Ribonuclease A:

Exploring the Function of the Active-Site Lysine Residue in Catalysis and Inhibition

By

June M. Messmore

A dissertation submitted in partial fulfillment

of the degree of

Doctor of Philosophy

(Biochemistry)

UNIVERSITY OF WISCONSIN-MADISON

1999

Reader's Page

A dissertation entitled

Ribonuclease A: Exploring the Function of the Active-Site Lysine Residue in Catalysis and Inhibition

submitted to the Graduate School of the
University of Wisconsin-Madison
in partial fulfillment of the requirements for the
degree of Doctor of Philosophy

by

June M. Messmore

Degree to be awarded: December 19___ May 19___ August 19 99

Approved by Dissertation Readers:

Ronald T. Raines
Major Professor

May 28th, 1999
Date of Examination

Virginia S. Hinshaw
Dean, Graduate School

Ribonuclease A: Exploring the Function of an Active-Site Lysine in Catalysis and Inhibition

June M. Messmore

Under the supervision of Professor Ronald T. Raines

at the University of Wisconsin-Madison

ABSTRACT

Structural analyses had suggested that the active-site lysine residue of RNase A (Lys41) may interact preferentially with the transition state for covalent bond cleavage, thus facilitating catalysis. Site-directed mutagenesis and chemical modification were combined (1) to probe the role of Lys41 in catalysis, (2) to provide a chemical on/off switch for RNase A activity in *in vitro* applications, and (3) to probe the analogy of uridine 2',3'-cyclic vanadate to the catalytic transition state. In addition to studying inhibition by the uridine vanadate, inhibition by a polyvanadate species was also characterized.

Results indicate the importance of positive charge and the donation of a single hydrogen bond in catalysis. Chemical modification can reversibly modulate the activity of ribonuclease by a factor of 30,000. A polyvanadate species, apparently decavanadate, was observed to be a hyperbolically competitive inhibitor of RNase A whose binding is sensitive to ionic strength. Lastly, studies of uridine 2',3'-cyclic vanadate, using RNase A variants altered at position 41, showed that any interaction between this vanadate species and Lys41 is not highly analogous to the interaction between the transition state and Lys41.

Acknowledgements

There are literally dozens of people whose contributions I ought to point out. Thank you to all of you and if I have not mentioned you specifically, know that I remember your efforts and absolutely appreciate it.

Thanks to ALL members of the Raines Lab, past and present. I am particularly grateful to Steve delCardayre who taught me 90% of everything I know about molecular biology. And to Jeung-Hoi Ha for her scientific and personal guidance in the early stages. I am grateful to Brad Kelemen whose scientific opinion and skills as a listener I value greatly. I am indebted to Jed Thompsen for the synthesis of enzymatic substrates and for his unfailing wittiness. I am also indebted to two talented young women, Dana Fuchs and Juneko Grilley, with whom I had the pleasure to work during their undergraduate years. Last and most of all, I am indebted to Barbra Fisher (nee Templer) for her friendship and counsel, not to mention all the free meals.

Thanks to the whole Raines Lab, not only for the scienctific support but also for being such a willing audience to my culinary experimentations over the years, see (Tlusty et al., 1986).

Dr. Darrell McCaslin's expertise and wry sense of humor were instrumental in all things calorimetric. Thanks Darrell.

Thanks to Mom and Dad, and my brothers Gene and Jay for understanding when I was absent from their lives and welcoming me when I was there. Thanks a million-fold to Tom Brownlee, the solid rock in my life, a pretty good cook in his own right, and my own personal computer help-desk.

Gratitude to Ron, for his patience.

Table of Contents

List of Tables

List of Figures and Schemes

List of Abbreviations

ATP	adenosine 5' triphosphate
C>p	cytidine 2',3'-cyclic phosphate
csa	cysteamine
DNA	deoxyribonucleic acid
DTT	dithiothreitol
DTNB or Ellman's reagent	5,5'-dithio-bis(nitrobenzoic acid)
HEPES	N-2-hydroxyethylpiperazine-N'-2-ethanesulfonic acid
HIV	human immunodeficiency virus
IC_{50}	inhibitory concentration decreasing activity by 50%
ITC	isothermal titration calorimetry
K41C	cysteine in the place of residue Lys41
K41CAA	S-acetamidinocysteine in the place of residue Lys41
K41CAm	S-(carbamoylmethyl)cysteine in the place of residue Lys41
K41CEA	S-aminoethylcysteine in the place of residue Lys41
K41CET	S-ethyltrimethylaminocysteine in the place of residue Lys41
K41CPA	S-aminopropylcysteine in the place of residue Lys41
MeOH	methanol
MES	2-(N-morpholino)ethanesulfonic acid
MPP	3-mercaptopropyl-1-phosphate
NaOAc	sodium acetate
NTB	2-nitro-5-thiobenzoic acid
PAGE	polyacrylamide gel electrophoresis

pdb.	Brookhaven protein data bank
p*I*	isoelectric point
poly(C)	poly(cytidylic acid)
RI	placental ribonuclease inhibitor
RNA	ribonucleic acid
RNase	ribonuclease
RNase A	bovine pancreatic ribonuclease A
RPA	ribonuclease protection assay
SDS	sodium dodecylsulfate
TEA	triethylamine
TLC	thin layer chromatography
Tris	2-amino-2-hydroxymethylpropane-1,3-diol
TS	transition state
$_{tx}$	subscript denoting pertinence to the rate limiting transition state
U>p	uridine 2',3'-cyclic phosphate
UMP	uridine 3'-monophosphate
Up(4-nitrophenol) or UpAR	uridine 3'-(4-nitrophenylphosphate)
UpA	uridylyl(3'→5') adenosine
UTP	uridine triphosphate
UVC	uridine 2',3'-cyclic vanadate monohydrate
V_{10}	decavanadate

Chapter 1

Introduction

Historical Perspective

In 1920, the observation was made that a boiled aqueous extract of porcine pancreas was capable of turning yeast nucleic acids into nucleotides, without liberating either purine or pyrimidine bases or inorganic phosphate (Jones, 1920). Jones correctly surmised that this transformation resulted from a single active agent. In 1939, an apparently homogeneous sample of protein was isolated from bovine pancreases by ammonium sulfate fractionation and recrystallization (Kunitz, 1939). This protein possessed the same activity against yeast RNA as that first observed by Jones and it came to be called ribonuclease or RNase. To put the work of Jones, Kunitz, and other contemporaries into proper perspective, one must be realize that the early histories of RNA and ribonuclease were interlocking puzzle pieces. The distinction between RNA and DNA was not completely understood until c.1930 (Chargraff, 1955), and the correct chemical structure of ribonucleic acids was not deduced until c.1952 (Brown & Todd, 1955). The study of the enzyme helped elucidate the structure of RNA, while the nature of the enzyme necessarily remained unclear as long as the chemical structure of the substrate remained unknown.

Through the mid 1940's the tenor of research was profoundly affected by World War II (WWII). One effect of the war was to create relationships between industry and academic science. During the war, the Armour meat packing company became involved in the development of blood products for the war effort and thus acquired expertise in biochemical separations. After the war was over, this company, which one now associates with the slogan "the dogs kids love to bite" and Vienna sausages, not with biochemical research, decided to invest some of its considerable excess capital of bovine pancreases in the philanthropic advancement of science. Exactly why and how the folks at Armour came to decide to undertake a large-scale purification of ribonuclease may be lost to history, but

an appreciation for the impact of this decision remains. Fred Richards has given an account of his time in the laboratory of Linderstrom-Lang, how he was introduced to the Armour ribonuclease, and the importance of this enzyme to post-war biochemistry (Richards, 1992).

> "In early 1954 Chris Anfinsen was in the middle of one of his many visits to the Carlsberg Laboratory. This time he had appeared with a bottle containing 10 grams of crystalline bovine pancreatic ribonuclease! This very large sample was given to him free by the Armour company...Armour used the procedures, then recently developed by Moses Kunitz at the Rockefeller Institute, to prepare 1 kilogram of the pure enzyme from their normal slaughterhouse material. Samples of this single lot were given out free to any laboratory in the world that could demonstrate a need and a reasonable research project. It is hard to over emphasize the significance of this decision. Over the years a large number of groups were able to move forward the frontiers of research in enzyme structure and mechanism and to compare their results knowing that the starting material in each project was identical. There were no strings attached to the gifts. The company only asked that good science be done. For most biochemists, contracts and patenting were not even on the horizon in those days. Nirvana had we only known it!
>
> Chris kindly doled out aliquots of his precious hoard to other members of the laboratory...When Chris ended this particular stay and returned to the U.S., he still had most of the ribonuclease in the bottle. None of us used very much. As is well known, Chris made good use of the rest during the next decade (See Nobel Lecture (Anfinsen, 1973).)"

Richards, too, made good use of the Armour ribonuclease discovering and studying ribonuclease S, the partial proteolysis product of ribonuclease (Richards & Vithayathil, 1959), and ultimately reporting its crystal structure.

The rapid progression of knowledge and techniques in the years following WWII has been referred to as "the first golden era of protein science (Neurath, 1995)." Ribonuclease and the scientists that studied it were clearly among the vanguard during this period. In addition to Anfinsen and Richards, another noteworthy group that chose to work with ribonuclease in the years immediately following WWII was the team of Stanford Moore and William Stein, and like Anfinsen, these two researchers were ultimately awarded a

Nobel Prize for their accomplishments (Moore & Stein, 1973). They chose to work on ribonuclease not only because of its availability but also because it was relatively small (13.7 Kdalton) and stable (Manning, 1993). By employing newly developed chromatographic fractionation techniques, they discovered that two forms of ribonuclease existed in the Kunitz preparation (Hirs, 1953). The forms were dubbed RNase A and B and were shown to differ only by a carbohydrate chain attached to RNase B (Plummer, 1964). Moore and Stein and post-doctoral fellows in their laboratory also determined the amino acid sequence of RNase A, the first enzyme and second protein (after insulin) for which such information became available (Hirs, 1960; Smyth, 1963).

Between 1955 and 1963, Stein and Moore's group played a key role in what Stein referred to as "a sort of serial-story" that culminated in the development of a cohesive picture of the mechanistic roles of His12 and His119 (Stein, 1964). In 1955, it was discovered that photoinactivation was accompanied by a loss of histidine (Weil, 1955). In 1959, it was simultaneously discovered, by Barnard in England and Gundlach in Stein and Moore's laboratory, that carboxymethylation of a uniquely susceptible histidine residue inactivated the enzyme (Barnard & Stein, 1959; Gundlach, 1959). This residue turned out to be His119. By 1963, Crestfield in Stein and Moore's laboratory had pinpointed a second active-site histidine residue, also critical for enzymatic activity. It occurred at position 12 (Crestfield & Stein, 1963). Chemical modification studies on RNase S initially seemed at odds with Crestfield's observations (Vithayathil & Richards, 1960), but later studies with RNase S confirmed the importance of His12 (Finn & Hofmann, 1965).

It had been realized about a decade earlier that RNase catalyzed two related reactions (Markham & Smith, 1952). The chain of RNA phosphodiester linkages was, first

of all, cleaved by the transphosphorylation occurring between the incoming 2' hydroxyl and the departing 5' hydroxyl of the adjacent base. In the second reaction, the cyclic phosphodiester, which formed as the result of the transphosporylation, is hydrolyzed, leaving a 3' monophosphate (Fig 1.1). The cyclic product can be thought of as an intermediate, though later studies have shown that the two reactions almost never occur sequentially on the same enzyme molecule, the cyclic product nearly always being released to solution before hydrolysis can occur (Thompson *et al.*, 1994).

During the same years when the original histidine modification studies were ongoing, kinetic and spectrophotometric observations were also implicating two active-site histidine residues. Findlay, Herries, Rabin, and coworkers looked at catalytic activity as a function of pH, and varied solvents, inhibitors, and buffers (Findlay *et al.*, 1961; Findlay *et al.*, 1962). They concluded that two ionizing groups, both bearing a positive charge when protonated, participated in catalysis. From the bell-shaped pH-rate profile, with its maximum near neutral pH, they concluded that one functioned as an acid and one as a base. Findlay *et al.* proposed that His119 acted as an acid, protonating the leaving group in transphosphorylation, and as a base, deprotonating the water nucleophile in hydrolysis. The other histidine, later realized to be His12, was postulated to act as the base in transphosphorylation, deprotonating the 2' O nucleophile and as the acid in hydrolysis, protonating the 2' O leaving group (Fig 1.2.). This mechanistic proposal has withstood the test of time, appearing in many basic biochemistry textbooks. More importantly, it is still consistent with all known mechanistic data, even though other mechanistic proposals have been put forth from time to time (Witzel, 1962; Breslow & Labelle, 1986). Recently,

enzymes with alanine or fluorohistidine residues at positions 12 and 119 have been shown to behave in accordance with predictions arising from their "textbook" roles (Jackson *et al.*, 1994; Thompson & Raines, 1995).

Rabin and coworkers were among the first to propose a mechanistic role for Lys41 (Deavin *et al.*, 1966), a residue whose catalytic participation had also been strongly implicated by unique reactivity with reagents such as fluorodinitrobenzene (Hirs *et al.*, 1961). They attributed Lys41's apparent effects on catalysis to an ability to bind the substrate through the partially-charged non-bridging phosphoryl oxygens, noting that this could be accomplished either by virtue of electrostatic interactions or hydrogen bonding. Roberts pointed out that this binding would be strengthened by increased charge density on these oxygen atoms in a phosphorane dianion intermediate (Roberts, 1969). Usher and Eckstein showed that both ribonuclease reactions proceed in-line (Eckstein, 1968; Usher *et al.*, 1970; Usher *et al.*, 1972), and thus lent support to the concept that both steps were of a concerted nature. In this conception of the mechanism, the role of Lys41 shifts from stabilizing charge-build-up on a pentavalent dianion intermediate to stabilizing charge build-up on a pentacoordinate transition state, the role for Lys41 that has become commonplace in textbooks. Like the acid-base roles for the histidine residues, this hypothesis has persisted over the better part of three decades. However, a number of alternatives and variations have been brought forth and the emergent picture has been somewhat less clear than for the histidines. The existence or non-existence of a pentavalent or phosphorane intermediate has been an enduring source of contention.

In 1967, the three-dimensional structure of ribonuclease was announced (Kartha *et al.*, 1967; Wyckoff *et al.*, 1967). It was only the fourth protein and second enzyme structure to

be solved. In less than 20 years the level of knowledge had progressed from little information about the enzyme's primary structure to detailed information about the tertiary structure. Eric Barnard commented in 1969 that "We have left the era of groping in the dark, feeling with chemical probes for prominent features of the molecule. The crystallographers have switched on the lights." He also wondered "should, then, the enzyme chemist now cry, like Othello, that his occupation is gone?" But Barnard concluded, rightly so, that such a lament might be premature (Barnard, 1969).

Over the past 30 years a wealth of crystallographic data has accumulated. Much of it has been reviewed (Wlodawer, 1985). At the present time, RNase A, B, and S, and minor modifications thereof, account for over 60 Protein Data Bank entries. Crystallographic studies, on the whole, have tended to support the textbook roles of the three key active-site participants. But certain crystal structures have raised provocative questions. For instance, the joint neutron, x-ray diffraction study with the coordination complex uridine 2',3'-cyclic vanadate monohydrate (UVC) bound in the active site showed Lys41 closer to the 2' oxygen than to the non-bridging phosphoryl oxygen (Wlodawer *et al.*, 1983). This observation is especially remarkable since UVC has been believed to be a reasonable analog of the transition state. Should one conclude that a deprotonated lysine residue functions as the base in transphosphorylation, or that the structure is not accurate enough to draw mechanistic conclusions, or that uridine vanadate is a less than faithful mimic of the transition state? Another instance of a crystal structure intimating an alternative mechanistic hypothesis comes from the structure with cytidine 3'–phosphate bound in the active site (Zegers *et al.*, 1994). The 2' OH appears to be hydrogen bonded to both His12 and Lys41, while the non-bridging phosphoryl oxygens are hydrogen bonded only to the

mainchain carbonyl of Phe120 and water molecules. The authors take this topology to imply that the role of Lys41 in transphosphorylation is to work in conjunction with His12 to activate the 2' oxygen nucleophile.

Any proposal of an alternative role for Lys41 must be in accord with what has recently been learned about the transition state from ^{18}O isotope effects (Sowa et al., 1997). This study, using a slow phosphodiester substrate, showed a loss of bond order in the rate-limiting transition state to both the leaving group oxygen and the non-bridging phosphoryl oxygens. It is difficult to reconcile these observations with a mechanism other than an associative, concerted one.

Many mechanistic proposals, both new and well-accepted, can be tested directly in ways that were not possible prior to the advent of site-directed mutagenesis. Site-directed mutagenesis followed by careful study of the variant proteins provides an avenue for characterization and. quantification of the contributions of individual catalytically important residues. Knowles properly points out that site-directed mutagenesis is a more powerful technique than previously existed, yet warns that it can give results that are difficult to interpret. He likens the use of chemical modification reagents in deducing catalytic roles to attempts to understand an automobile engine by firing a shell through it. He likens mutagenesis to putting a square tire on one wheel of the car (Knowles,1987).

The birth of the modern era of "protein engineering" can be pinpointed to the late 1970's. In 1977, somatastatin became the first polypeptide to be heterologously over-expressed, and then in 1978, Smith first achieved site-specific mutagenesis. However, in the era of protein engineering, RNase A studies have lagged somewhat behind other proteins. The second protein to be sequenced and the fourth to have its three-dimensional structure

solved, RNase A was no where near the top of the list of proteins to be successfully cloned and over-expressed. It was not successfully produced recombinantly until approximately a decade after somatostatin. The reason for this lag was not that researchers had exhausted the study of RNase A, or that site-specific variants were not potentially interesting, but that the heterologous expression of this enzyme proved difficult.

The first limited success with RNase A and modern DNA technology was achieved in 1987, when a synthetic gene for RNase A was expressed as a fusion to beta-galactosidase (Nambiar *et al.*, 1987). This work and other early work, with either synthetic genes or the rat RNase gene, suffered from low yields, due to cytotoxicity and proteolytic degradation, inefficient purification schemes, and undesirable modifications (for a brief review, see delCardayre et al., 1995). A breakthrough occurred when the bovine pancreatic RNase cDNA, which had been previously cloned (Raines & Rutter, 1989), was fused to the pelB leader sequence and expressed from a plasmid under the control of the T7 promoter (delCardayre & Raines, 1994). The result was an insoluble but fully processed protein, which could be isolated at yields as high as 50 mg/L of culture (delCardayre *et al.*, 1995). Mutated proteins could be expressed and purified thusly, with lower, yet still substantial yields. The tight control of the T7 promoter system and the insolubility of the protein greatly ameliorated problems with cytotoxicity and proteolysis.

The beginnings of the research reported herein coincide roughly with this breakthrough by delCardayre et al. Other researchers have previously reported mutants at position 41 similar to those to be covered presently, but no other group has subjected their proteins to as thorough study, presumably due in part to the limited quantities of available protein.

Scope of this work

In order to gain insight into the role of Lys41, we have varied the amino acid residues at position 41 and performed steady-state kinetic measurements with the variant enzymes using several substrates. This examination has allowed for quantitative assessment of the magnitude of catalytic contribution by Lys41 in both the transphosphorylation and hydrolysis reactions. The choice of substitutions has made possible the consideration of the relative importance of hydrogen bonding and Coulombic interactions. This work is discussed in chapter two.

We have used the varying transition state binding abilities possessed by these variants to probe for the similarity of uridine 2',3'-cyclic vanadate to the chemical transition state. The results of this work are adressed in chapter three.

The control of ribonucleolytic activity is important in molecular biological manipulations of RNA. Chapters four and five discuss two new strategies for controlling RNase activity. Chapter four discusses a new inhibitor for wild-type RNase that was fortuitously discovered in the course of the work discussed in chapter three. Chapter five discusses a novel strategy that can be employed when RNase activity is needed in one stage of an experiment, but is detrimental in subsequent steps.

Figure 1.1 Ribonuclease catalyzes two reactions. This figure was originally presented by Markham and Smith in 1952.

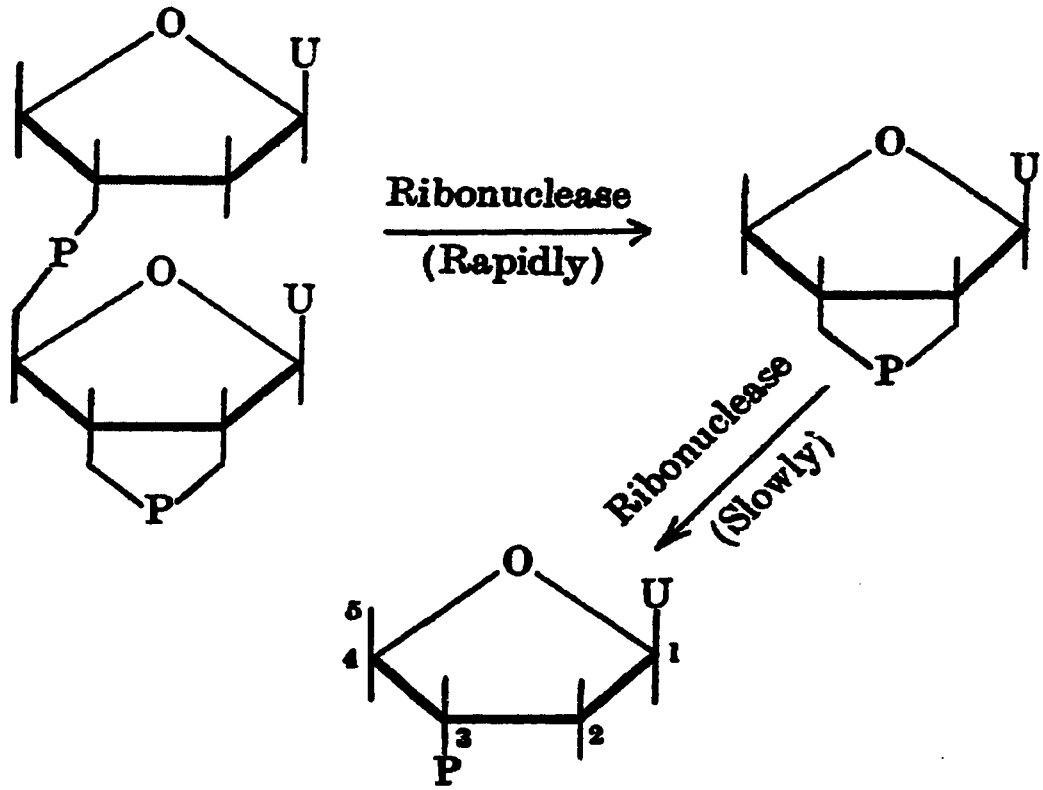
O
U
P
O
U
P
Ribonuclease
(Rapidly)
O
U
P
Ribonuclease
(Slowly)
O
U
5
4
1
3
2
P

Figure 1.2 Mechanism of the transphosphorylation and hydrolysis reactions catalyzed by ribonuclease A. His12 and His119 participate as acid and base.

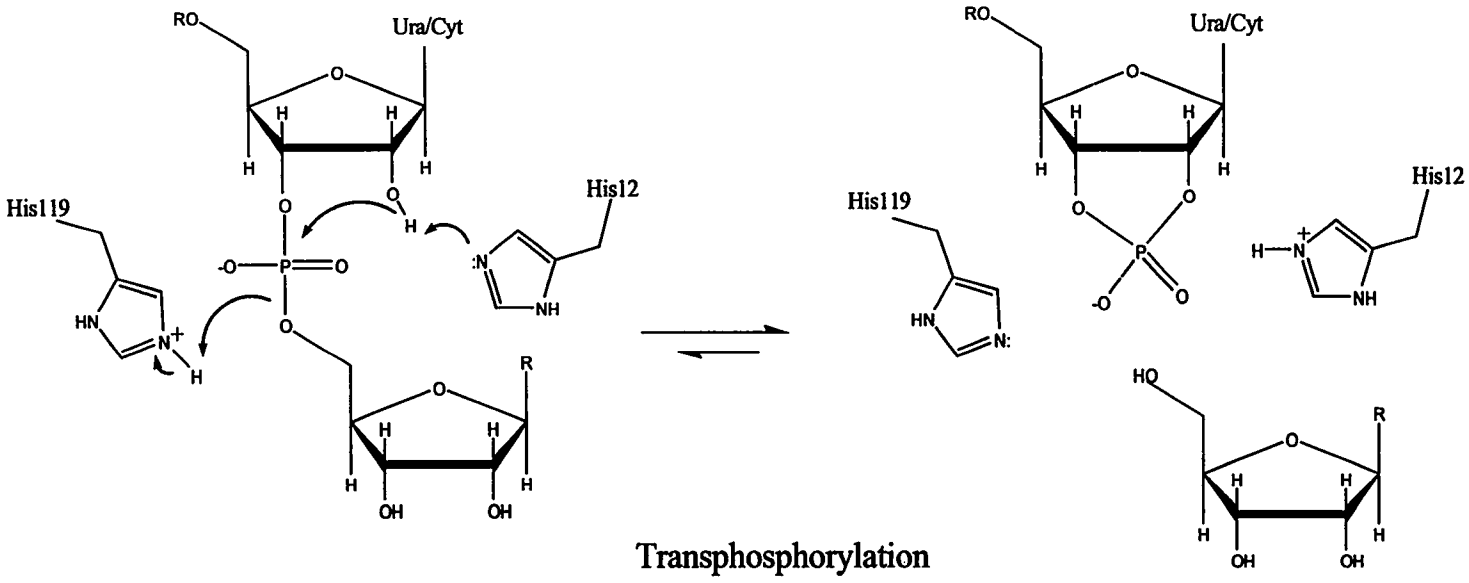

Transphosphorylation

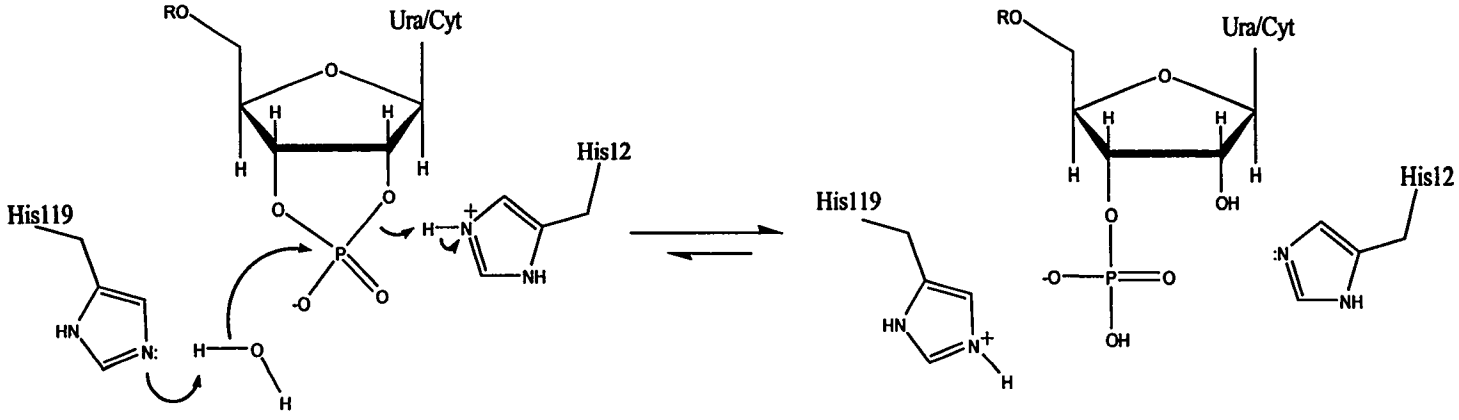

Hydrolysis

Chapter 2

Kinetic Properties of Variants of Ribonuclease A at Position 41

Portions of this chapter published in the *Journal of the American Chemical Society* as: Messmore, J. M., Fuchs, D. N., Raines, R. T. Ribonuclease A: Revealing Structure-Function Relationships with Semisynthesis. (**117**, 8057-8060)

Introduction

Life as we know it would be impossible without catalysis. Enzymes serve as both the workhorses and traffic cops within the world of biomolecules. They have evolved amazing powers of catalysis in order to sustain the highly specific, heavily coupled, non-equilibrium, and fast-paced chemical processes necessary for organism viability. Most biological reactions would be far too slow to accommodate life on the familiar time scale without the aid of enzymes. For example, the half-life of a peptide bond has been estimated to be seven years (Kahne & Still, 1988) or several hundred years (Radzicka & Wolfenden, 1996). How many millennia would it take just to digest lunch? Yet a molecule of chymotrypsin, a digestive protease, can turn over as fast as 7 times per second (Baumann *et al.*, 1970). For many enzyme-catalyzed reactions we can not even assess true catalytic power because of the difficulty of assessing the corresponding uncatalyzed reaction rate. RNase A is not such an enzyme; the relevant uncatalyzed rates are known (Thompson *et al.*, 1995). We also have significant structural information about this protein, and consequently can attempt to dissect the sources of ribonuclease-associated rate enhancements of RNA hydrolytic cleavage.

To consider the uncatalyzed and catalyzed rates of RNA cleavage, it is necessary to consider the two steps, transphosphorylation and hydrolysis, separately (Figure 1.1). Data have been published for both steps. The non-enzymatic first-order rate constant, k_{uncat}, for transphosphorylation of uridylyl 3'→5'adenosine (UpA) at pH 6 and 25 °C, has been determined to be 5×10^{-9} sec^{-1} (Thompson *et al.*, 1995). Compare this value to the pseudo first-order rate constant (*V/K*) for 1 μM RNase A and UpA (delCardayre *et al.*, 1995). The value of *V/K*, under the same conditions, is 2.3 s^{-1}. The catalyzed reaction is faster by a factor of $\sim5\times10^{8}$, a value that is affected by the arbitrary choice of 1 μM enzyme as the standard state. The rate constant for uncatalyzed hydrolytic ring opening of cytidine 2',3'–cyclic phosphate (C>p) at 25 °C, and pH 6 has been estimated to be 4×10^{-9} s^{-1} (Eftink &

Biltonen, 1983). *V/K* for C>p and 1μM enzyme under similar conditions has been determined to be 1.9×10^{-3} s^{-1}(this work), for an acceleration of rate by a factor of $\sim 5 \times 10^{5}$. Another manner of comparing catalyzed and uncatalyzed reactions stems from Eyring's theory of absolute reaction rates and the definition of the steady-state parameter k_{cat}/K_m (Wolfenden, 1976). The value k_{uncat} reports to us on the energy barrier between the unbound substrate and the unbound transition state, while the parameter k_{cat}/K_m reports to us on the energy barrier between the unbound substrate and the rate-limiting, enzyme-bound transition state. The ratio of k_{uncat} to k_{cat}/K_m can be viewed as the dissociation constant of the transition state from the enzyme (K_{tx}), assuming both reactions go through similar transition states (Figure 2.1). The free energy of the interaction between the enzyme and the transition state, the binding energy utilized in lowering the activation barrier of the catalyzed reaction, ΔG_{tx}, is thus given by $RT*\ln(K_{tx})$. Using this manner of analysis, RNase A has been calculated to bind to the transition state for cytidine 2'-3'-cyclic phosphate hydrolysis with $\Delta G_{tx} = -15.9$ kcal/mol. Similarly, the computed value of ΔG_{tx} for UpA transphosphorylation by RNase A is -20.0 kcal/mol. However, because the catalyzed reaction appears to have a step other than the chemical transformation as the rate limiting step (Thompson *et al.*, 1995), the computed value must be taken as a limit; the actual value of ΔG_{tx} for UpA transphosphorylation may be more negative.

A number of features of the enzyme have been identified as probable contributors to this sizeable transition state binding energy. Evidence for the contributions of specific features came originally from chemical modification studies, then from X-ray and NMR structural data and from conservation across species. A crystal structure of RNase A with a putative transition state analog bound in the active site demonstrates that five groups are placed intimately with respect to the active site (Wlodawer *et al.*, 1983). These groups are the His12 imidazole, the His119 imidazole, the Gln11 side chain amide, the backbone amide N-H between residues 119 and 120, and the Lys41 primary amine (Figure 2.2). The

involvement of four of these groups also concurs with other lines of evidence, while evidence for the involvement of backbone groups in protein function is intrinsically harder to obtain. His119 has been shown to act as an acid in transphosphorylation, where it serves to protonate the 5' oxygen leaving group. Its role is believed to be reversed in hydrolysis, where it is widely accepted to act as a base, deprotonating the incoming water nucleophile. His12 is believed to act as a base in transphosphorylation, deprotonating the 2' hydroxyl nucleophile, and as an acid in hydrolysis, protonating the 2' oxygen leaving group. Gln11, like His12 and His119, is conserved in pancreatic-type ribonucleases across many evolutionarily distant species (Beintema, 1987). Gln11's role has been recently assigned to be the orientation of the substrate and prevention of non-productive binding modes (delCardayre *et al.*, 1995). A number of proposals have been put forth as to Lys41's role in catalysis (see below). Away from the immediate site of phosphoryl transfer, several other amino acid side chains are known to be involved in substrate binding and specificity. Thr45 enforces the specificity of RNase A, determining that reactions take place only at phosphoryl groups that are 3' to pyrimidines (delCardayre & Raines, 1994). Lys66, Arg10, and Lys7 bind phosphoryl groups at sites directly before and after the reacting phosphoryl (P0 and P2, respectively) (Richardson *et al.*, 1990; Parés *et al.*, 1991; Templer, 1997). These four residues are also conserved in almost all known pancreatic-type ribonucleases [Residue 66 in the wallaby is an exception (Beintema, 1987)].

Of all the RNase A residues known to play a role in binding and catalysis, Lys41 is perhaps the most intriguing and enigmatic. Its large contribution to catalysis was apparent even in the earliest chemical modification study (Hirs *et al.*, 1961). The most widely cited of Lys41's proposed roles is stabilization of negative charge on the non-bridging phosphoryl oxygens, in either a pentacoordinate (phosphorane) intermediate or an associative transition state. However Lys41's deprotonation does not show the expected effect (or any effect) in pH–rate profiles (Eftink & Biltonen, 1983). The side chain is highly

disordered in many crystal structures (Borah *et al.*, 1985) (Alber *et al.*, 1982). In the crystal structure with uridine vanadate, the putative transition state analog, the side chain is relatively more ordered, as one might expect. Here, however, the primary amino group of Lys41 actually lies closer to the 2' oxygen (within 2.8 Å) than to the nearest of the nonbridging oxygens (within 3.4 Å). In addition, neutron diffraction data clearly show a hydrogen bond between the 2' oxygen and Lys41 (Wlodawer *et al.*, 1983).

Over Lys41's long history, most of the conceivable roles have been proposed. Lys41 is positively charged and capable of hydrogen bond donation, so it is quite logical to propose a direct interaction with a substrate's non-bridging phosphoryl oxygens, which are negatively charged and capable of hydrogen bond acceptance. But at what stage is this interaction important? Originally it was assigned to a ground state role (Deavin *et al.*, 1966). But several years later it was proposed that this interaction would be strengthened as the reaction progressed to a pentacoordinate intermediate, where the nonbridging oxygens would presumably bear increased negative charge (Roberts *et al.*, 1969). Evidence for an intermediate exists for some uncatalyzed and small-molecule-catalyzed phosphoryl transfer reactions (Westheimer, 1968; Breslow & Labelle, 1986; Breslow, 1991). However, in the enzymatic case of transphosphorylation or hydrolysis, proposal of an intermediate is not necessary. Lys41 may simply serve to stabilize the phosphorane-like transition state. If the enzyme stabilizes a phosphorane intermediate, it will also stabilize the transition states flanking that intermediate, so whether or not an intermediate exists, Lys41's role will be similar. The possibility that Lys41's primary function is to interact with the 2' hydroxyl rather than the nonbridging oxygens has also been given some attention. The residue's position in the uridine vanadate crystal structure suggests that Lys41 serves the role usually ascribed to His12, a role that is not particularly compatible with Lys41's apparent pK_a of ~9 (Brown & Bradbury, 1976; Jentoft *et al.*, 1981). Another possibility is that a partial negative charge develops on the 2' oxygen, as it acts as an attacking nucleophile or leaving

group, and a charge - charge interaction or hydrogen bond with Lys41 facilitates that development (Zegers *et al.*, 1994).

Although the present work does not definitively settle what roles Lys41 does and does not play, it does serve to clarify what aspects of Lys41 are important in those roles and addresses Lys41's importance relative to other residues known to participate in ground state and transition state binding. The method we report for studying Lys41 utilizes not only site-directed mutants at position 41, but also Cys41 mutant proteins that have been chemically modified. This approach was undertaken in order to increase the variety of structures available for study. Combining these two techniques has the unique advantage of allowing for non-natural amino acid structures without substantially increasing side chain bulk, the major disadvantage associated with the chemical modifications in the absence of previous mutagenesis. Pioneers in combining these two techniques include Mildvan, Hartman, and Kirsch (Pease *et al.*, 1987; Smith & Hartman, 1988; Planas & Kirsch, 1990).

A number of conventional mutational studies on RNase A at Lys41 have been reported. The mutants investigated have fallen into two categories, K41R RNase A and variants that lack a positive charge because Lys41 was replaced with a glycine or alanine residue. Kinetic data for K41R for the transphosphorylation step have been reported by two groups, but each group used a different pH and buffer for their kinetic assays. The mutant was determined to have retained 2% of its activity at pH 5 (Trautwein *et al.*, 1991) and 0.2% of its activity at pH 7 (Tarragona-Fiol *et al.*, 1993). Since a number of factors differed between these two studies, it is difficult to pinpoint the source of the discrepancy as being solely a pH effect. Both studies agree that the parameter most greatly affected by this mutation is k_{cat}. K41G RNase A has been studied only for second step activity and was found to have 'none' (Laity *et al.*, 1993). K41A RNase A has been studied only in the context of porcine RNase A, and was found to have retained 2 - 5 % of wild-type activity, both in the transphosphorylation and hydrolysis steps (Miranda, 1990). Because this study used

recombinant RNase A protein obtained from cultured mammalian cells, it may have suffered from contamination with co-purified endogenous ribonucleases. Unlike the previous reports, our work compares a range of mutants under consistant assay conditions, and does so for both the transphosphorylation and hydrolysis steps.

Materials and Methods:

Protein Modification Reagents: Bromoethylamine·HBr, bromopropylamine·HBr, iodoacetamide, and bromoethyltrimethylamine·HBr were from Sigma Chemical (St. Louis, MO) and used without further purification. Chloroacetonitrile and all other chemicals used in chloroacetamidine·HCl synthesis were from Aldrich Chemical (Milwaukee, WI) and were also used without further purification.

Chloroacetamidine·HCl was synthesized from chloroacetonitrile, methanol and ammonium chloride as described by Schaefer and Peters (Schaefer & Peters, 1961)(Figure 2.3). Chloroacetonitrile (2.5 M) was reacted with methanol (solvent) in the presence of a catalytic amount of methoxide, which was generated *in situ* with trace amounts of Na. The resulting imidate, still in MeOH, was reacted with a stoichiometric amount of ammonium chloride. MeOH was evaporated off under vacuum and the product was washed several times with diethyl ether and dried under vacuum. The integrity and purity of the chloroacetamidine·HCl was confirmed by ^{1}H NMR (in CD_3OD; 4.85 ppm relative to tetramethylsilane, s, CH_2,) mass spectroscopy (EI, *m/e* 92; calc'd for $C_2H_5ClN_2$ 92.0141) and melting point (92-94 ^oC; uncorrected). The product was stable when stored under vacuum for one week or more.

Enzyme preparation: Mutations in the cDNA that codes for RNase A were made by the method of Kunkel (Kunkel *et al.*, 1987) using the following oligonucleotides,

AAGGTGTTAACTGGCCTGCATCGATC (for K41R), AAAGTGGTTAACTGG-ACAGCATCGATC (for K41C), AAGGTGTTAACTGGCGCGCATCGATC (for K41A), and AAGGTGTTAACTGGTTGGCATCGATC (for K41Q). Mutant cDNA's were expressed in *Escherichia coli* under the control of the T7 RNA polymerase promoter, and the resulting proteins were refolded and purified as previously described (delCardayre *et al.*, 1995). After purification, the new sulfhydryl group in the K41C enzyme was protected from inadvertent reactions such as air oxidation by reaction with 5,5'-dithio-bi(2-nitrobenzoic acid).

Immediately prior to alkylation, the sulfhydryl group of Cys41 was deprotected by treating the enzyme with dithiothreitol (0.1 mM) at 25 °C until one equivalent of 5-thio-2-nitrobenzoic acid had been released, typically for 25 minutes. Deprotected K41C RNase A was added to a freshly prepared solution of haloalkylamine (0.1 M) in 0.2 M Tris-HCl buffer, pH 8.3. The resulting solution was incubated 3 h at 30 °C. Chemically modified enzymes were separated from any unreacted or undeprotected K41C by cation exchange FPLC (Mono S column; Pharmacia, Piscataway, NJ) using a linear gradient of NaCl (0 – 0.20 M) in 50 mM HEPES-NaOH buffer, pH 7.7. The isolated yield of each cysteine-modified enzyme was at least 50%.

Enzymatic Assays: Polycytidylic acid [poly(C)] was from Sigma Chemical or Midland Reagent (Midland, TX) and was purified by precipitation from aqueous ethanol (70% v/v). Small aliquots of poly(C) stock solutions were quantitated for total cytidyl concentration by their absorbance at 268 nm. using $\epsilon = 6200\ M^{-1}cm^{-1}$ (Yakovlev *et al.*, 1992). Assays of poly(C) cleavage were performed at 25 °C in 0.10 M Mes-NaOH buffer, pH 6.0, containing NaCl (0.1 M). Cleavage of poly(C) was monitored by UV absorption at 250 nm using $\Delta\epsilon = 2380\ M^{-1}\ cm^{-1}$. Concentrations of poly(C) in assays ranged from 0.02 mM to 1 mM, in terms of individual cytidyl units. Enzyme concentrations ranged from 1 nM for wild-type to 8 μM for K41A.

Up(4-nitrophenol) was obtained as the 2',5' O-tetrahydropyranyl blocked material and was kindly provided by Dr. James E. Thompson and Dr. Tatiana Kutateladze. The deblocking procedure employed a strong cation exchange resin (Davis *et al.*, 1988). Before use, the resin was washed with 3 N HCl, then ethanol, and finally with water until the eluent was neutral. The blocked material in water was shaken for 20 minutes with resin (2 mg of BioRad Ag 50WX8 resin per μmole of material), and the resin was then removed by filtration through a syringe-tip filter. The pH of the deprotected material in solution was adjusted with NaOAc to pH 5, where stability is maximal (Dantzman & Kiessling, 1996). Up(4-nitrophenol) solutions thus prepared were kept at 4 °C and used within 72 h of deprotection. Small aliquots of the stock solution were quantitated on the basis of total 4-nitrophenol concentration by dilution into 0.01 N NaOH and measurement of absorbance at 400 nm, using $\epsilon = 18000\ M^{-1}cm^{-1}$ (Kezdy & Bender, 1962). Cleavage by enzymatic catalysis was monitored in the above MES-NaOH buffer at 25 °C by UV absorption using $\Delta\epsilon = 4560\ M^{-1}cm^{-1}$ at 330 nm (Thompson *et al.*, 1995). Concentrations of Up(4-nitrophenol) in assays ranged from 0.05 mM to 1 mM. Enzyme concentrations ranged from 24 nM for wild-type RNase A to 24 μM for K41A.

Cytidine 2',3'-cyclic phosphate (C>p) hydrolysis at 25 °C was monitored in 25 mM Mes-NaOH buffer, pH 6.0, containing NaCl (0.1 M). Hydrolysis was monitored by UV absorption at either 286 or 292 nm, using $\Delta\epsilon = 1570\ M^{-1}cm^{-1}$ or $760\ M^{-1}cm^{-1}$ respectively. Concentrations of C>p in assays ranged from 0.1 mM to 7 mM. Enzyme concentrations ranged from 300 nM for wild-type RNase A to 5 uM for K41A RNase A. Assays of K41A required measurements of absorbance changes over 6 h time periods.

Steady-state kinetic parameters were determined by fitting initial velocity data to a hyperbolic curve, using the programs Deltagraph (Deltapoint Software, San Francisco, CA) and HYPERO (Cleland, 1979), for visualization and standard error analysis, respectively. Both programs perform fitting operations using the Marquardt algorithm.

Results

We used recombinant DNA techniques to produce variants of RNase A in which Lys41 was changed to an alanine, a glutamine, an arginine, or a cysteine residue. In all cases, the purification method (delCardayre *et al.*, 1995) successfully produced pure proteins as judged by SDS/PAGE. The T_m of K41A RNase A was within 5 °C of that of the wild-type protein, and the circular dichroism spectrum of K41Q RNase A was indistinguishable from that of the wild-type enzyme, indicating the general ability of variants at position 41 to fold properly.

The change to cysteine introduces a solvent accessible sulfhydryl group to the native protein. This group was then alkylated with one of five halo-alkylamines and the enzyme re-isolated. In each of the resulting chemically modified enzymes, residue 41 contains a nitrogen separated from the main chain by either 4 atoms (as in lysine) or 5 atoms (as in arginine) (Figure 2.4). The following observations indicate that alkylation was specific for Cys41. First, exposure of the wild-type RNase A to the reaction conditions did not change its catalytic activity, indicating that fortuitous alkylation had not occurred near the enzyme active site. Second, no cysteine-modified enzyme had a retention time during cation exchange FPLC that was greater than that of wild-type RNase A, indicating that no more than one additional positive charge had been introduced.

An acetamidino group can suffer hydrolysis to form an amide. To ascertain the stability of the S-acetamidinocysteine RNase A (K41CAA), the enzyme was re-injected onto the FPLC column 10 days after it was originally isolated and several days after kinetic parameters had been assayed. At this point, the enzyme still appeared to be more than 95% pure.

We determined the ability of wild-type, variants, and modified ribonucleases to catalyze the transphosphorylytic cleavage and hydrolysis of several substrates. The values

of the steady-state kinetic parameters for cleavage of poly(C) by our ribonucleases are given in Table 2.1. The values for C>p are given in Table 2.2, and the values for Up(4-nitrophenol) in Table 2.3. In the case of lower-functioning variants (K41A, K41C, and K41Q) the experiments determining these parameters were unconventional in that the enzyme concentrations used were not minuscule relative to substrate concentrations. However, none of the assumptions necessary for using the classical Michaelis-Menton steady-state treatment were violated. In the design of these types of experiments, the steady-state assumption must be considered, *i.e.* the concentration of the enzyme-substrate complex, [E·S], cannot change appreciably during the course of the measured reaction. In the current case of our low-functioning mutants, this assumption should be met because the forward reaction is assumed to be negligible compared to the on and off rates. Therefore, a rapid pseudo-equilibrium is formed between the free enzyme and free substrate and the [E·S] complex. The reaction is never measured for long enough to shift significantly this equilibrium. A second consideration is whether or not the free substrate concentration remains essentially equal to the total substrate concentration. The K_m values that we have measured do not indicate very tight binding. If these K_m values are assumed to be equilibrium constants, simple calculations indicate that the concentrations of [E·S] are smaller, by more than an order of magnitude, than the substrate concentrations, and so the treatment of free substrate and total substrate as equal is valid.

As shown in Tables 2.1-2.3, dramatic differences are observed in the values of k_{cat}/K_m indicating that the mere presence of an alkylamine is not enough to effect efficient catalysis. Tables 2.1-2.3 present two energetic values that are derived from k_{cat}/K_m. ΔG_{tx} is a function of both k_{cat}/K_m and the uncatalyzed rate and reports on the total transition state binding energy. For these calculations, the uncatalyzed rate constant for poly(C) transphosphorylation has been assumed to be equal to that measured for UpA under identical conditions. $\Delta\Delta G_{tx}$ is a function of the enzyme variant's k_{cat}/K_m and wild-type

k_{cat}/K_m and reports on the change in ability to bind to the rate limiting transition state associated with the mutation or modification.

Discussion:

Three of the prepared variants, K41A, K41C, and K41Q, have in common that they remove the positively charged lysine side chain and replace it with a smaller, uncharged residue. In all three cases, the loss of ability to cleave poly(C) amounts to nearly a 10^5-fold reduction in k_{cat}/K_m. When one takes away an interacting functional group, such as is done in alanine mutagenesis, ΔG_{tx} decreases by an amount ($\Delta\Delta G_{tx}$) that is equal to that group's apparent contribution to the binding of the rate-limiting transition state (of course, the identity of that transition state could be altered upon mutation). It appears that, like alanine, cysteine and glutamine at position 41 do not participate in catalysis. These three mutant proteins all indicate that Lys41 contributes nearly 7 kcal/mol, or approximately one third of the total transition state binding energy.

If the groups involved in binding the transition state work independently of one another, then the total binding energy should be accounted for when one sums all the relevant individual contributions. Using the alanine mutants of RNase A at positions believed to be directly involved in catalysis and studied for their ability to catalyze transphosphorylation, such a summation adds up to a total reduction in ΔG_{tx} of ~ 25 kcal/mol (Table 2.4). It is interesting to note that the value of $\Delta\Delta G_{tx}$ for K41A RNase A indicates that the primary amine at position 41 provides the greatest contribution of any single feature of RNase A's catalytic machinery. In other words, 25 kcal/mol is slightly larger but surprisingly close to the value derived by comparing the uncatalyzed and catalyzed reaction rates. One possible reason for the excess is the fact that the value of 20.6 kcal/mol derived for transition state binding energy to a polymeric substrate [poly(C)] is actually only a lower limit. Another important consideration is the fact that reductions in

ΔG_{tx} are *apparent* contributions and can be skewed because of the complexity of an enzyme active site; residues have influence on each other's microenvironments and can act synergistically. Therefore consideration of any given mutational change as strictly isolated is not always appropriate.

The other two substrates investigated differ from poly(C) in significant ways. Whether or not these differences alter the mechanisms of the catalyzed or uncatalyzed reactions is unknown. Cyclic (second step) and linear (first step) phosphodiesters have quite comparable uncatalyzed rates of phosphoryl transfer. These rates are significantly faster than for hydrolysis of typical linear phosphodiesters, though for very different reasons. The second-step substrate, a five-membered cyclic phosphodiester, is strained and thus unstable. The resulting instability is nearly equivalent to the instability inherent in first-step substrates arising from the intramolecular positioning of the nucleophile. Up(4-nitrophenol) has a much faster uncatalyzed rate than does UpA, poly(C), or cyclic substrates because of the superior ability of the 4-nitrophenolate to act as a leaving group. The catalysis of the second or hydrolysis step is generally considered to be mechanistically equivalent to the first. This equivalence of mechanism is plausible since a water molecule is only a slightly weaker nucleophile than an alcohol and a primary alkoxide (first step) is only a slightly better leaving groups than a secondary alkoxide (second step). However, this equivalence has never been conclusively proven. The effect of a much more facile leaving group, such as 4-nitrophenolate, on the mechanism is also not known. It is unlikely that the enzyme assists in the proper positioning of the nitrophenol leaving group in the same way it does with nucleotide leaving groups (Thompson & Raines, 1995). The ramifications of this fact are also unclear. In spite of the differences between these three substrates, alterations of Lys41 reduce ΔG_{tx} by about the same proportion of wild-type ΔG_{tx} for all three substrates (Figure 2.5). The reduction amounts to about one third for the K41A enzyme. This

similarity in effect implies a similarity in mechanism for the turnover of all three substrates, at least in regard to the function of Lys41.

The result of modifying the cysteine-containing enzyme variant (K41C RNase A) with bromoethylamine is an enzyme (K41CEA RNase A) quite closely related in structure to wild type protein. Yet, its activity is less than 10% that of the wild-type enzyme. The difference in the two enzymes must lie in the differences between a thioether group and a methylene group. Although the angles of C-S-C bonds tend to be more acute than those of C-CH_2-C bonds, this difference is offset by the greater length of C-S bonds (Planas & Kirsch, 1991; Lide, 1994). Molecular modeling indicates that the primary amine groups in S-ethylaminocysteine (CEA) and lysine can be superimposed to within 0.1 Å. A more significant difference between CEA and lysine is their relative preference for gauche rather than anti torsion angles. The anti conformation of CC-CC bonds is favored by approximately 0.8 kcal/mol in model compounds (Allinger *et al.*, 1989; Gellman, 1991), and the average Lys41 torsion angle in the crystallographically-determined protein structure with uridine vanadate is (175° ± 3°). In contrast to CC-CC bonds, the gauche conformation of CS-CC bonds is favored by 0.05 - 0.20 kcal/mol (Gellman, 1991). Molecular modeling indicates that the CS-CC bond of an CEA residue at position 41 can be in the gauche conformation without disturbing the structure of the native protein. Thus, the thioether side chains at position 41 are likely to be less rigid and extended than the alkyl side chains. We therefore surmise that catalysis by K41CEA is not as efficient as that by wild-type RNase A because of the entropic cost of fixing a thioether in the all anti conformation.

Catalytic efficiency also depends on the length of the side chains of residue 41. RNase A variants that present a primary amine or guanidino group at the end of side chains longer than that of lysine are more active catalysts than is unmodified K41C RNase A. Thus, additional length is tolerated in the active site. Still, enzymes in which an NH group at position 41 is separated from the main chain by 4 atoms are more active than those with 5

intervening atoms. This result could arise from the additional conformational entropy or unfavorable torsion angles required by longer side chains.

Guanidino and acetamidino groups have the potential to bind simultaneously to more than one oxygen of a phosphoryl group. For example, a guanidino group is used to bind phosphoryl groups by the HIV-1 Tat protein (Calnan *et al.*, 1991) and by artificial receptors (Jubian *et al.*, 1992). Further, in Staphlococcal nuclease and ribonucleases of the T1 family, an arginine appears to play the role of Lys41 in RNase A (Saenger, 1991). We have replaced Lys41 with an arginine residue and an S-acetamidino (CAA) residue, which is a short analog of arginine. The $\Delta\Delta G_{tx}$ value for these enzymes is not greater than that for analogous enzymes that contain only a primary amino group in the side chain of position 41. Thus, the enzyme is unable to take advantage of an additional potential hydrogen bond, at least as presented by arginine or CAA. Either there is no value to an additional hydrogen bond over and above those already present [from Lys41, Gln11 and the main chain at Phe120 (Figure 2.2)], or an additional hydrogen bond is sterically excluded in spite of arginine's and CAA's flexibility.

The catalytic role most commonly attributed to Lys41 is in stabilizing the excess negative charge built up on the nonbridging phosphoryl oxygens during transphosphorylation. It has been assumed by many that this stabilization occurs by Coulombic interactions (Fersht, 1985; Eftink & Biltonen, 1987). But it has been proposed that the stabilization occurs by way of a strong, short hydrogen bond involving partial transfer of the proton (Gerlt & Gassman, 1993).

The salient features of a lysine residue are its positive charge and its capacity to hydrogen bond. Three of the 5 cysteine-modified enzymes as well as arginine share both of these features. In general, it is not a simple matter to distinguish the contribution of Coulombic forces from that of a hydrogen bond. What follows is the simplest explanation that is consistent with the data.

Perhaps the most interesting modified enzymes are the S-ethyltrimethyl-aminocysteine enzyme (K41CET RNase A), which possesses a positive charge but no candidate for hydrogen bond donation, and the S-(carbamoylmethyl)cysteine enzyme (K41CAm RNase A), which has an amide N-H for potential hydrogen bond donation but no charge. The low activity for the K41CET argues against the efficacy of simply a charge - charge interaction in transition state stabilization. All else being equal, Coulombic interactions diminish only as the inverse of distance. An increased distance between the positive center and the phosphoryl oxygens, relative to that in K41CEA, is imposed by the three methyl groups. Inspection of structural data suggests that the methyl groups could be accomodated in the vicinity of the phosphoryl oxygens with out imposing any structural perturbations on the protein. In the absence of structural perturbations, this distance is not far enough to fully explain the greater than 10^4-fold reduction in k_{cat}/K_m.

The strength of a hydrogen bond is expected to correlate inversely with the pK_a of the proton being donated, inasmuch as hydrogen bonding involves some extent of proton transfer (Hine, 1975; Jencks, 1987). Increases in pK_a do indeed correspond to increases in $\Delta\Delta G_{tx}$ for modified enzymes having side chains of comparable length [(K41CEA to K41CAA to K41CAm) and (K41CPA to K41R)]. The three $\Delta\Delta G_{tx}$ values for enzymes with side chain lengths comparable to lysine, however, do not follow an expected linear pattern. This lack of linearity could arise because the pK_a of each side chain depends on its particular environment in the native protein. For example, the pK_a of Lys41 has been determined to be near 9 (Brown & Bradbury, 1976; Jentoft *et al.*, 1981), even though the model compound butylammonium has a pK_a of 10.6. Different side chains may be affected to different extents. Another, perhaps more significant, source of non-linearity is that charged species tend to participate in stronger hydrogen bonds than do uncharged species. This phenomenon has been observed for proteins (Fersht *et al.*, 1985) as well as small molecules, including amines (Meot-Ner, 1984). If one compares two highly isosteric

modified enzymes, K41CAA versus K41CAm, positional effects on pK_a should be minimized. The two enzymes differ only slightly structurally, having either a C-NH_2 or a C=O group next to the terminal NH_2. Here, a difference in pK_a (model compounds in aqueous solution (Albert *et al.*, 1948; Bordwell, 1988)) of 2.7 pH units corresponds to 4 kcal/mol. This value is consistent with other data on the relative strengths of charged and uncharged hydrogen bonds in protein - ligand interactions (Thorson *et al.*, 1995).

It is noteworthy that, although K41CAm lacks a formal charge and has a relatively high pK_a, it still appears to contribute, albeit modestly, to catalysis. This result provides further evidence of the importance of a hydrogen bond donated by residue 41. It should also be noted that K41Q has not been included in this discussion of catalysis and pK_a. It is, in fact, a worse catalyst than K41CAm presumably because glutamine has a shorter side chain than does S-(carbamoylmethyl)cysteine and cannot reach into the active site.

Conclusion

Site-directed mutagenesis followed by chemical modification has enabled the study of related enzymes that have more subtle changes in their active sites than would have been possible with site-directed mutagenesis alone. Lys41 apparently contributes about one third of the total transition state binding energy. The correlation of high k_{cat}/K_m values and low pK_a values and the low activity of K41CET support not only the role of Coulombic forces, but also of hydrogen bond donation in catalysis at position 41.

Table 2.1: Steady-State Kinetic Parameters for Catalysis of Poly(C) Cleavage by Ribonuclease A Variants[a].

RNase A	k_{cat} (s^{-1})	K_m (mM)	k_{cat}/K_m ($M^{-1}\times s^{-1}$)	ΔG_{tx} (kcal/mol) [b]	$\Delta\Delta G_{tx}$ (kcal/mol) [c]
wild-type	604 ± 47	0.091 ± 0.022	$(6.5 \pm 1.2) \times 10^6$	-20.6	0.0
K41A [d]	0.031 ± 0.009	0.34 ± 0.11	$(9.1 \pm 3.5) \times 10$	-14.0	6.6
K41C	0.026 ± 0.004	0.36 ± 0.12	$(7.3 \pm 1.5) \times 10$	-13.9	6.8
K41R	4.4 ± 0.3	0.091 ± 0.016	$(4.8 \pm 0.6) \times 10^4$	-17.7	2.9
K41Q	0.023 ± 0.001	0.20 ± 0.03	$(1.2 \pm 0.1) \times 10^2$	-14.2	6.5
K41CEA	43 ± 3	0.075 ± 0.016	$(5.2 \pm 1.5) \times 10^5$	-19.1	1.5
K41CAA	11.0 ± 0.4	0.041 ± 0.006	$(2.6 \pm 0.3) \times 10^5$	-18.7	1.9
K41CPA	12.9 ± 0.4	0.12 ± 0.01	$(1.1 \pm 0.1) \times 10^5$	-18.2	2.4
K41CAm	0.074 ± 0.007	0.25 ± 0.05	$(3.0 \pm 0.3) \times 10^2$	-14.7	5.9
K41CET	nd	nd	$<2.3 \times 10^2$ [e]	< -14.5 [e]	>6.1 [e]

[a] Data were obtained at 25 °C in 0.10 M MES buffer, pH 6.0, containing NaCl (0.10 M).

[b] $\Delta G_{tx} = RT \ln k_{uncat} / (k_{cat}/K_m)$. The value of k_{uncat} for poly(C) cleavage is assumed to be the same as for another linear phosphodiester, UpA. This value was determined to be 5×10^{-9} s^{-1} (Thompson *et al*, 1995).

[c] $\Delta\Delta G_{tx} = RT \ln (k_{cat}/K_m)_{w.t.} / (k_{cat}/K_m)_{variant}$

[d] Average of four independent preparations of enzyme.

[e] Assuming $K_m \geq 0.1$ mM

nd = not determined due to the technical difficulties involved.

Table 2.2: Steady-State Kinetic Parameters for Catalysis of Cytidine 2',3'-Cyclic Phosphate Hydrolysis by Ribonuclease A Variants[a].

RNase A	k_{cat} (s^{-1})	K_m (mM)	k_{cat}/K_m ($M^{-1} \times s^{-1}$)	ΔG_{tx} (kcal/mol) [b]	$\Delta\Delta G_{tx}$ (kcal/mol) [c]
wild-type	2.6 ± 0.5	1.39 ± 0.26	$(1.9 \pm 0.2) \times 10^{3}$	-15.9	0.0
K41A	0.0008 ± 0.0002	2.68 ± 0.68	$(2.8 \pm 0.4) \times 10^{-1}$	-10.7	5.2
K41R	0.034 ± 0.016	1.69 ± 0.16	$(2.0 \pm 0.1) \times 10^{1}$	-13.2	2.7
K41CEA	0.050 ± 0.01	4.14 ± 0.19	$(1.21 \pm 0.03) \times 10^{2}$	-14.3	1.6

[a] Data were obtained at 25 °C in 0.10 M MES buffer, pH 6.0, containing NaCl (0.10 M).

[b] $\Delta G_{tx} = RT \ln k_{uncat} / (k_{cat}/K_m)$. The value of k_{uncat} for C>p hydrolysis taken from Eftink & Biltonen (1983), $4 \times 10^{-9}\ s^{-1}$.

[c] $\Delta\Delta G_{tx} = RT \ln (k_{cat}/K_m)_{w.t.} / (k_{cat}/K_m)_{variant}$

Table 2.3: Steady-State Kinetic Parameters for Catalysis of Uridine 3'-(4-nitrophenylphosphate) Cleavage by Ribonuclease A Variants[a].

RNase A	k_{cat} (s^{-1})	K_m (mM)	k_{cat}/K_m ($M^{-1} \times s^{-1}$)	ΔG_{tx} (kcal/mol) [b]	$\Delta\Delta G_{tx}$ (kcal/mol) [c]
wild-type [d]	18.8 ± 0.6	0.33 ± 0.05	$(5.7 \pm 0.6) \times 10^4$	-13.1	0.0
K41A	nd	nd	$(6.2 \pm 1.0) \times 10^0$	-7.7	5.4
K41R	0.20 ± 0.01	0.21 ± 0.03	$(9.5 \pm 0.9) \times 10^2$	-10.6	2.4
K41CEA	0.86 ± 0.07	0.13 ± 0.03	$(6.2 \pm 0.9) \times 10^3$	-11.8	1.3

[a] Data were obtained at 25 °C in 0.10 M MES buffer, pH 6.0, containing NaCl (0.10 M).

[b] $\Delta G_{tx} = RT \ln k_{uncat} / (k_{cat}/K_m)$. The value of k_{uncat} for uridine 3'-(4-nitrophenylphosphate) cleavage taken from Dantzman & Kiessling (1996), $1.5 \times 10^{-5}\ s^{-1}$.

[c] $\Delta\Delta G_{tx} = RT \ln (k_{cat}/K_m)_{w.t.} / (k_{cat}/K_m)_{variant}$

[d] From Thompson & Raines (1995).

Table 2.4: Summary of Alanine Mutagenesis and Catalysis of Transphosphorylation.

RNase A	Proposed Role	$\Delta\Delta G_{tx}$ * (kcal/mol)	Reference
Q11A	Orientation of substrate	0.3	(delCardayre *et al.*, 1995)
K7A, R10A, K66A	P0 and P2 subsites	3.5	(Fisher *et al.*, 1998)
H12A	General base	5.4	(Thompson & Raines, 1995)
K41A	Selective stabilization of the transition state	6.7	This work
T45A	Pyrimidine specificity B1 subsite	1.6	(delCardayre & Raines, 1994)
N71A	B2 subsite	2.2	(Tarragona-Fiol *et al.*, 1993)
H119A	General acid	5.7	(Thompson & Raines, 1995)
	Total	**25.4**	

* All data pertain to poly(C) cleavage with the exception of that for N71A ribonulease A.

Figure 2.1 Scheme for measuring the enzymatic affinity for the transition state (see Wolfenden, 1976). $K_E^{\ddagger}$ is the equilibrium constant for achieving the enzyme-bound transition state; $K_{UN}^{\ddagger}$ is the equilibrium constant for achieving the unbound transition state without the aid of a catalyst; K_{tx} is the dissociation constant for the transition state and the enzyme. The two transition states are assumed to decay at the same rate, which is a function of temperature and Planck's constant, h, and Boltzmann's contant, k_b.

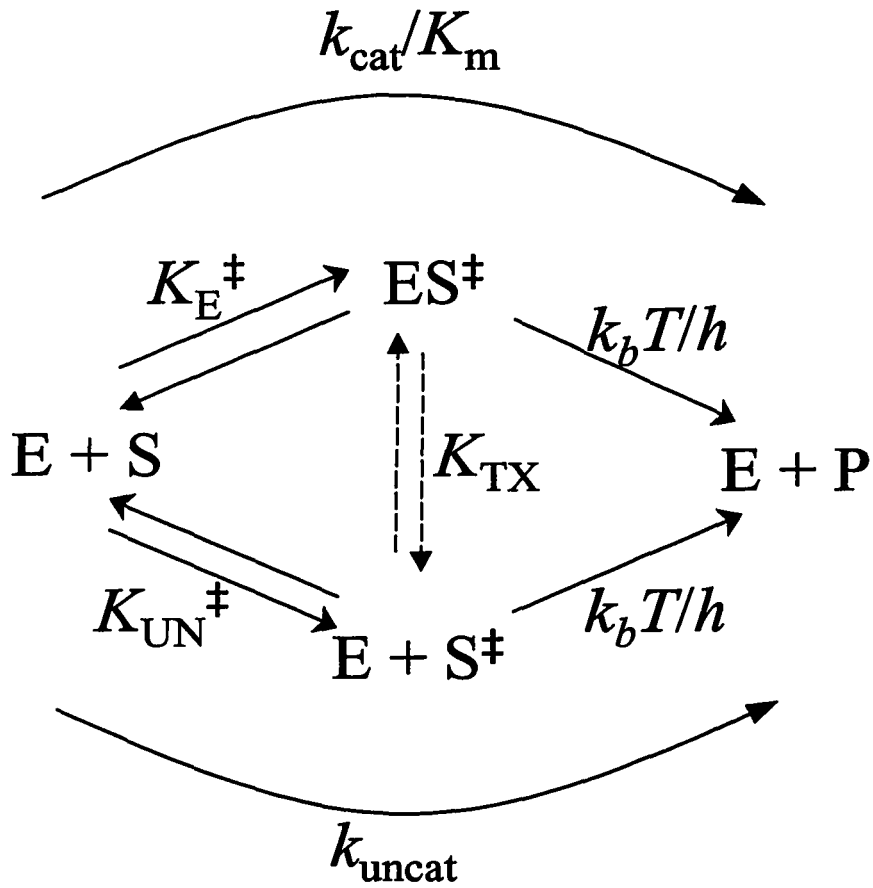

$$k_{uncat} = K_{UN}^{\ddagger}\,(k_bT/h)$$

$$k_{cat}/K_m = K_E^{\ddagger}\,(k_bT/h)$$

$$K_{tx} = K_{UN}^{\ddagger} / K_E^{\ddagger}$$

$$K_{tx} = k_{uncat}\,(k_{cat}/K_m)$$

Figure 2.2 Structure of the active site of ribonuclease A bound to uridine 2',3'-cyclic vanadate monohydrate. The structure was refined at 2.0 Å from x-ray and neutron diffraction data collected from crystals grown at pH 5.3. The side chain of Phe120 and the uracil base are not shown. (coordinates from pdb:6RSA, Wlodawer *et al*, 1983)

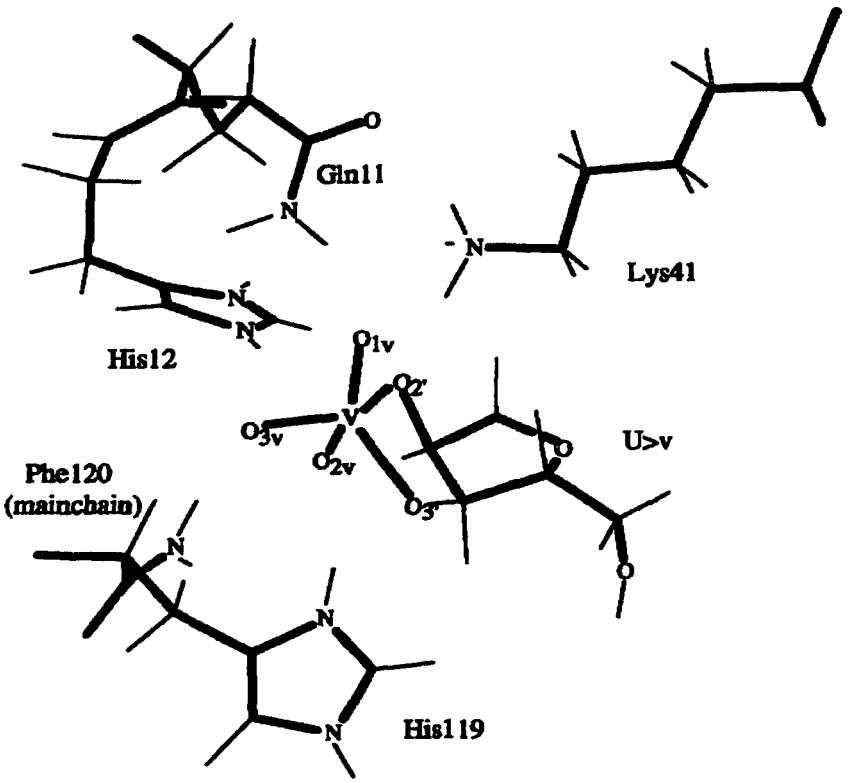
Gln11
Lys41
His12
U>v
Phe120
(mainchain)
His119

Figure 2.3 Scheme for the synthesis of chloroacetamidine•HCl from chloroacetonitrile. Because methoxide in step one is regenerated, it need be present only in catalytic amounts. The methoxide was produced by addition of a small amount of metallic Na.

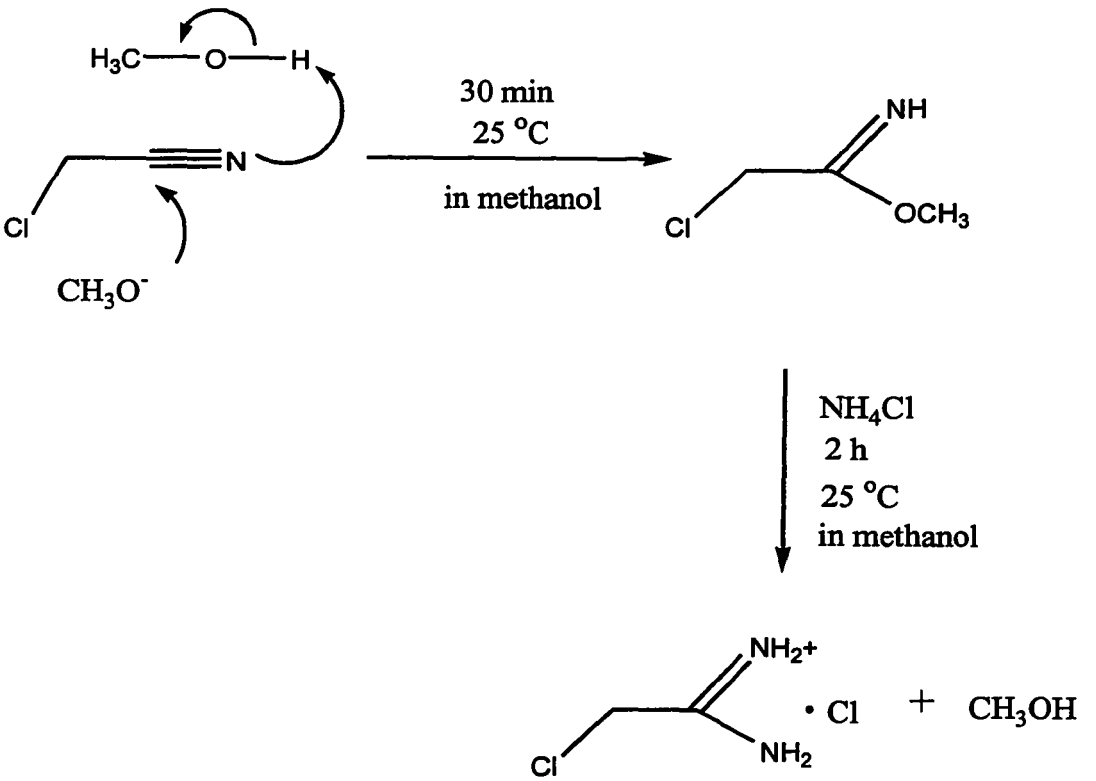
H3C
O
H
N
Cl
CH3O-
30 min
25 °C
in methanol
NH
OCH3
Cl
NH4Cl
2 h
25 °C
in methanol
NH2+
• Cl
+
CH3OH
NH2
Cl

Figure 2.4 Chemical modifications made to the sulfhydryl group of K41C RNase A.

Halo-alkylamine	Side Chain		Protein Abbreviation
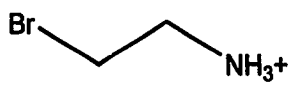	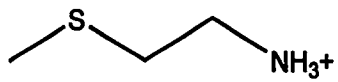	S-(aminoethyl)cysteine	K41CEA
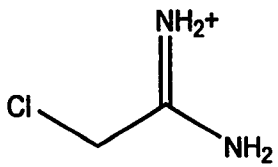	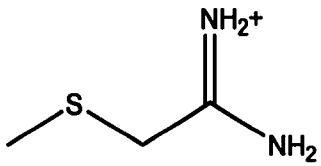	S-acetamidinocysteine	K41CAA
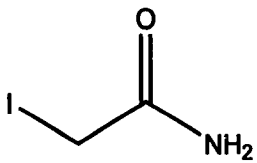	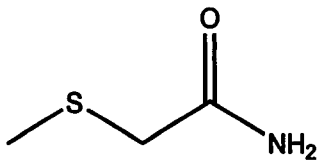	S-(carbamoylmethyl)cysteine	K41CAm
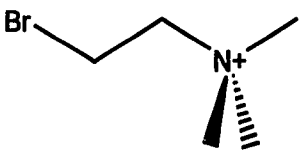	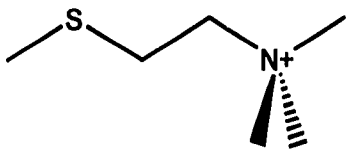	S-((trimethylamino)ethyl)cysteine	K41CET
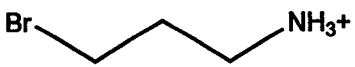	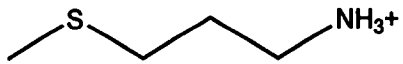	S-(aminopropyl)cysteine	K41CPA

Figure 2.5 Comparison of the effects of alteration at position 41 on the catalysis of transphosphorylation and hydrolysis. All reaction rates were measured at 25 °C in 0.10 M MES buffer, pH 6.0, containing NaCl (0.10 M).

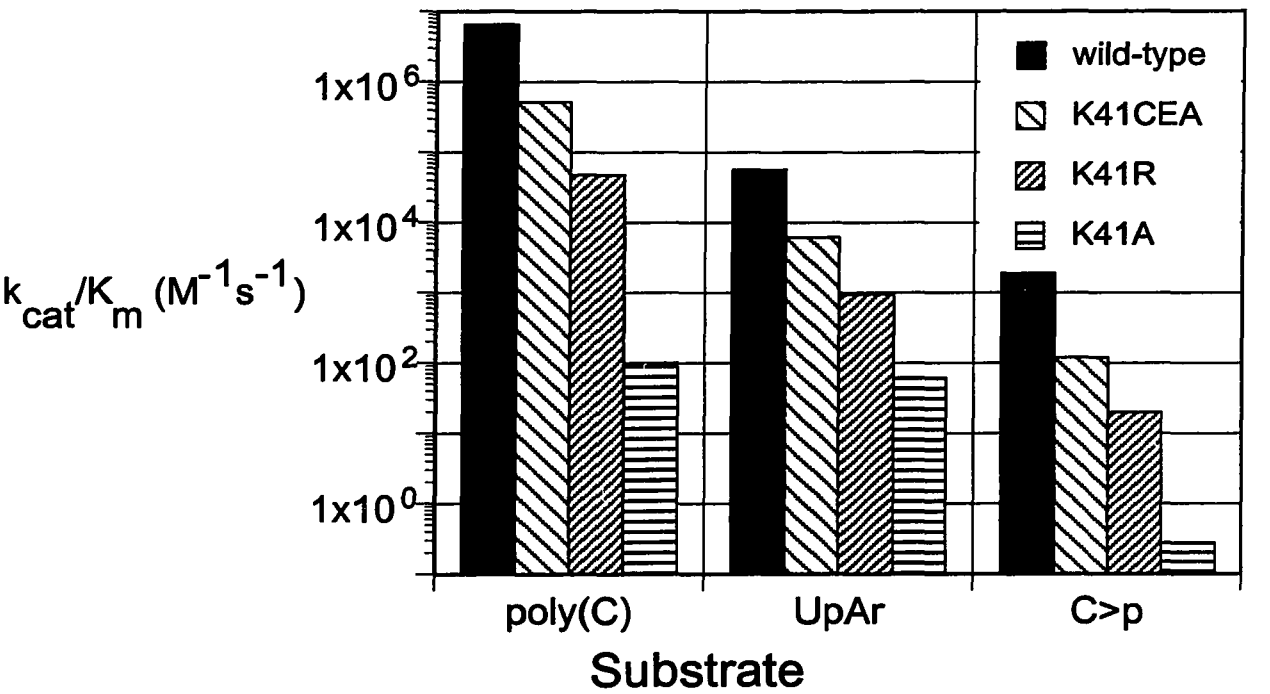
wild-type
K41CEA
K41R
K41A
1x10^6
1x10^4
1x10^2
1x10^0
k_cat/K_m (M^-1s^-1)
poly(C)
UpAr
C>p
Substrate

Chapter 3

Reexamination of Uridine Vanadate as a Transition State Analogue for Ribonuclease A Catalysis

In preparation for submission to *Biochemistry*.

Introduction

Modern enzymological theory posits that an important aspect of understanding the energetic basis of catalysis entails describing how forces acting between an enzyme and its substrate(s) improve as the transition state (TS) is formed (Pauling, 1948; Jencks, 1966; Eftink & Biltonen, 1983). The transition state, the most energetic species along a reaction pathway, is fleeting, having a lifetime of approximately 10^{-12} seconds, and is not amenable to direct study (Lolis & Petsko, 1990). Molecules whose ground state structures mimic the TS for a particular enzymatic reaction can be useful experimentally in probing the means by which the enzyme lowers the activation barrier of chemical transformation. How, then, is a molecule judged to be a mimic or an analogue of a transition state? Additionally, to what degree of scrutiny does the analogy hold true? In short, how high is the quality of the mimicry or analogy? These are important questions to consider when interpreting structural or kinetic studies of molecules believed to be transition state analogues.

A criterion for judging TS analogy is suggested by the equation (from Figure 2.1):

$$K_{tx} = k_{uncat}/(k_{cat}/K_m). \qquad \text{(eq. 3.1)}$$

If a molecule provides an accurate "snap shot" of the transition state, its dissociation constant from the enzyme (K_d) should equal K_{tx} (Wolfenden, 1969). The molecule's competitive inhibition constant, K_i, is a measure of its thermodynamic dissociation constant, and thus the value of K_i should approximate K_{tx}, as well as correlate linearly with $1/(k_{cat}/K_m)$. Combined knowledge of K_i for a particular inhibitor and an estimate of the corresponding value of K_{tx} does not supply a sufficient criterion for judging inhibitor→TS analogy. A tightly bound inhibitor may opportunistically take advantage of interactions that have nothing to do with the enzyme-TS complex. Conversely, subtle imperfections in TS mimicry can increase K_i without substantially altering the fact that the inhibitor resembles

the TS more closely than a ground state. Bartlett and Marlowe have therefore argued that a more appropriate criteria for assessing TS analogy is obedience to the correlation of K_i with K_m/k_{cat} over a range of values (Bartlett & Marlowe, 1983). This type of relationship is illustrated by free energy profiles in Figure 3.1.

Two methods exist for systematically altering the variables K_i and K_m/k_{cat}. One method employs a range of inhibitors that mirror a range of substrates. This method has been applied to proteases, using a phosphonate, a phosphonamidate, or an aldehyde group in the inhibitory peptidyl analogue in place of the scissile amide. The other method involves systematic alteration of the active site. This second method may be somewhat more generally applicable, because it does not require the enzyme to accommodate a variety of substrates (Phillips *et al.*, 1992). It does however require structural knowledge of the active site and the ability to alter that active site systematically by site-directed mutagenesis and/or chemical modifications. Both approaches, altering the substrates and inhibitors in parallel, and altering the enzyme, have been used successfully in a number of enzyme systems to show distinct correlations between substrate K_m/k_{cat} values and the K_i's of their related putative TS mimics (Thompson, 1973; Hanson *et al.*, 1989; Smith *et al.*, 1994).

Vanadate complexes have been proposed as TS analogues for phosphoryl transfer reactions. These proposals reflect the fact that V(V) can form stable pentoxy complexes, some of which adopt the trigonal bipyramidal geometry presumed to occur in phosphoryl displacement reactions. The first evidence of a vanadate complex' capacity for specific inhibition of a phosphoryl transfer enzyme was observed as a synergism in RNase A inhibition. Uridine and vanadate, in combination, inhibit this enzyme more strongly than would be predicted from adding up their individual inhibitory abilities (Lindquist *et al.*, 1973). Vanadate was presumed to combine with uridine and water to form the 1:1:1 complex, uridine 2',3'-cyclic vanadate monohydrate (UVC) (Figure 3.2A), and this complex

was presumed to mimic the TS. The existence in the active site of this predicted complex was verified by structural studies, where the observed geometry was somewhat distorted from the predicted trigonal bipyramid (Figure 3.2B) (Alber *et al.*, 1982; Wlodawer *et al.*, 1983). A recent structural study indicates that the degree of distortion is greater than was appreciated previously (Wladkowski *et al.*, 1998).

The degree to which UVC represents TS analogy is uncertain. The joint x-ray and neutron diffraction structural study and the recent high-resolution study both raise this issue (Wlodawer *et al.*, 1983; Wladkowski *et al.*, 1998). Two active-site residues were determined to be in positions not congruent with their commonly accepted mechanistic roles. This observation calls into question at least one of the following: the details of the crytallographic models, the nature of UVC as a TS mimic, or the commonly-held conception of the catalytic mechanism. Studies have used the structure of UVC bound to RNase A as a starting point for computational investigations (Bruenger *et al.*, 1985; Wladkowski *et al.*, 1995). The relevance of these studies depends in great measure on the relevance of the starting point.

The current work takes the approach of enzyme active-site alteration, using RNase A variants and uridine and vanadate in order to assess the correlation of K_i with K_m/k_{cat}. Changes have been made exclusively at position 41, one of the two residues found in an unexpected position in the RNase A•UVC structure (see Figure 3.3). The results will therefore focus on the interactions between UVC and Lys41, and the degree to which these interactions correspond to the interactions in the TS.

Experimental Procedures

Materials. Wild-type RNase A and the K41A, K41R, and K41C variants were produced and purified as described in Chapter 2. K41C RNase A was modified with

bromoethylamine to yield K41CEA RNase A, and re-purified as described. Up(4-nitrophenol) was obtained as the 2',5'-O-tetrahydropyranyl blocked material and was a generous gift from Drs. James E. Thompson and Tatiana G. Kutateladze. Sodium vanadate was obtained from Aldrich Chemical (Milwaukee, WI). All other chemicals were obtained from Sigma Chemical (St. Louis, MO).

Preparation of uridine/vanadate-containing buffers. Concentrated uridine solutions (1 M) were prepared in 0.010 M sodium succinate buffer, pH 6.0, containing NaCl (0.10 M). The concentration of these stocks was determined spectrophotometrically in H_2O by assuming that $\epsilon = 9.9 \times 10^3\ M^{-1}cm^{-1}$ at 260 nm (Beaven *et al.*, 1955). Sodium vanadate was dried for 1 h at 115 °C and cooled in a dessicator before weighing. It was then dissolved in water to 0.06 M, while heating gently. The pH after dissolution was 9.2 and no visible color was present, indicating the absence of appreciable amounts of decavanadate species (Goddard & Gonas, 1973; & Chapter 4 herein). The uridine and vanadate stock solutions were added to 0.010 M sodium succinate buffer, pH 6.0, containing NaCl (0.10 M). After preparing each solution, the pH was re-adjusted to 6.0 with dilute HCl and the solutions were passed through a 0.22 micron filter. To insure that all species were at equilibrium, buffers were incubated at room temperature overnight, and the pH re-checked prior to use in enzyme assays.

Enzyme assays. The substrate chosen for uridine and vanadate inhibition studies was uridine 3'-(4-nitrophenylphosphate), which undergoes RNase A catalyzed transphosphorylation to release 4-nitrophenol. Even though Up(4-nitrophenol) is a relatively slow substrate, the large change in extinction coefficient associated with this reaction makes for a rather sensitive assay. More importantly, 4-nitrophenol can be monitored at a wavelength well away from uridine's peak absorbance, allowing for use of much greater uridine concentrations.

Blocked Up(4-nitrophenol) was deblocked and handled as detailed in Chapter 2. The initial rate of release of *p*-nitrophenol from Up(4-nitrophenol) was followed at 330 nm and pH 6.0, in the buffers discussed above. Protein concentrations were below 7 μM, and Up(4-nitrophenol) concentrations ranged from 0.03 mM to 1 mM. The uncatalyzed rate is not negligible compared to some of the slower initial velocities measured; a rate constant for non-enzymatic transphosphorylation at pH 6.0 has been reported to be $k = \sim 1.5 \times 10^{-5}\ s^{-1}$ (Dantzman & Kiessling, 1996). In order to account properly for background rates of uncatalyzed substrate cleavage, control measurements were made in the buffered solutions absent any enzyme. These rates were in general agreement with the reported rate constant, and were subtracted from the total observed rate to give the catalyzed rate.

UMP inhibition. Inhibition by uridine 3'-monophosphate (UMP) was measured by determining the initial velocities of enzyme-catalyzed transphosphorylation of Up(4-nitrophenol) at varying levels of UMP and substrate. Reactions were performed in 0.1 M MES-NaOH buffer, pH 6.0, containing 0.1 M NaCl. Enzyme concentrations ranged from 7 nM for wild-type enzyme to 13 μM for the K41A variant. UMP concentrations ranged from 0.06 to 4.3 mM. Assays were otherwise identical to those used for UVC inhibition (see above). Because the initial velocity was only measured for 2% or less of the total reaction, the amounts of UMP generated enzymatically are negligible compared to the added UMP levels, and so were disregarded.

In the case of the K41A variant, the value of K_i determined by inhibition of enzymatic activity was verified by comparison with the value of K_d measured by isothermal titration calorimetry. Similar experiments have been described previously for wild-type RNase A (Wiseman *et al.*, 1989). UMP was injected by a series of microinjections into a solution of enzyme (2.5 μL of 12.8 mM UMP per injection into the ~1.3 mL cell containing 0.36 mM enzyme), until the heat generated upon each individual injection, resulting from

the exothermic nature of protein ligand binding, had approached a constant level. This titration was done in a MicroCal MCS system, using ORIGIN software (MicroCal Software, Northhampton, MA) to fit the data as described by Wiseman *et al* (1989). The value of K_d was thus obtained.

Data analysis. Initial velocity data were grouped into sets by enzyme variant and sodium vanadate concentration. Data sets were collected and analyzed according to these groupings. For each data set, initial velocities were measured not only with uridine plus vanadate, but in the absence of inhibitors, and inhibited by uridine alone or vanadate alone, at the particular concentrations in question. The measured inhibition by vanadate, in the absence of uridine, was probably the result of inhibitory effects of one or several minor, multimeric vanadate species, not $H_2VO_4^-$ itself. No K_i value for vanadate can be derived because the nature of the actual inhibitor moiety and its concentration relative to $[H_2VO_4^-]$ remain unclear (Chapter 4). Consequently, each concentration of vanadate was treated separately, and the derived inhibition parameter was considered simply as a correction factor, applying only to that particular set of conditions, not as a distinct binding constant. Data from a set were fitted by multiple regression analysis to simultaneous equations, sharing the parameters K_m, V_{max}, $K_i$ur, K_{cV}, and [UVC]/K_i. $K_i$ur denotes the competitive inhibition constant for uridine, K_{cV}, the apparent competitive inhibition constant for vanadate. [UVC]/K_i denotes the ratio of the concentration of the uridine-vanadate inhibitor (UVC) to its K_i. Analysis was performed with unweighted data using GraFit Software (Erithicus Software, Palo Alto, CA) and the following equations

$$v_0 = \frac{V_{max} \times [\text{Up(4-nitrophenol)}]}{K_m + [\text{Up(4-nitrophenol)}]} \qquad \text{eq. 3.2}$$

if neither uridine nor vanadate was present,

$$v_0 = \frac{V_{max} \times [\text{Up(4 - nitrophenol)}]}{\left(K_m \times \left(1 + {[\text{uridine}]}/{K_i\text{ur}}\right)\right) + [\text{Up(4 - nitrophenol)}]}$$

eq. 3.3

if uridine was present alone,

$$v_0 = \frac{V_{max} \times [\text{Up(4 - nitrophenol)}]}{\left(K_m \times \left(1 + {[\text{NaVO}_3]}/{K_{cV}}\right)\right) + [\text{Up(4 - nitrophenol)}]}$$

eq. 3.4

if vanadate was present alone,

$$v_0 = \frac{V_{max} \times [\text{Up(4 - nitrophenol)}]}{\left(K_m \times \left(1 + {[\text{NaVO}_3]}/{K_{cV}}\right) \times \left(1 + {[\text{uridine}]}/{K_i\text{ur}}\right) \times \left(1 + {[\text{UVC}]}/{K_i}\right)\right) + [\text{Up(4 - nitrophenol)}]}$$

eq. 3.5

if uridine and vanadate were both present.

When the set of data was collected on only one occasion, reported errors are the standard errors derived from this analysis. If the data set for the particular [uridine], [vanadate], enzyme variant combination was collected several times, using different preparations of the enzyme or buffers, then reported errors are standard deviations of the average [UVC]/K_i value.

Correlation analyses. Relationships between kinetic parameters (expressed as logarithmic values) across the range of enzyme variants were determined using the GraFit program for linear regression. The program determined slope, *r* value, and standard error, employing explicit weighting for the previously determined errors associated with the individual kinetic parameters.

Results

Uridine and vanadate were tested for the ability to synergistically inhibit RNase A and three variants. Practical considerations severely limited the amounts of uridine and vanadate that could be used in order to observe the inhibition due to UVC. Uridine is itself a weak inhibitor ($K_i = 15$ mM under the current assay conditions), and large uridine concentrations overwhelm measurements of inhibition. $H_2VO_4^-$, the dominant monomeric vanadate species at pH 6, has been reported to be non-inhibitory (Leon-Lai *et al.*, 1996). However, our current experience indicates that the inhibition by $H_2VO_4^-$ at concentrations above 0.4 mM is not negligible. Because vanadate species can participate in complex equilibria, we presume that the reports of $H_2VO_4^-$ itself being non-inhibitory are accurate and that inhibition arises from multimeric vanadate species. (These observations will be elaborated upon in Chapter 4.) Data were collected working within these concentration constraints. All of the RNase A variants studied were capable of being inhibited at levels in excess of those that would be expected from uridine plus vanadate, in the absence of any formation of complex. This synergy of inhibition was apparent at both concentrations of vanadate tested (0.1 and 0.4 mM). It was therefore possible in all cases to determine a value of $[UVC]/K_i$, using expressions for competitive inhibition (eq. 3.2 – eq. 3.5). Figure 3.4 shows initial velocity data for the two limiting cases – wild-type RNase A and the K41A variant. The values determined are presented in Table 3.1 and Figure 3.5. Additionally,

synergistic inhibition was observed with 5 mM uridine and 0.1 mM vanadate for wild-type RNase A and the K41CEA variant (data not shown).

The values of K_m/k_{cat}, which will presently be discussed in terms of correlation with [UVC]/K_i values, were determined previously and are available in Chapter 2. In order to compare binding of the product (a ground state) with the binding of UVC, the inhibition constant (K_p) for UMP was measured, for all four enzymes. These values are listed in Table 3.2. For K41A RNase A, this value was also verified by measuring the K_d of the RNase A•UMP complex via isothermal titration calorimetry. The binding of another ground state, namely the substrate, can be reflected in the value of the steady-state parameter, K_m. Because the forward progress on the enzyme of the hydrolysis of C>p is slow compared to C>p's dissociation rate (del Rosario & Hammes, 1970; Eftink & Biltonen, 1983), the K_m of C>p constitutes a case where a K_m can be appropriately treated as a dissociation constant, reporting on ground state binding. Values of K_m for C>p can also be found in the previous chapter.

Discussion

The value of K_i for UVC is somewhat elusive. In order to get from the determined parameter, [UVC]/K_i, to an explicit value for K_i, it would be necessary to know how much UVC is actually present in solution. It would also be crucial to know if other forms of a 1:1 complex exist, and if so, which form or forms can bind to the enzyme. The original characterization of the equilibrium constant for UVC formation, done by means of utraviolet-visible spectroscopy, rested on the faulty assumption that there was a single major species, possessing 1:1 stoichiometry (Lindquist *et al.*, 1973). The authors noted that irregularities in their data suggested the possibility of a minor 2:1 uridine:vanadate species, as well. Subsequent studies have proposed a range of structures, with stoichiometries of 2:1

and 2:2 (Figure 3.6). More recent work, based on ^{51}V, ^{1}H, and ^{13}C NMR spectroscopy, indicates that a 2:2 nucleoside:vanadate dimer predominates in solution under most conditions (Tracey *et al.*, 1990). A 2:2 species is also observed crystallographically (Angus-Dunne *et al.*, 1995). The work of Tracey *et al.* indicates that tetrahedral and pentacoordinate 1:1 complexes occur in solution, but in only minor proportions. The formation constant for the pentacoordinate complex (*i.e.* UVC), has been estimated to be $1.8 \pm 1.5\ M^{-1}$, at pH 7 (Tracey & Leon-Lai, 1991). The value estimated for the cyclic tetrahedral complex (*i.e.* UVC minus H_2O) is $4.5 \pm 1.1\ M^{-1}$. In addition, non-cyclic 1:1 nucleoside:vanadate complexes may occur at very low levels (Tracey *et al.*, 1990). Some uncertainty clearly persists in the quantitative description of minor 1:1 uridine vanadate species in solution. This uncertainty impacts on our ability to state a value of K_i with confidence.

A K_i value of 0.45 μM has been reported for wild type RNase A and UVC at pH 7. This value was calculated based on previously published estimated values of the equilibrium constants for the 1:1 and 2:2 complexes (Leon-Lai *et al.*, 1996). We have measured a value of 6.5 for the ratio $[UVC]/K_i$, for wild-type RNase A, at 15 mM uridine and 0.1 mM vanadate. If we employ the same equilibrium constants, though they were determined under slightly different conditions of pH and buffer strength and may provide an incomplete description of the equilibria involved, we would expect the following concentrations of uridine vanadate complexes, 0.047 mM 2:2 and 2.9 μM 1:1 (see appendix). This calculation gives a K_i value of 0.45 μM for the present work, in close agreement with that published for pH 7. The enzyme was not present at high enough concentrations to shift the equilibrium. At 15 mM uridine and 0.4 mM vanadate, we have determined $[UVC]/K_i$ to be 16.4. Under these conditions, the 2:2 complex would be

expected to be present at 0.19 mM and the 1:1 complex at 5.9 μmolar, leading to an estimate for K_i of 0.36 μM, also in close agreement with the published value.

Even though tight binding alone is not rigorous proof of TS analogy, the comparison of UVC's binding affinity with other related molecules' is noteworthy. 2'-deoxy-2'-fluorouridilyl(3'→5')adenosine (fUpA) is an analogue of UpA, a substrate for the transphosphorylation-step. The reported dissociation constant for the RNaseA•fUpA complex is 0.4 mM (pH 5.5)(Anonov *et al.*, 1978). The K_m for U>p, a substrate for the hydrolysis step, is probably reflective of a dissociation constant (Eftink & Biltonen, 1983). It has been determined to be 2.2 mM at pH 6.0 and 2.1 mM at pH 5.5 (Schultz *et al.*, 1998). Uridine 3'–monophosphate, the product of the hydrolysis step, binds somewhat more tightly than the substrate but still has a K_i of only 72 μM at pH 6.0. Evidently, the calculated affinity of RNase A for UVC at pH 6.0 is greater than for any of these ground state molecules, by more than two orders of magnitude. Although a K_i value of 0.4 μM is many orders of magnitude larger than the value estimated for K_{tx} (~2×10^{-12} M for hydrolysis, see Chapter 2), it is nonetheless the tightest binding constant reported for any related molecule. If we have over-estimated the amount of UVC present, we will have over-estimated K_i. It is possible, given the difficulty of studying minor nucleoside vanadate species, that the true value of K_i is lower than 0.4 μM and thus more reflective of K_{tx}.

Fortunately, we need only relative measurements of binding in order to assess the correlation of K_i with K_m/k_{cat}. The dilemma of poorly-characterized equilibria of multiple complexes can be side-stepped. Because we can measure inhibition for all the enzymes in question under a constant set of conditions, UVC concentration, though unknown, should be constant. If K_m/k_{cat} exhibits a linear correlation with K_i, then it also does so with K_i/[UVC]. Such correlations, which were investigated over a range of K_m/k_{cat} values

spanning 4 or more orders of magnitude, are presented on a logarithmic scale in Figures 3.7 -3.9. The results are similar for the two different sets of vanadate concentrations, and are essentially parallel. The lines are expected to be parallel because [UVC] is altered in a constant manner while individual K_i values do not change. Increases in K_i correspond to increases in K_m/k_{cat} for several substrates, representing both of the reactions that RNase A catalyzes. The coefficients of correlation, r values, are above 0.8. Such high values indicate that UVC most likely interacts with the residue at position 41 in a way that mimics the TS. The probability that a value of r exceeding 0.8 has arisen from random sources, in the absence of true correlation, is 20%, for a sample of four data points (Bevington, 1969).

The slope of the correlation line is meaningful. If K_i were to mirror K_{tx} perfectly, the value of the slope would be unity (Thompson, 1973). In practice, the TS and its imperfect analogue can show differential levels of sensitivity to ligand or active-site changes. Peptide aldehydes as analogues for the serine protease elastase are reported to exhibit a slope of 0.74 (Thompson, 1973). Peptide analogues containing a phosphonate linkage, when compared with substrates for the zinc protease thermolysin, exhibit a slope of 1.05 (Bartlett & Marlowe, 1983). A peptide analogue with a phosphonamidate linkage yielded a slope of 1.03 when alterations were made at a catalytic arginine in carboxypeptidase A (Phillips *et al.*, 1992). The linear correlations of UVC inhibition and catalytic changes, resulting from alterations made to RNase A at position 41, show slopes that are much shallower, in the range of 0.25 to 0.36.

Examining the differences between correlations using different substrates serves to ask whether UVC mimics the TS of hydrolysis better than the TS of transphosphorylation, and thus indirectly probes the similarity of the transition states for these two reactions. A cyclic substrate would appear to be the species that UVC resembles most closely, because both molecules lack the ability to access the 5' nucleotide binding subsites. But this

resemblance only applies to ground state features and is irrelevant to electronic or spacial similarities specific to the TS. Because Lys41 appears to make a greater absolute contribution to K_{tx} for better substrates, the slope of the correlation line is less when plotted against K_m/k_{cat} values for the more facile transphosphorylation step. This difference is small and well within error and does not indicate gross differences in the quality of analogy of UVC to one or the other TS. The choice of substrate does not alter the central observation that UVC is only a marginal to fair TS mimic.

The transphosphorylation of poly(C) by wild-type RNase A appears to be limited by a step other than the chemical transformation (Thompson *et al.*, 1995). Therefore, K_m/k_{cat} might not be fully reflective of K_{tx} for the chemical transition state. Rather, the actual value of log K_{tx} could be lower than log K_m/k_{cat}. The slope of the true correlation between K_i and K_{tx} may be even shallower than the slope, shown in Figure 3.7, of the correlation between log K_i/[UVC] and log K_m/k_{cat}.

The substrate and the product can also be considered weak mimics of the TS, as they are inevitably related. By extension, a mimic of the substrate or product is in some sense also a mimic of the TS. The relationship between substrate and TS is especially important if the enzyme uses uniform binding to stabilize both the Michaelis complex and the TS. One must ask the question "does the analogue mimic the TS simply by trivial mimicry of the substrate or product?" A logarithmic plot of K_m and K_p values vs. [UVC]/K_i demonstrates little correlation (Figure 3.10). The binding of UVC, like that of the TS, is much more sensitive to changes at position 41 than is K_m or K_p, as would be expected if UVC were a reasonable analogue. The correlation of K_p with K_m/k_{cat} serves as a threshold. Shallower correlations disqualify an inhibitor from being considered to be TS-like. The slope of the plot of K_p for uridine 3'–phosphate and K_m/k_{cat} (Figure 3.11) is smaller than that seen for UVC indicating that UVC bears more resemblance to the TS than does the product.

Conclusion

The contribution of Lys41 to transition state binding is mimicked to a limited extent by the interaction between this residue and UVC. The mimicry or analogy is judged to be mediocre, and far off the level of analogy exhibited by some good TS analogues in other enzymes. This mediocrity is evidenced by the shallow slope of the correlation lines (Figures 3.7 through 3.9) and can also be expressed as a free energy profile (Figure 3.12). The deficit in the sensitivity of K_i values to changes in k_{cat}/K_m may indicate that the charge on one or more of UVC's vanadyl oxygen atoms differs significantly from the charge on the corresponding phosphoryl oxygen atom in the enzyme-bound transition state. The impact of UVC structural and binding data on the mechanistic understanding of RNase A must be viewed accordingly. V-O bonds in vanadates can exhibit a rather wide spectrum of strengths and polarities (Krauss & Basch, 1992; Ray *et al.*, 1995). Likewise, P-O bonds in the transition states of phosphoryl transfer reactions can exhibit a variety of alterations in bond order (Cleland & Hengge, 1995). That the interactions of a given enzymatic residue with any particular vanadate should fail to mimic faithfully a catalytically important interaction is therefore perhaps not so surprising. The current observations argue for a measure of skepticism against detailed and/or quantitative conclusions regarding a residue's role in transition state binding based solely on vanadate data.

Appendix: Concentrations of Uridine Vanadate Species

(After Leon-Lai et al., 1996)

$Vi + U \overset{K_1}{\leftrightarrows} UVC$ $\quad [Vi][U]K_1 = [UVC]$ $\quad K_1 = 3.0\ M^{-1}$

$2\ Vi + 2\ U \overset{K_2}{\leftrightarrows} U_2V_2$ $\quad [Vi]^2\ [U]^2K_2 = [U_2V_2]$ $\quad K_2 = 5 \times 10^7\ M^{-3}$

$[V_{tot}] = [Vi] + [UVC] + 2[U_2V_2] + [E^{\cdot}UVC]$ levels of any other possible species assumed negligible

assume $[E^{\cdot}UVC] << [Vi]$,
$[U] = [U_{tot}]$

$$[V_{tot}] = [Vi] + 2[U_2V_2] + [UVC] = K_3[U][Vi] + 2K_2[U]^2[Vi]^2 + [Vi]$$

where Vi is free monomeric vanadate, U is uridine, UVC is the inhibitory 1:1 uridine vanadate complex, and U_2V_2 is the 2:2 uridine vanadate complex. $[V_{tot}]$ is the total concentration of added sodium vanadate, and $[U_{tot}]$ is the total concentration of added uridine.

If $[V_{tot}] = 1.0 \times 10^{-4}$ M and $U = 1.5 \times 10^{-2}$ M, then $[Vi] = 4.7 \times 10^{-5}$ M, $[UVC] = 2.1 \times 10^{-6}$ M, $[U_2V_2] = 2.5 \times 10^{-5}$ M.	If $[V_{tot}] = 4.0 \times 10^{-4}$ M and $U = 1.5 \times 10^{-2}$ M, then $[Vi] = 1.1 \times 10^{-4}$ M, $[UVC] = 5.1 \times 10^{-6}$ M, $[U_2V_2] = 1.4 \times 10^{-4}$ M.

Table 3.1: Ratio of the Concentration of Uridine Vanadate Complex to K_i Value[a]

RNase A	[Uridine] (mM)	[$NaVO_3$] (mM)	[UVC]/K_i	Independent Data Sets
wild-type	15	0.1	6.5 ± 1.6	3
wild-type	15	0.4	16.4 ± 3.0	3
K41CEA	15	0.1	0.9 ± 0.1	2
K41CEA	15	0.4	2.7 ± 0.3	1
K41R	15	0.1	0.57 ± 0.22	2
K41R	15	0.4	2.8 ± 0.3	1
K41A	15	0.1	0.37 ± 0.11	1
K41A	15	0.4	0.43 ± 0.28	2

[a] Data were obtained at 25 °C in 0.010 M sodium succinate buffer, pH 6.0, containing NaCl (0.10 M). Inhibition was measured against the substrate Up(4-nitrophenol).

Table 3.2: Inhibition Constants for Uridine 3'-Monophosphate[a]

RNase A	K_i (μM)
wild-type	72 ± 12
K41CEA	57 ± 5
K41R	46 ± 3
K41A	260 ± 120 [b]

[a] Data were obtained at 25 °C in 0.10 M MES buffer, pH 6.0, containing NaCl (0.10 M), versus Up(4-nitrophenol) substrate.

[b] The K_d for the UMP•RNase A complex measured by isothermal titration calorimetry in the above buffer was 410 ± 70 μM.

Figure 3.1 Representation of catalysis and related inhibition by a moiety that is a faithful mimic of the transition state. The left profile depicts reactions which are catalyzed and uncatalyzed. $\Delta G_{uncat} = -RT \ln (k_{uncat}h/k_bT)$ and $\Delta G_{tx} = -RT \ln(k_{cat}/K_m)/k_{uncat}$. The right profile depicts binding of analogous inhibitory species where $\Delta G_{assoc} = -RT \ln (1/K_i)$. Note that changes in ΔG_{tx} are mirrored in changes in ΔG_{assoc}.

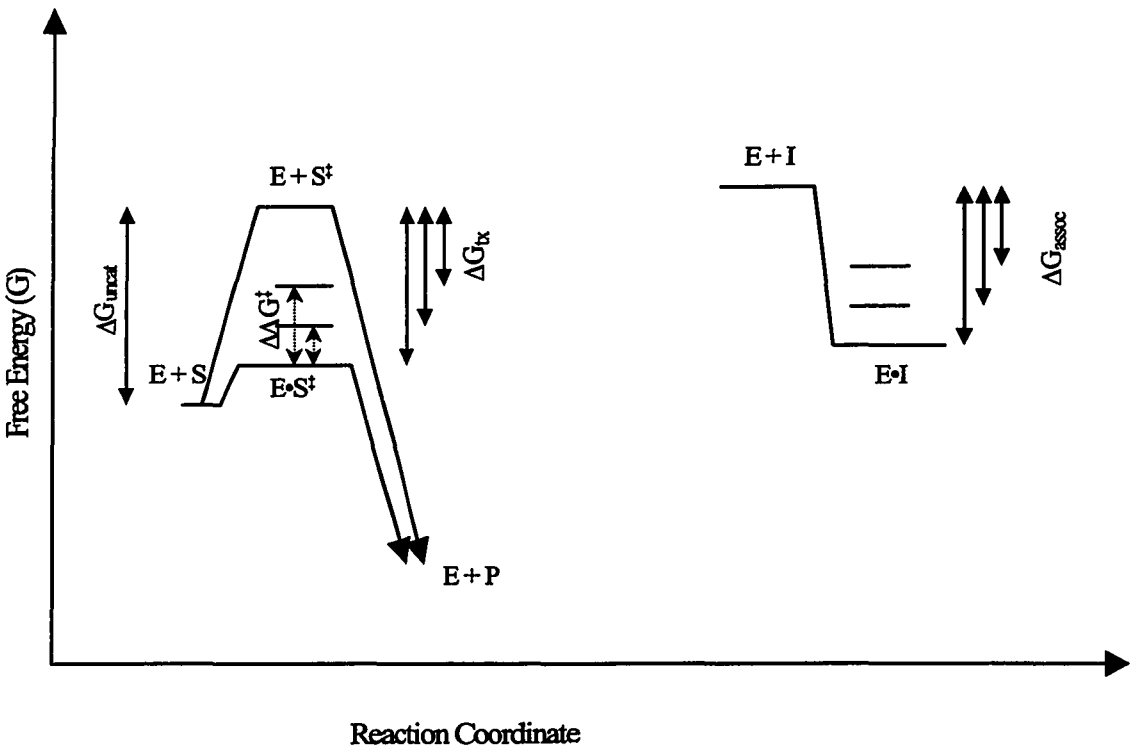
Free Energy (G)
E+S‡
E+S
E•S‡
E+P
E+I
E•I
ΔGuncat
ΔΔG‡
ΔGtx
ΔGassoc
Reaction Coordinate

Figure 3.2 (A) Structure of the vanadyl portion of the uridine vanadate monohydrate complex, as proposed by Lindquist *et al.* (1973).

(B) Structure of same, observed in the active site of ribonuclease A, by x-ray crystallographic analysis. (Wlodawer, 1983). The angle denoted by arrow is 166°, compared to the 180° expected for a perfect trigonal bipyramid.

A)

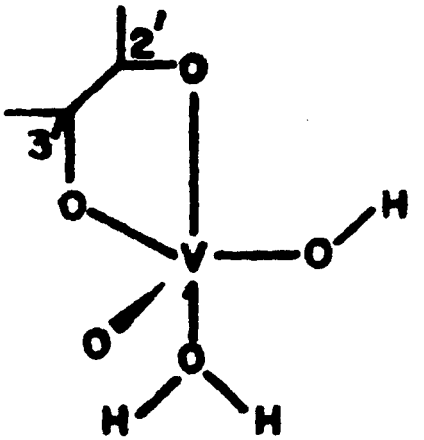

B)

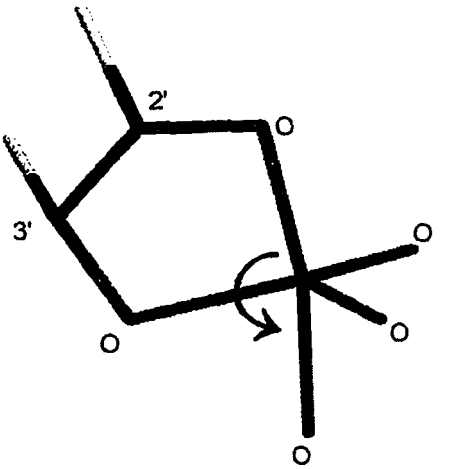

Figure 3.3 Stereoview of the structure of the active site of ribonuclease A bound to UVC. The structure was refined to 2.0 Å from X-ray and neutron diffraction data collected from crystals grown at pH 5.3 (pdb:6rsa; Wlodawer *et al*, 1983). The distance from Lys41 (top) to the 2' oxygen (yellow; ---) is 2.8 Å. The distance from Lys41 to the nearest nonbridging oxygen is 3.5 Å. The distance from His12 (right) to the nearest oxygen (yellow; ---) is 2.7 Å, while the distance to the 2' oxygen is 3.0 Å. The histidine at the lower left is His119.

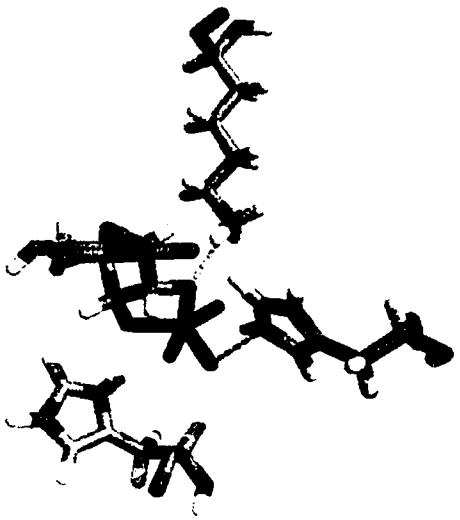

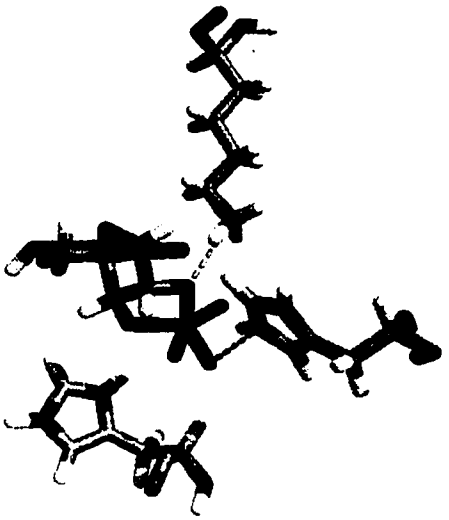

Figure 3.4 Initial velocity data for inhibition of (A) wild-type and (B) K41A ribonuclease A by the UVC. Curves were fit to eq. 3.2 - 3.5. A theoretical curve has also been included (calculated via eq. 3.5, with [UVC/K_i] set to zero), to illustrate the behavior that would be observed in the absence of synergism, *i.e.*, in the absence of UVC formation and binding.

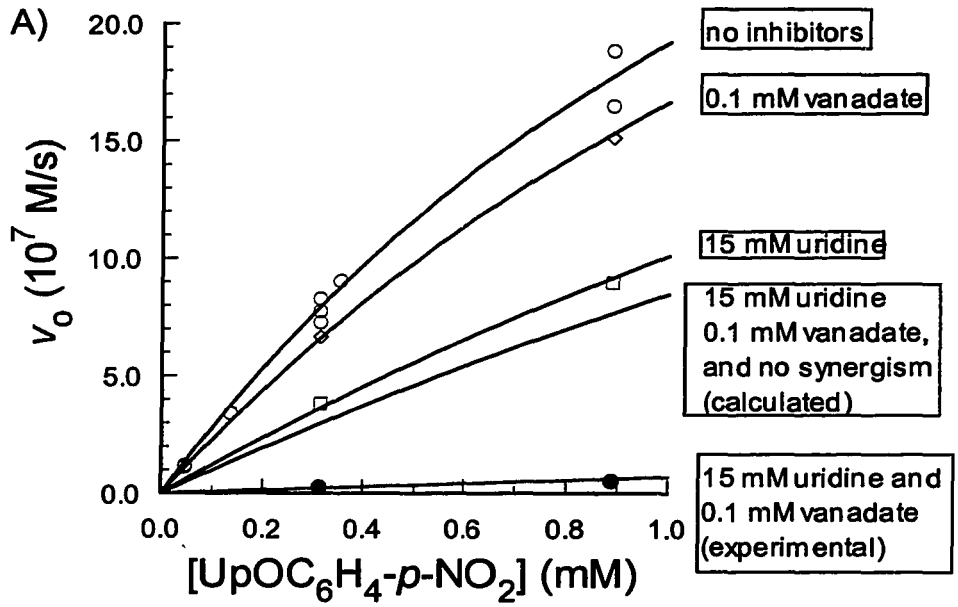
A)
20.0
15.0
10.0
5.0
0.0
v_o (10^7 M/s)
0.0
0.2
0.4
0.6
0.8
1.0
[UpOC$_6$H$_4$-*p*-NO$_2$] (mM)
no inhibitors
0.1 mM vanadate
15 mM uridine
15 mM uridine
0.1 mM vanadate,
and no synergism
(calculated)
15 mM uridine and
0.1 mM vanadate
(experimental)

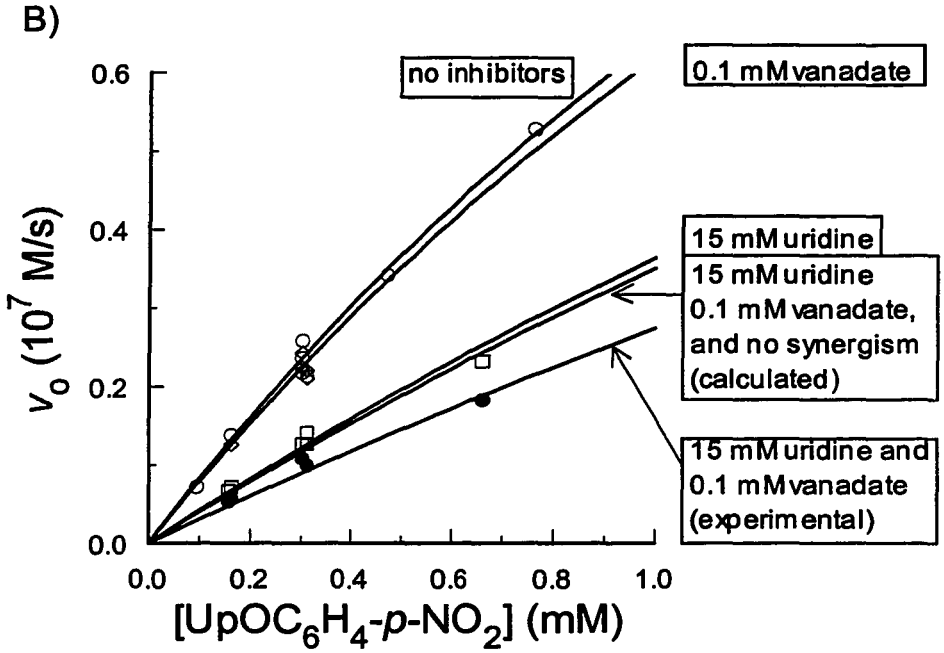
B)
0.6
0.4
0.2
0.0
v_o (10^7 M/s)
0.0
0.2
0.4
0.6
0.8
1.0
[UpOC$_6$H$_4$-*p*-NO$_2$] (mM)
no inhibitors
0.1 mM vanadate
15 mM uridine
15 mM uridine
0.1 mM vanadate,
and no synergism
(calculated)
15 mM uridine and
0.1 mM vanadate
(experimental)

Figure 3.5 Values of K_i/[UVC] for inhibition of Up(4-nitrophenol) cleavage by wild-type ribonuclease A and the K41CEA, K41R, and K41A variants. Data are presented on a logarithmic scale. The values shown are the $\log_{10}$ of the inverse of the values given in Table 3.1. Ribonuclease A variants are arranged from highest to lowest catalytic efficiency.

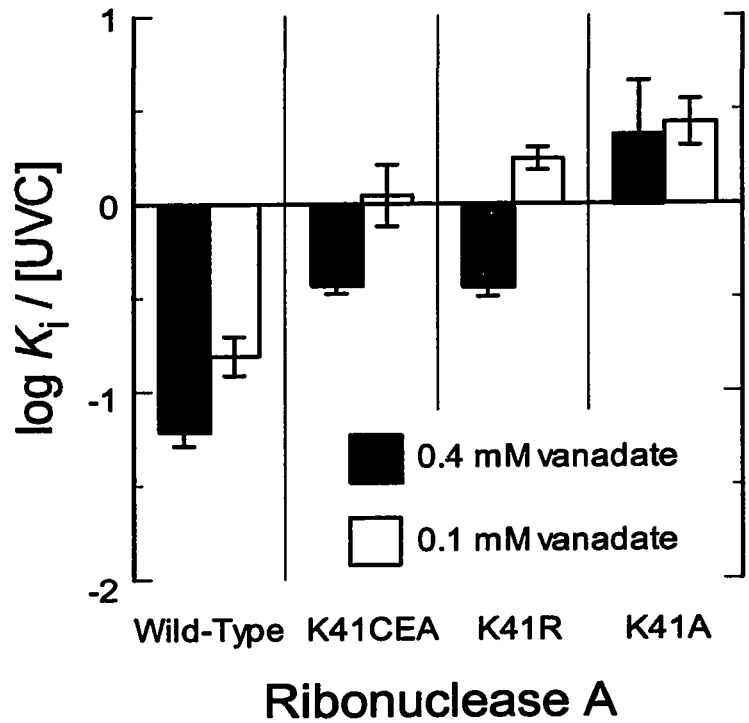
1
0
-1
-2
log K_i / [UVC]
0.4 mM vanadate
0.1 mM vanadate
Wild-Type
K41CEA
K41R
K41A
Ribonuclease A

Figure 3.6 Proposed structures for diol•V(V) complexes, such as uridine vanadate. (A) and (B) 2:1 complexes proposed by Geraldes and Castro (1989). (C) 2:2 complex with 1 bridging oxygen (Gresser & Tracey, 1986). (D) 2:2 complex with 1 bridging oxygen and 2 bridging diol species (Gresser & Tracey, 1986). (E) 2:2 complex with 3 bridging oxygens (Tracey & Leon-Lai, 1991) (F) Alternative 2:2 complex with 3 bridging oxygens (Richter & Rehder, 1991). This structure differs from that in (E) in that the alcohol oxygens participate in coordination to two vanadates. (G) 2:2 complex where V is octahedral (Harnung *et al.*, 1993). (H) 2:2 complex with 2 bridging oxygens. Note that the V atoms in this structure are significantly distorted from trigonal bipyramidal. According to the authors, this structure supercedes those in (C), (D) and (E) (Angus-Dunne *et al.*, 1995).

A)

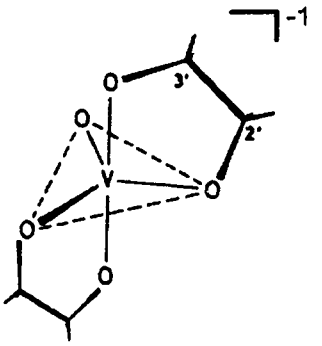

B)

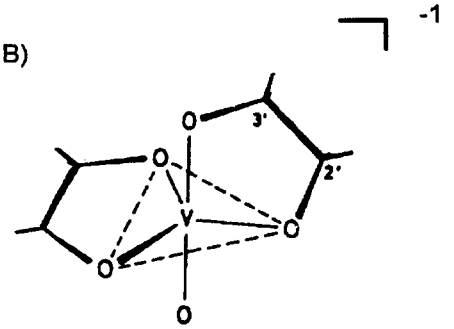

C)

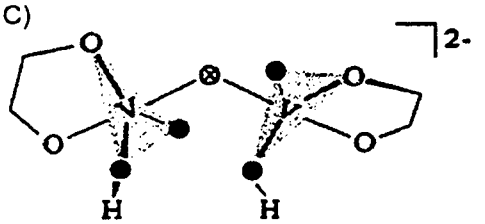

D)

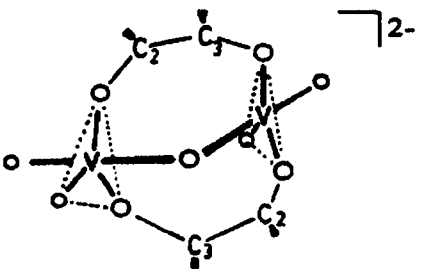

E)

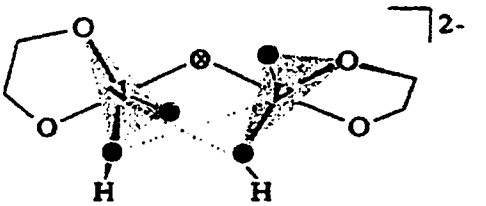

F)

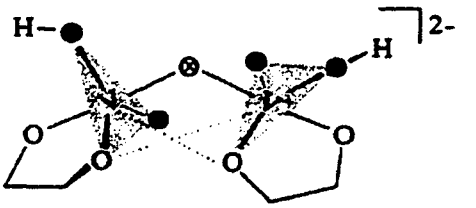

G)

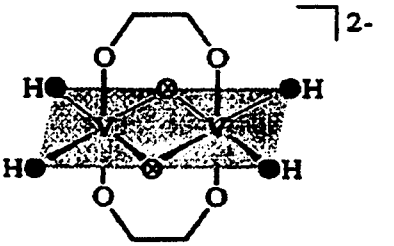

H)

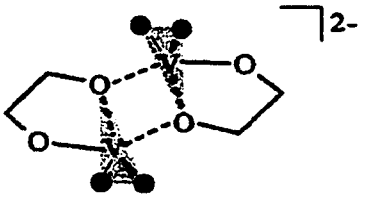

Figure 3.7 UVC inhibition versus Poly(C) cleavage. Plot of log (K_i/[UVC]) versus log (K_m/k_{cat}) for the cleavage of poly(cytidylic acid) by ribonuclease A and variants. Values of K_m/k_{cat} were obtained from initial velocity data measured at 25 °C in 0.10 M MES-NaOH buffer pH 6.0, containing NaCl (0.10 M). Values of K_i/[UVC] (Table 3.1) were from data collected at 25 °C in 0.010 M sodium succinate buffer, pH 6.0, containing 0.10 M Na Cl, with Up(4-nitrophenol) as substrate. Open circles (○) denote 0.1 mM $NaVO_3$ and 15 mM uridine. Closed circles (●) denote 0.4 mM $NaVO_3$ and 15 mM uridine. The upper line was derived by linear regression of the 0.1 mM $NaVO_3$ data, while the lower line was derived from the 0.4 mM $NaVO_3$ data.

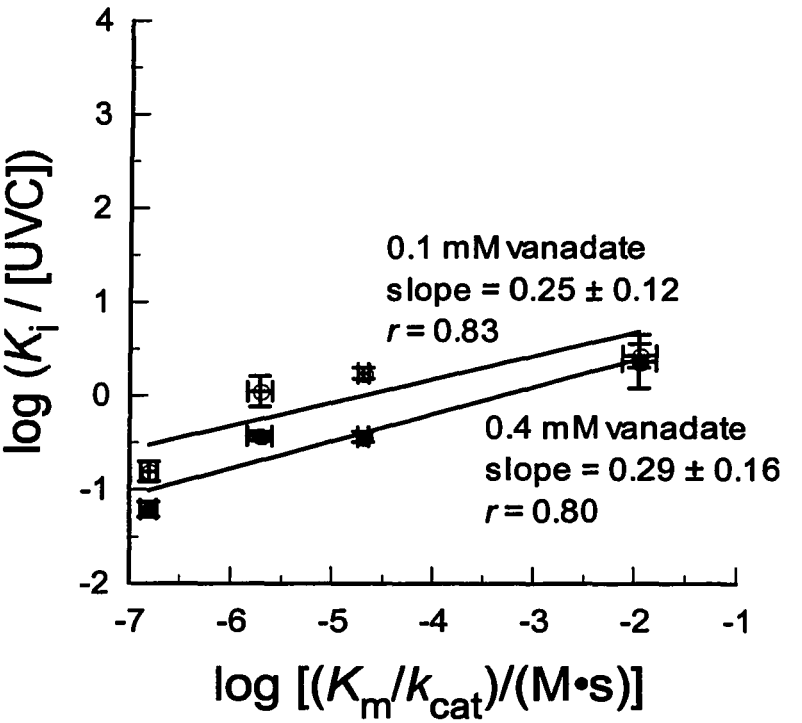
4
3
2
1
0
-1
-2
log (K_i / [UVC])
0.1 mM vanadate
slope = 0.25 ± 0.12
r = 0.83
0.4 mM vanadate
slope = 0.29 ± 0.16
r = 0.80
-7
-6
-5
-4
-3
-2
-1
log [(K_m/k_{cat})/(M•s)]

Figure 3.8 Plot of log (K_i/[UVC]) versus log (K_m/k_{cat}) for the cleavage of Up(4-nitrophenol) by ribonuclease A and variants. Values of (K_m/k_{cat}) were obtained from initial velocity data measured at 25 °C in 0.10 M MES-NaOH buffer pH 6.0, containing NaCl (0.10 M). Values of (K_i/[UVC]) (Table 3.1) were from data collected at 25 °C in 0.010 M sodium succinate buffer, pH 6.0, containing 0.10 M NaCl, with Up(4-nitrophenol) as substrate. Open circles (○) denote 0.1 mM $NaVO_3$ and 15 mM uridine. Closed circles (●) denote 0.4 mM $NaVO_3$ and 15 mM uridine. The upper line was derived by linear regression of the 0.1 mM $NaVO_3$ data, while the lower line was derived from the 0.4 mM $NaVO_3$ data.

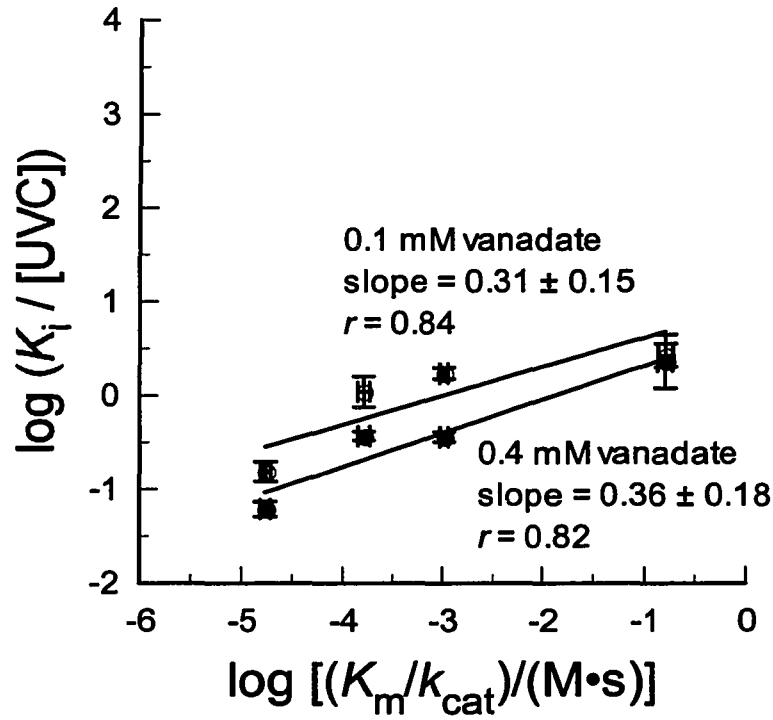
0.1 mM vanadate
slope = 0.31 ± 0.15
r = 0.84
0.4 mM vanadate
slope = 0.36 ± 0.18
r = 0.82
log (Ki / [UVC])
log [(Km/kcat)/(M•s)]
4
3
2
1
0
-1
-2
-6
-5
-4
-3
-2
-1
0

Figure 3.9 UVC inhibition versus C>p hydrolysis. Plot of log (K_i/[UVC]) versus log (K_m/k_{cat}) for the hydrolysis of cytidine 2',3'-cyclic phosphate by ribonuclease A and variants. Values of K_m/k_{cat} were obtained from initial velocity data measured at 25 °C in 0.10 M MES-NaOH buffer, pH 6.0, containing NaCl (0.10 M). Values of K_i/[UVC] (Table 3.1) were from data collected at 25 °C in 0.010 M sodium succinate buffer, pH 6.0, containing 0.10 M NaCl, with Up(4-nitrophenol) as substrate. Open circles (○) denote 0.1 mM $NaVO_3$ and 15 mM uridine. Closed circles (●) denote 0.4 mM $NaVO_3$ and 15 mM uridine. The upper line was derived by linear regression of the 0.1 mM $NaVO_3$ data, while the lower line was derived from the 0.4 mM $NaVO_3$ data.

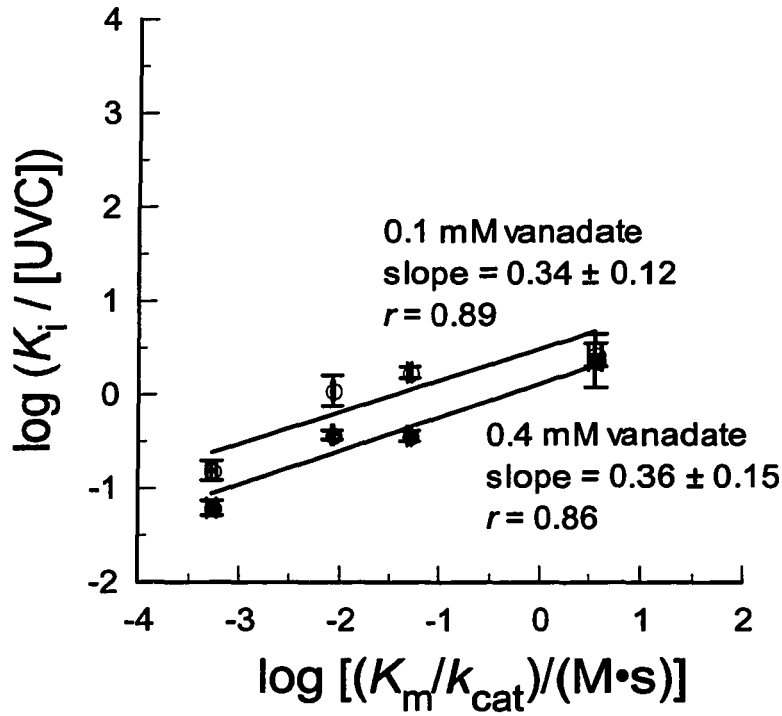
0.1 mM vanadate
slope = 0.34 ± 0.12
r = 0.89
0.4 mM vanadate
slope = 0.36 ± 0.15
r = 0.86
log (Ki / [UVC])
log [(Km/kcat)/(M•s)]
4
3
2
1
0
-1
-2
-4
-3
-2
-1
0
1
2

Figure 3.10 UVC inhibition versus ground state binding. K_m and K_p show an absence of correlation with UVC binding. These data are listed in Tables 3.1 and 3.2. Values of K_i/[UVC] (Table 3.1) are from data collected at 25 °C in 0.010 M sodium succinate buffer, pH 6.0, containing NaCl (0.10 M), with Up(4-nitrophenol) as substrate. Values of K_m for C>p (closed circles (●), x-axis value) were obtained from initial velocity data at 25 °C in 0.025 M MES-NaOH buffer pH 6.0, containing NaCl (0.10 M). Values of K_p for UMP (open circles (○), x-axis value) were obtained from initial velocity data measured at 25 °C in 0.10 M MES-NaOH buffer, pH 6.0, containing NaCl (0.10 M) with Up(4-nitrophenol) as substrate and added UMP as competitive inhibitor. The value of the dissociation constant for UMP and ribonuclease A from calorimetry is also included for comparison.

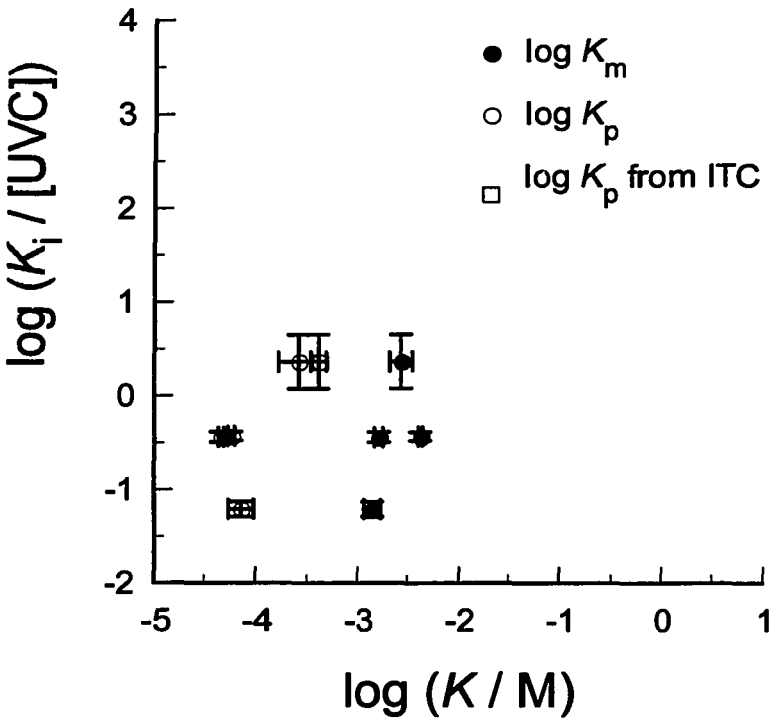
log K_m
log K_p
log K_p from ITC
log (K_i / [UVC])
log (K / M)
4
3
2
1
0
-1
-2
-5
-4
-3
-2
-1
0
1

Figure 3.11 UMP inhibition versus C>p hydrolysis. The weak correlation shows that UMP is not an "analogue" of the transition state. Values of K_m/k_{cat} for C>p hydrolysis were obtained from initial velocity data measured at 25 °C in 0.025 M MES-NaOH buffer pH 6.0, containing NaCl (0.10 M). Values of K_i/[UVC] (Table 3.1) were obtained at 25 °C in 0.010 M sodium succinate buffer, pH 6.0, containing NaCl (0.10 M) with Up(4-nitrophenol) as substrate.

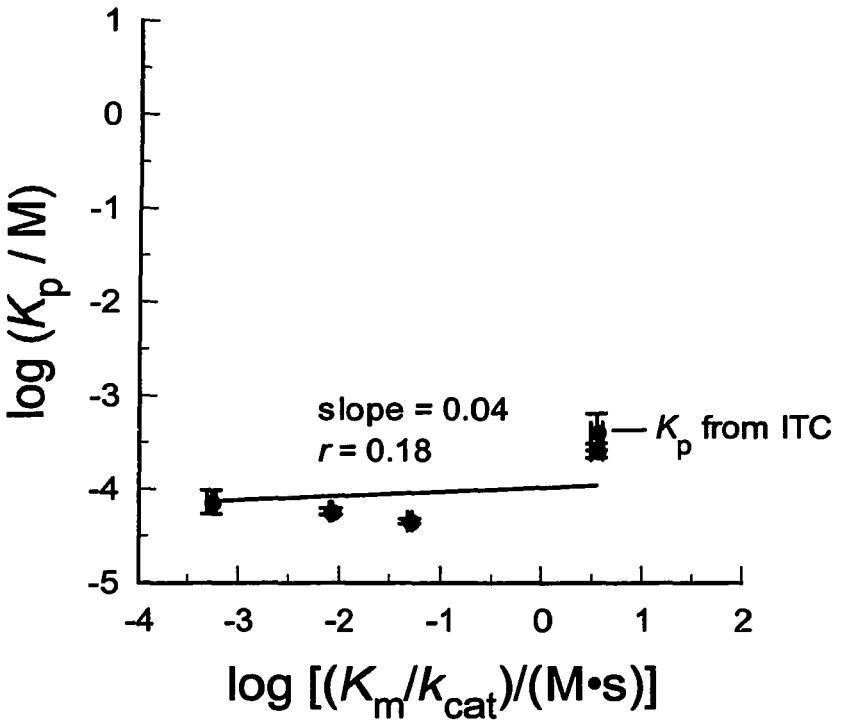
1
0
-1
-2
-3
-4
-5
log (K_p / M)
slope = 0.04
r = 0.18
K_p from ITC
-4
-3
-2
-1
0
1
2
log [(K_m/k_{cat})/(M•s)]

Figure 3.12 Representation of catalysis by ribonuclease A and related inhibition by UVC, drawn to scale. The left profile depicts the energy barrier for the uncatalyzed hydrolysis of C>p and the energy barriers for hydrolysis of C>p catalyzed by wild-type ribonuclease A and several variants. $\Delta G_{uncat} = -RT \ln (k_{uncat}h/k_bT)$. $\Delta G_{tx} = -RT \ln(k_{cat}/K_m)/k_{uncat}$. The right profile depicts the energetic consequences of these same variants binding to the complex formed by uridine and vanadate. $\Delta G_{assoc} = -RT \ln (1/K_i)$. For wild-type ribonuclease A, the value assumed for K_i is that given by Leon-Lai (1996). For the other protein variants, K_i has been adjusted by the relative ratios of K_i/[UVC] determined herein. Each dotted line represents one RNase A variant. If UVC were a perfect mimic of S‡ ,then the four dotted lines would be parallel.

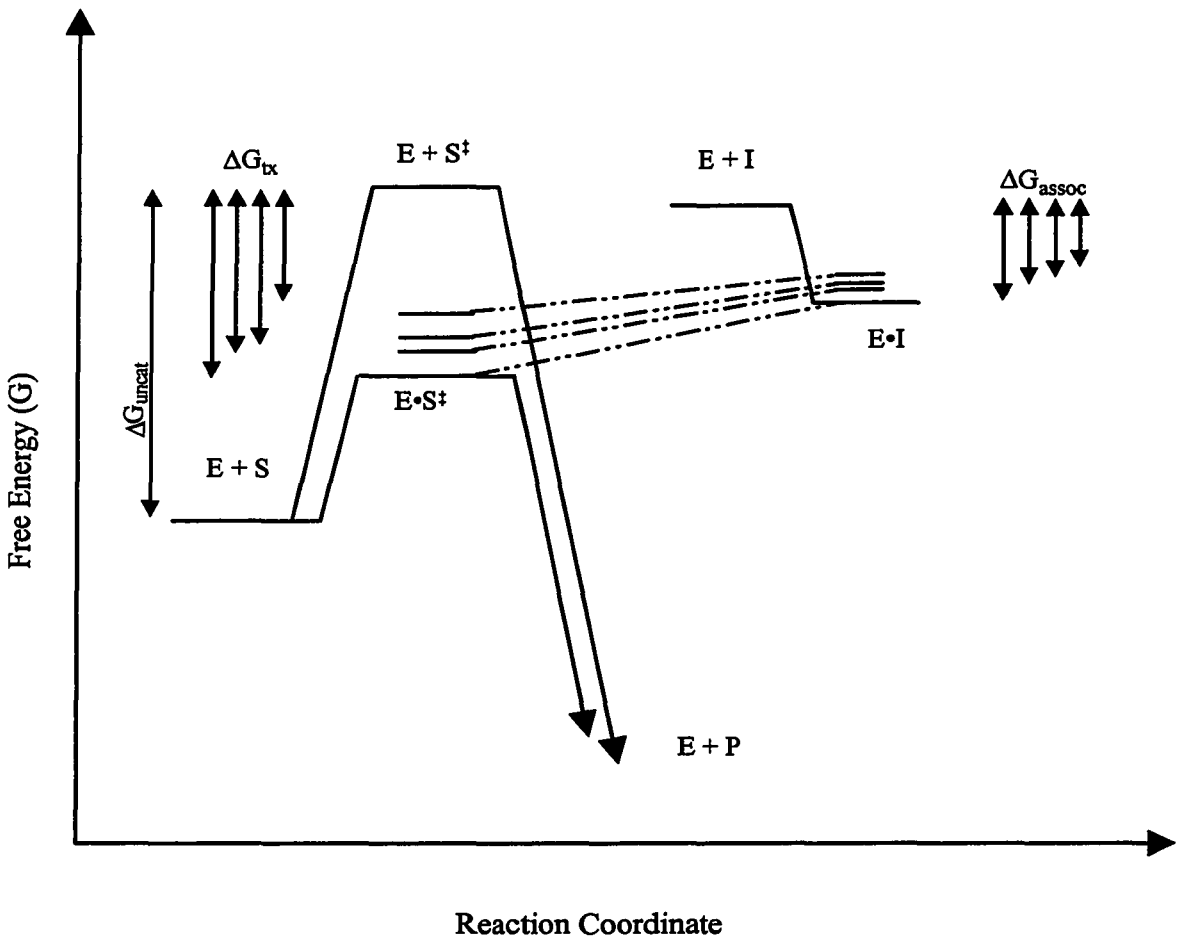
ΔG_tx
E + S‡
E + I
ΔG_assoc
ΔG_uncat
E•I
E•S‡
E + S
E + P
Free Energy (G)
Reaction Coordinate

Chapter 4

Inhibition of Ribonuclease A by Decavanadate

Introduction

Successful isolation of cytoplasmic mRNA often depends on adequate suppression of the endogenous ribonucleolytic activity. The ribonuclease suppression strategies that have proven useful have varied depending on the tissue source and the conditions necessary for the achievement of particular experimental goals (Poulson, 1977; Berger & Birkenmeier, 1979). A number of inhibitors of bovine pancreatic ribonuclease A (RNase A) have proven to be valuable in isolations of RNA from both pancreatic and non-pancreatic tissue sources, presumably because the problematic ribonucleases in non-pancreatic tissues bear some structural relationship to the pancreatic enzyme. Consequently, any new strategies in RNase A inhibition may have application in recombinant DNA technology.

Vanadium(V) in aqueous solutions occurs in a number of oxometalate forms collectively termed vanadates. In neutral, dilute solutions the predominant species $H_2VO_4^-$ is often simply referred to as vanadate. When solutions are not dilute, the speciation of vanadium oxometalates is fairly complex (Petterson, 1994; Rehder, 1995). This complexity is illustrated by Figures 4.1. Monomeric vanadate predominates only at concentrations below 5 mM or at pH values above 8 (Figure 4.1b). The species that occur at higher concentrations or under neutral to mildly acidic conditions are multimers that arise through the sharing of oxo ligands. The structures of some known multimers are shown in Figure 4.2. In addition to its capacity for self-association, vanadate also possesses the capability of forming complexes with a variety of biochemically important ligands. Alcohols, carboxylic acids, amines, and phosphates can all participate (Crans, 1995). A single vanadium can be coordinated to as many as 7 atoms, but 4 or 5 coordinating atoms is more typical. A variety of geometries have been observed, including tetrahedral, octahedral and trigonal bipyramidal. Multimeric oxovanadates can form larger complexes with additional ligands. When free thiols act as ligands, they can participate in redox chemistry, resulting in the reduction of vanadium(V) to vanadium(IV). The stabilities of vanadate coordination

complexes fall within a wide spectrum, and in many cases, thermodynamic and kinetic stability is not yet carefully characterized.

RNase A is a much studied enzyme and has often served as a prototypical enzyme in the development of new biochemical research methods. Indeed, the first of many vanadium-containing enzyme inhibitors was an inhibitor of RNase A (Lindquist *et al.*, 1973). Subsequently, monomeric and polymeric oxovanadates have been reported to inhibit a variety of phosphoryl processing enzymes (Crans, 1994; Stankiewicz *et al.*, 1995). Polymeric oxovanadates have been described as inhibitors for approximately one dozen enzymes. Nevertheless, with the notable exception of the originally-reported nucleoside complexes, vanadates, polymeric or otherwise, have not been reported to inhibit RNase A. Polymeric oxovanadates exist as polyanions at physiological pH's. Likewise, many of the reported inhibitors of RNase A are polyanions, such as heparin, polyvinylsulfate, aurintricarboxylic acid, and polymers of acidic amino acids (Richards & Wyckoff, 1971; Hallick *et al.*, 1977). Given the precedent for polyanionic inhibitors and the historical link between vanadate and RNase A, one might make the incorrect assumption that if polymeric oxovanadates could inhibit RNase A someone would have discovered and reported such inhibition by now. The historical gap notwithstanding, we report direct observations that support the conclusion that RNase A is indeed strongly inhibited by a polymeric oxovanadate. The data suggest that this inhibitor is decavanadate.

Materials and Methods

Materials. RNase A and variants thereof were produced and purified as described in Chapter 2 and elsewhere (delCardayre *et al.*, 1995). Sodium metavanadate, $NaVO_3$, was obtained from Aldrich Chemical (Milwaukee, WI). Poly(cytidylic acid) [poly(C)] was from Midland certified reagents (Austin, TX). Uridine 2',3'-cyclic phosphate (U>p) was from Sigma Chemical (St. Louis, MO). The buffers 2-(*N*-morpholino)ethanesulfonic acid (MES),

imidazole, and sodium succinate were from Sigma Chemical (St. Louis, MO). Tris-HCl was from Fisher (Chicago, IL).

IC_{50}. RNase A catalyzes the cleavage of poly(C) and the hydrolysis of U>p. If U>p was used as the substrate, it was present at a concentration of 1.1 mM. If poly(C) was used as the substrate, it was present at a concentration of 50 μM. These substrate concentrations are roughly half the value of K_m. The reaction volume was 0.80 mL, and the pathlength was 1.0 cm. Vanadate solutions were added to the reaction mixtures in 2 μL volumes. Enzyme was added last, to a final concentration of 0.20 μM in the case of U>p and 1.0 nM in the case of poly(C). The initial rates of reaction of U>p hydrolysis and poly(C) cleavage were monitored by changes in the ultraviolet absorbance, at 286 and 250 nm, respectively.

Concentrated stock solutions of sodium metavanadate were typically prepared at 40 – 200 mM. A series of dilutions from concentrated stocks was tested until a dilute solution was identified that reduced the initial velocity by a factor of 50% (± 10%). The final concentration of vanadate present in the 50% inhibited assay is reported as the IC_{50} value. This value reflects only the total concentration of vanadate and does not attempt to report on the concentration of any individual species. This value will be greater than the K_i or K_d value by at least a factor equal to the number of vanadium atoms in the actual inhibitor.

Isothermal Titration Calorimetry. The thermodynamic parameters of vanadate binding to RNase A were investigated by isothermal titration calorimetry (ITC). ITC was performed with a Micro Calorimetry System (MCS) calorimeter from MicroCal (Northhampton, MA). All experiments were performed at 25 °C. Binding experiments are generally performed by injecting ligands into dilute protein solutions (Cooper & Johnson, 1994). The inverse approach of injecting protein into ligand was adopted here, in order to avoid the sizable and complex background signals that are observed upon dilution of a concentrated, multimer-containing vanadate solution.

A concentrated solution of RNase A (~7 mg/ml) was dialyzed against 30 mM sodium succinate buffer, pH 6.0, overnight prior to the ITC experiment. A 0.20 M metavanadate solution had been prepared as detailed below in order to maximize the proportion of vanadate that was present as the decamer. Within 30 min of beginning the experiment, this solution was diluted in 30 mM succinate buffer, pH 6.0, to 0.20 mM metavanadate, *i.e.*, ~20 μM decavanadate. Both vanadate and protein solutions were degassed by vacuum.

The reference cell was filled with water. The degassed protein solution was placed in the 250 μL injection syringe, while the degassed, dilute vanadate solution was transferred to the MCS sample cell. A small aliquot of protein solution was retained for protein quantitation ($\epsilon^{0.1\%} = 0.72$ at 278 nm). Each 10 μL injection of protein occurred over 12.6 s, and injections were made at intervals of 240 s. Controls were performed using buffer alone in the syringe in place of the protein solution or buffer alone in the cell in place of the ligand solution. The heat of dilution of protein into buffer was deemed negligible. The small exothermic signal resulting from injecting buffer into the dilute vanadate was used to correct the experimental data before fitting. Data were fitted using the ORIGIN software (MicroCal Software, Northhampton, MA). Fitting gave least-squares estimates of the the binding parameters n, ΔH and K_{assoc}.

Decavanadate Stock Solutions. Solutions were prepared from sodium metavanadate at concentrations above 40 mM, in 0.6 M NaCl. HCl was used to adjust the pH to between 3 and 5. Because pH values were slow to stabilize, the pH was checked 24 h later to insure that equilibrium had been established. Under these conditions, only trace amounts of non-decavanadate oxovanadium species would be expected to be present (Petterson *et al.*, 1983). Stock solutions at these high concentrations appeared very bright yellow to orange in color and were stored at room temperature and for over several months, as long as no precipitation had occurred.

Steady-State Kinetics and Inhibition of Poly(C) Cleavage. Poly(C) was purified by precipitation from aqueous ethanol (70% v/v) prior to use. Small aliquots of poly(C) stock solutions were quantitated for total cytidyl concentration by their absorbance, assuming $\epsilon = 6200\ M^{-1}cm^{-1}$ at 268 nm (Yakovlev *et al.*, 1992). Assays of poly(C) cleavage were performed at 25 °C in 10 mM Tris-HCl buffer, pH 7.0, containing NaCl (0.10 M). Decavanadate was added, from the concentrated stock, immediately before enzyme addition. Cleavage of poly(C) was monitored by UV absorption at 250 nm, assuming that $\Delta\epsilon = 2380\ M^{-1}cm^{-1}$ (delCardayre & Raines, 1994). Steady-state kinetic parameters were determined by fitting initial velocity data to the Michaelis-Menton equation, using the program DELTAGRAPH (Deltapoint Software, San Francisco, CA). The subsequent hyperbolic fit of $(K_m/V)_{apparent}$ was also made with DELTAGRAPH.

Results

Studies of inhibitory organo-vanadate complexes, such as the study of uridine vanadate reported in the previous chapter, require inorganic vanadate solutions as background controls. In the process of performing such controls, it was observed that (1) vanadate dissolves very slowly into water but more quickly into buffered or weakly acidic aqueous solutions, and (2) stock solutions prepared thusly were highly inhibitory to RNase A. These initial observations were surprising because monomeric vanadate had been reported previously not to bind to the enzyme (Leon-Lai *et al.*, 1996). Additionally, Lindquist (Lindquist et al., 1973) had noted that small fractions of decavanadate present in their system had not interfered with RNase A activity. Upon further investigation of this unexpected inhibition, we became aware that previous exposure to pH's below 7.0 was the single most critical factor predicting inhibition.

Solution History and Inhibition. IC_{50} values were determined as a function of the storage pH of an 80 mM $NaVO_3$ solution. The pH of these solutions had been adjusted to

varying levels with 3 N HCl. Lower pH values were noted to correlate with the visual observation of a yellow chromophore. IC_{50} results are shown in Table 4.1. Similar trends were observed for IC_{50} determinations in other assay buffer systems. Solutions of 10 mM imidazole-HCl at pH 7.0, 30 mM sodium succinate at pH 6.0, and 10 mM MES-NaOH at pH 6.0 all gave results similar to 10 mM Tris-HCl at pH 7.0. Similar results were also observed with poly(C) as the substrate (Table 4.2).

If acidified $NaVO_3$ solutions were diluted into the Tris-HCl assay buffer 42 h prior to the addition of enzyme and substrate, IC_{50} values increased 8- to 9-fold. In contrast, dilutions of acidified $NaVO_3$ made within 1-2 hours of assaying resulted in inhibitory capabilities not distinguishable from dilutions made and used immediately. Full activity of inhibited RNase A solutions can be recovered by dialyzing the enzyme against 1 M NaCl and then against dilute buffer.

Vanadate is known to oligomerize to dimers, tetramers, pentamers, and decamers. Of these, only decavanadate is slow to disassemble upon dilution (Goddard & Gonas, 1973), and only decavanadate possesses absorptivity in the visible range, accounting for the observed yellow color. These facts suggest that decavanadate is the reversible inhibitor responsible for the observed loss of RNase A activity (see Discussion section). Further characterizations of the inhibition are based on this assumption.

Protein Vanadate Binding. Isothermal titration calorimetry was used to demonstrate and measure the binding of decavanadate to RNase A in the absence of substrate. Protein was injected into a solution of vanadate that had been prepared so that the proportion of decavanadate was maximized. Both protein and decavanadate were buffered with 30 mM sodium succinate, pH 6.0. An exothermic reaction was observed, as shown in Figure 4.3a. Least-squares estimates of binding parameters give a value of 12.3 ± 0.3 for n, the number of equivalents of monomeric vanadium bound per protein molecule. This number is consistent with binding to decavanadate; deviation from 10.0 may arise from

errors in protein quantitation or inhomogeneity of vanadate species. If one assumes that all the vanadate is present as decavanadate and that the stoichiometry of binding is 1:1, the K_d derived from calorimetric data is 1.4 ± 0.3 μM. This fit is shown in Figure 4.3b.

Kinetic model of inhibition. Steady-state kinetic analysis of inhibition indicates that the vanadate inhibitor is competitive against poly(C) (Figure 4.4a). When $(K_m/V_{max})_{apparent}$ is plotted versus vanadate concentration, the linear relationship expected for simple competition is not observed. The relationship can be fit to a hyperbola (Figure 4.4b). The implications of this relationship are discussed below.

Discussion

Vanadate forms a multitude of complexes and has versatile redox chemistry. Accordingly, the possible mechanisms for loss of enzymatic activity by vanadate are multiple. The fact that RNase A activity is recoverable after dialysis rules out any irreversible reaction with the protein. It might also be conceivable for the vanadate to interact with the substrate in such a way as to make it unavailable to the enzyme. The calorimetric data indicate, however, that vanadate binds to protein even in the absence of substrate (Figure 4.3); a substrate-vanadate interaction is not necessary to explain the loss of enzymatic activity. Moreover, the loss of enzyme activity is observed at vanadate concentrations far below that of the substrate.

If vanadate does not alter the protein irreversibly and does not sequester the substrate, then it must either participate in or constitute by itself a reversible inhibitor. Because functional groups of buffers can potentially participate in vanadate complexes, buffer concentrations were kept low (10 - 30 mM) and a number of unrelated buffers were employed. Changing the buffer species did not significantly alter the results, and therefore we conclude that inhibition does not require coordination to a buffer functional group. A complex composed of vanadate and substrate could form in sufficient quantities to act as an

inhibitor. This possibility seems difficult to reconcile with the fact that inhibition was observed with both cyclic mononucleotide and linear polymeric substrates.

Even if no other ligand is involved, vanadates can self associate into a number of configurations that are known to inhibit various enzymes. Vanadate dimers, tetramers, and pentamers interconvert on the time-scale of milliseconds to seconds (Crans et al., 1990). The storage conditions of vanadate should therefore not influence which multimeric forms are present several minutes after dilution into an assay buffer solution. The results in Table 4.1 are not consistent with species that respond rapidly to pH and concentration changes. Decavanadate, on the other hand, decomposes to monomeric vanadate with a half-life of hours (Goddard & Gonas, 1973). Not only is decavanadate the most likely candidate for our observed inhibition, it is stable enough to allow for some characterization of this inhibition, because our kinetic assays and calorimetry experiments can be performed on a time scale of fractions of the half-life of decavanadate in dilute solution.

Decavanadate is known to be the vanadate assemblage responsible for inhibiting several kinases and phosphorylases, as well as the glycolytic enzyme aldolase (Crans, 1994; Stankiewicz *et al.*, 1995). Reported K_i and IC_{50} values range from 62 μM for hexokinase, to 45 nM for phosphofructokinase (Choate & Mansour, 1979; Boyd *et al.*, 1985). The IC_{50} values observed for RNase A are within this range. (Note: the IC_{50} values in Tables 1 and 2 are expressed in terms of $[V]_{total}$, which is $10\times[V_{10}]$.)

The enzymes inhibited by decavanadate, including RNase A, are all preorganized to bind phosphoryl groups at multiple sites. However, decavanadate inhibition is by no means a general property of all such enzymes. Creatine kinase, pyruvate kinase, galactokinase, and inorganic pyrophosphatase are all enzymes of this class not affected by decavanadate (Boyd *et al.*, 1985). Likewise, inhibition by decavanadate is not simply a consequence of being cationic. High isoelectric point (p*I*) does not necessarily correlate with susceptibility to decavanadate inhibition. RNase A has a p*I* of 9.3 (Ui, 1971). The isoelectric point of

pyruvate kinase (cow muscle) is 8.9 (Cardenas et al., 1973); under conditions of neutral pH it is not inhibited by decavanadate. The isoelectric point of phosphofructokinase (pig liver) is only 5.0 (Massey & Deal, 1973); yet it is inhibited. The ability of decavanadate to act as an enzyme inhibitor is more selective than one might initially expect.

Where decavanadate inhibition has been characterized carefully, it has not tended to follow a simple competitive model. In the case of hexokinase, decavanadate behaves noncompetitively with respect to both ATP and glucose (Boyd *et al.*, 1985). In the case of phosphofructokinase, decavanadate inhibition behaves in a complex allosteric fashion. Hexokinase inhibition is antagonized by positive allosteric effectors and is synergistic with ATP, suggesting that decavanadate may interact with both the substrate and effector binding sites (Choate & Mansour, 1979). For RNase A, with respect to poly(C), the data likewise suggest a model with more subtlety than a simple competition with the substrate for the active site. Inhibition is less severe at higher levels of the substrate (Figure 4.4a), but the slope replot (Figure 4.4b) fits a hyperbola better than a straight line. One model capable of explaining this pattern arises from an inhibitor that can bind to the enzyme in a fashion that does not preclude substrate binding and turnover, yet alters K_m. In this model

$$(K_m/V_{max})_{\text{apparent}} = K_m \times \left(\frac{1 + {}^{[I]}\!/_{K_i}}{1 + {}^{[I]}\!/_{K_I}} \right) \times \frac{1}{V}$$

where $K_i = {}^{[E][I]}\!/_{[EI]}$ and $K_I = {}^{[ES][I]}\!/_{[EIS]}$ (Roberts, 1977). Figure 4.4b shows the least-squares fit to this equation where K_i = 0.41 μM V_{10} and K_I = 11.5 μM V_{10}. The data that indicate this model are minimal, and so the assignment of the inhibition as hyperbolic competitive is preliminary. As more data are collected, perhaps an even more complex picture of inhibition will emerge. It should be noted that at least one other scenario is capable of accounting for the observed inhibition pattern. The hyperbolic dependence of

K_m/V_{max} on vanadium concentration may be an artifact of an unexpected equilibrium, inasmuch as decavanadate has been reported to form even larger complexes such as octadecavanadate and to incorporate additional ligands (Pope & Muller, 1994). The concentration of an unidentified inhibitory vanadate species might appear hyperbolic over the concentration range studied. Still, hyperbolic competitive inhibition is not unexpected for a large polyanionic ligand inasmuch as its binding is likely to have profound effects on the electrostatic potential of the protein and may thereby alter K_m.

A limited amount of decavanadate inhibition data has been collected at varying pH's and salt concentrations, as well as with protein variants possessing an altered charge (Table 4.2). The pK_a of $HV_{10}O_{28}^{5-}$ is 6.14 (Petterson *et al.*, 1983). The dependence of inhibition on pH has not been studied sufficiently to draw concrete conclusions, but it is interesting to note that the differences in IC_{50} values are not dramatic between pH 6.0 and pH 7.0. It is clear from the data at varied NaCl concentrations and from the mutation of cationic residues that binding to decavanadate is mediated in large part by Coulombic forces. RNase A has a total of fourteen arginine and lysine residues and has significant patches of exposed positive electrostatic potential around the active site. The dimensions of the active-site cleft in the area of greatest positive potential are sufficient to accommodate decavanadate. This positive potential is reduced in the K41A and K7A/R10A/K66A variants (Figure 4.5). These changes appear to be reflected in the variations in IC_{50} values.

Decavanadate appears to bind to RNase A with an affinity on par with two other small molecules that are known to have some value in laboratory RNA manipulations. Aurintricarboxylic acid has been reported to have an IC_{50} value near 1 μM (Hallick *et al.*, 1977), and vanadyl(IV)uridine has a K_i of 12 μM (Lindquist *et al.*, 1973). Also comparable is the IC_{50} near 2 μM observed for tyrosine-glutamic acid copolymers of M_r ~3500 (Sela, 1962). Decavanadate does not have nearly the affinity (K_d = ~10^{-13} M) of the 50 kDa ribonuclease inhibitor protein (RI) (Vicentini *et al.*, 1990), which is also often used

experimentally to suppress ribonucleolytic activity in mammalian tissues and extracts. But unlike RI, decavanadate is inexpensive and easy to prepare. Decavanadate is not prone to oxidation, as is vanadyl(IV)uridine. The value of decavanadate in stabilizing RNA is, however, compromised for several reasons. It will likely be less effective against ribonucleases that have less cationic surfaces. Its efficacy will likely be diminished under high ionic strength conditions. If used under pH and concentration conditions where it is metastable, decavanadate will have a limited lifetime. Finally, its inhibition of RNase A is hyperbolic rather than absolute, yielding, at high decavanadate concentrations an enzyme with an apparent K_m of $K_m(K_I/K_i)$.

Even if decavanadate does not prove to be practically useful, the observation that decavanadate is an RNase A inhibitor does raise the possibility that other polyoxo-metalate species may be capable of inhibiting RNase A as well as other ribonucleases. It also raises a consideration of some importance for kinetic studies at high vanadium concentrations, such as those that attempt to answer questions about phosphoryl transfer transition states. In such studies, one must take steps to avoid misattributing inhibition that is actually due to decavanadate as being due to other vanadium species, because very low concentrations of decavanadate can significantly impact enzyme activity. The K_i and K_d values for the RNase A•decavanadate complex, under conditions of low ionic strength, are on the order of 1 μM.

Table 4.1: IC_{50} Values for $NaVO_3$ Inhibition of the Hydrolysis of Uridine 2',3'-Cyclic Phosphate by Ribonuclease A[a].

pH	IC_{50}[b] (μM)
9.5 [c]	> 1000
9.1	100
9.0	55
8.2	20
6.2	2.7
2.7	2.7

[a] Assays were performed at 25 °C in 10 mM Tris-HCl buffer with a substrate concentration of 1.1 mM uridine 2',3'-cyclic phosphate.

[b] IC_{50} values are expressed as total added [VO_3^-].

[c] The pH of 9.5 was the initial pH, before any adjustment.

Table 4.2: Effect of Salt, pH, and Active-Site Charge on IC_{50} values of Decavanadate for Catalysis by Ribonuclease A.

RNase A	Buffer	[NaCl]	pH	Substrate	IC_{50} (μM)[a]
wild-type	10 mM Tris-HCl	0 mM	7.0	U>p	2.7
wild-type	10 mM Tris-HCl	100 mM	7.0	U>p	10
wild-type	10 mM Tris-HCl	290 mM	7.0	U>p	50
wild-type	0.10 M MES-NaOH	100 mM	6.0	poly(C)	40
wild-type	30 mM Na•Succinate	0 mM	6.0	poly(C)	17
wild-type	10 mM Tris-HCl	100 mM	7.0	poly(C)	12
K41A	0.10 M MES-NaOH	100 mM	6.0	poly(C)	150
K7A/R10A/K66A	0.10 M MES-NaOH	100 mM	6.0	poly(C)	> 600

[a] Vanadate was prepared as decavanadate. IC_{50} values are expressed as total added $[VO_3^-]$.

Figure 4.1. Distribution and predominance diagrams for vanadium (V) species in aqueous solution. (A) Distribution diagram for 40 mM vanadium in 0.6 M NaCl at 25 °C [from (Petterson *et al.*, 1983)]. Fi is defined as the ratio of vanadium existing as a particular a species to total vanadium. (B) Predominance diagram for vanadium species in 0.6 M NaCl at 25 °C (Petterson, 1994). V_1' denotes HVO_4^{2-}, V_1'' denotes $H_2VO_4^-$, V_2 denotes $V_2O_7^{4-}$, V_2' denotes $HV_2O_7^{3-}$, V_2'' denotes $H_2V_2O_7^{2-}$, V_4 denotes $V_4O_{12}^{4-}$, V_5 denotes $V_5O_{15}^{5-}$, V_{10} denotes $V_{10}O_{28}^{6-}$, V_{10}' denotes $HV_{10}O_{28}^{5-}$, V_{10}'' denotes $H_2V_{10}O_{28}^{4-}$, and V_{10}''' denotes $H_3V_{10}O_{28}^{3-}$. V_2O_5 exists primarily as a solid.

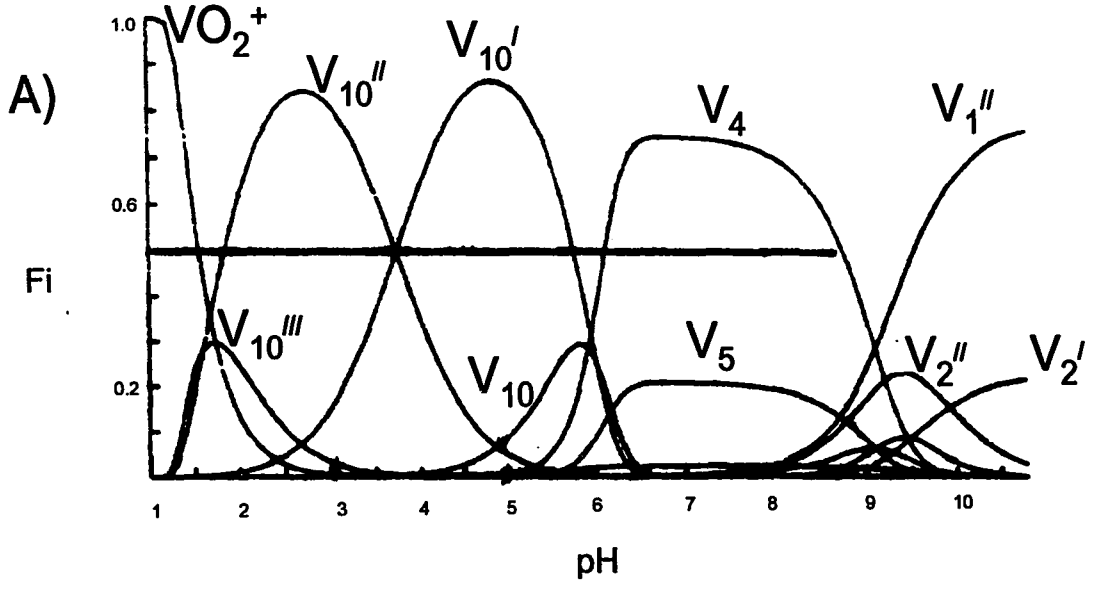
A)
Fi
1.0
0.6
0.2
VO_2^+
V_{10}''
V_{10}'
V_4
V_1''
V_{10}'''
V_{10}
V_5
V_2''
V_2'
1 2 3 4 5 6 7 8 9 10
pH

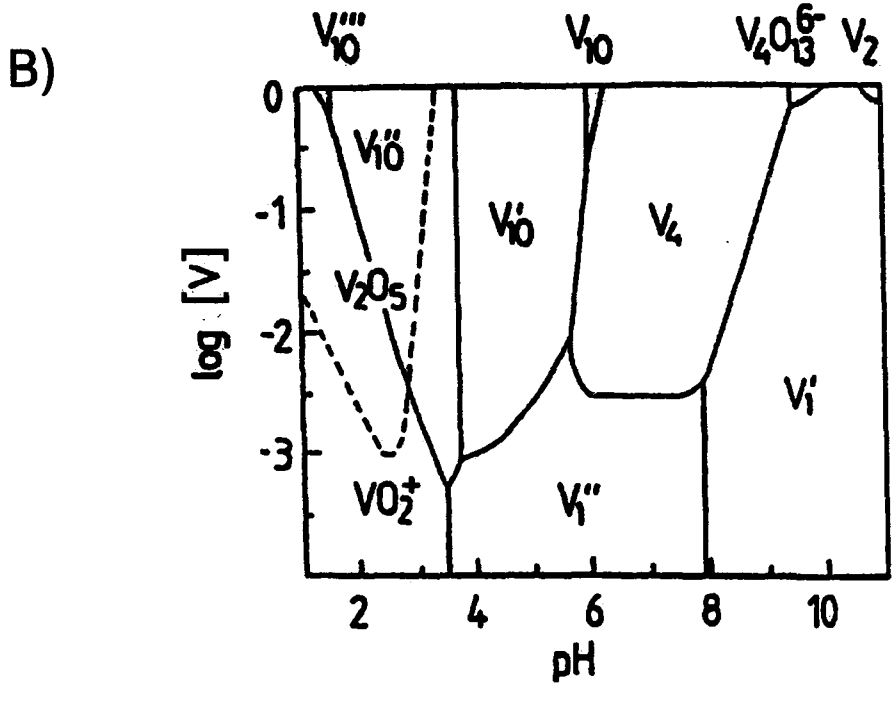
B)
V_{10}''''
V_{10}
$V_4O_{13}^{6-}$
V_2
0
-1
-2
-3
log [V]
V_{10}''
V_{10}'
V_4
V_2O_5
V_1'
VO_2^+
V_1''
2 4 6 8 10
pH

Figure 4.2 Representative monomeric and multimeric oxovanadate structures. Decavanadate is shown in the lower right quadrant. Taken from (Rehder, 1995) and references therein.

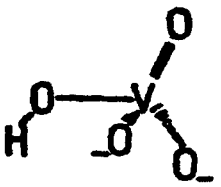

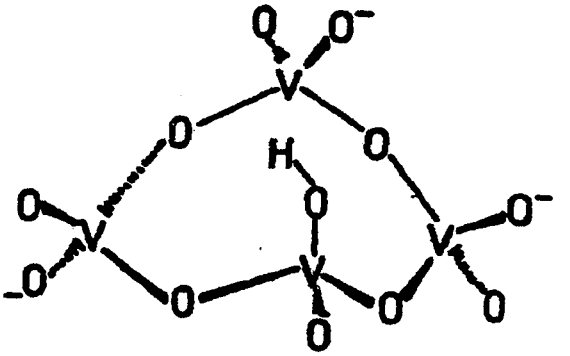

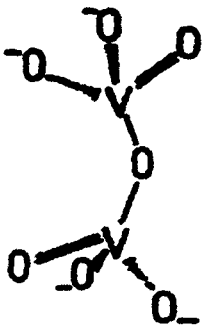

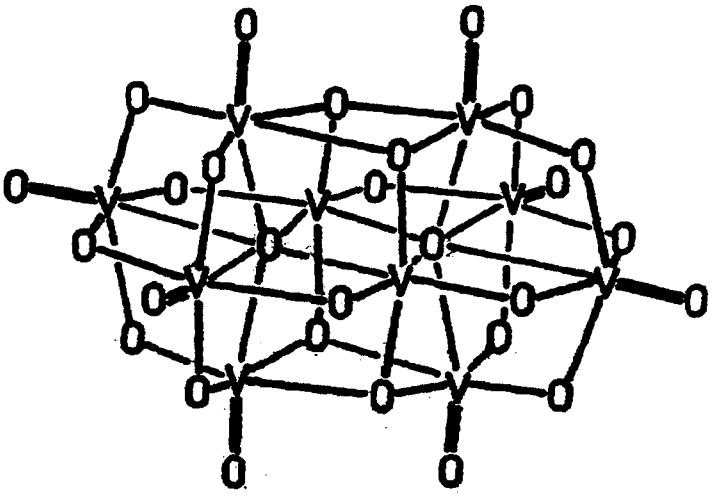

Figure 4.3 Thermograms for the binding of ribonuclease A to decavanadate. (A) The upper graph shows the heat released upon injection of protein to the decavanadate solution. (B) The lower graph is a plot of the heat released versus the molar ratio of RNase A to decavanadate. The concentration of decavanadate is taken to be [total vanadate] divided by ten. Binding was measured by isothermal titration calorimetry at 25 °C in 30 mM sodium succinate buffer, pH 6.0.

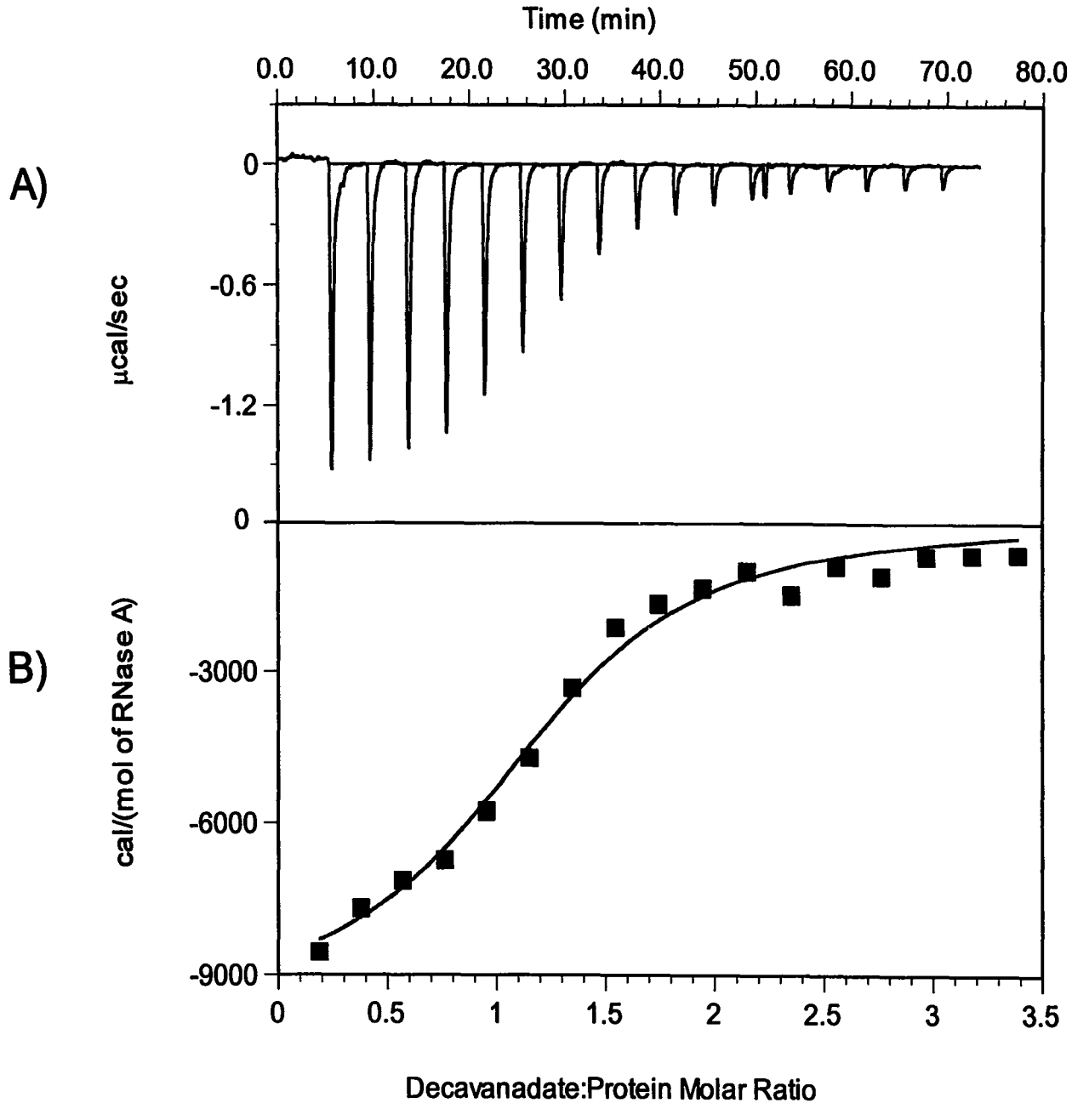
A)
B)
Time (min)
0.0
10.0
20.0
30.0
40.0
50.0
60.0
70.0
80.0
µcal/sec
0
-0.6
-1.2
cal/(mol of RNase A)
0
-3000
-6000
-9000
0
0.5
1
1.5
2
2.5
3
3.5
Decavanadate:Protein Molar Ratio

Figure 4.4 The effect of decavanadate on the steady-state kinetic parameters of poly(C) cleavage by ribonuclease A. (A) Lineweaver-Burke plots at varying levels of decavanadate: 130 μM $NaVO_3$ (◇), 65 μM $NaVO_3$ (◆), 13 μM $NaVO_3$ (O), and not inhibited (▲). Experiments were performed in 10 mM Tris-HCl buffer, pH 7.0, at 25 °C (B) Slope replot of the above data fit to the equation:

$$(K_m/V)_{\text{apparent}} = K_m \times \left(\frac{1 + {[I]}/{K_i}}{1 + {[I]}/{K_I}} \right) \times \frac{1}{V}$$

where K_i and K_I are 0.41 and 11.5 μM, respectively. [$NaVO_3$] divided by 10 is the assumed decavanadate concentration, [I].

A)

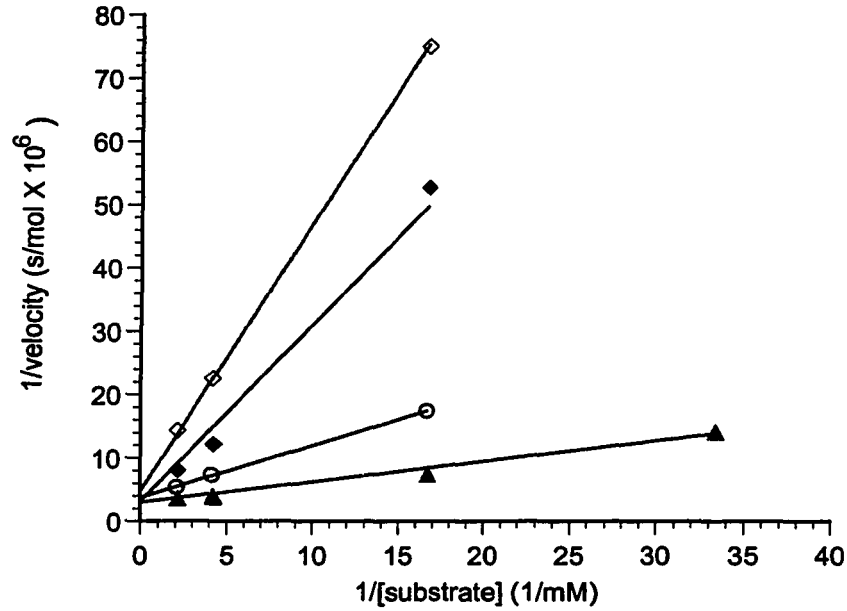
1/velocity (s/mol X 10^6)
80
70
60
50
40
30
20
10
0
0
5
10
15
20
25
30
35
40
1/[substrate] (1/mM)

B)

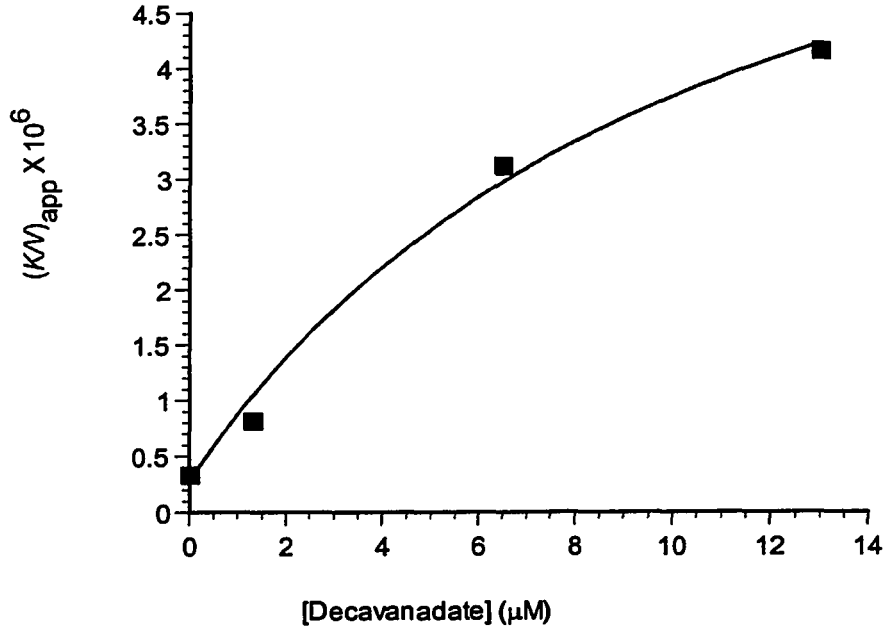
(K/V)app X10^6
4.5
4
3.5
3
2.5
2
1.5
1
0.5
0
0
2
4
6
8
10
12
14
[Decavanadate] (μM)

Figure 4.5 Electrostatic potential maps of the surface of decavanadate and of wild-type ribonuclease A and two charge variants. The atomic coordinates for ribonuclease A are from pdb:6RSA and the decavanadate structure was obtained from the Cambridge data base. The coordinates for K41A ribonuclease A are derived from pdb:6RSA with the relevant site change to alanine made via manual editing of the pdb file. The coordinates for K7A/R10A/K66A are from pdb:3RSK. Maps were created using GRASP (Nicholls *et al.*,1991). Each of the 18 bridging surface oxygens of decavanadate was assigned a charge of $-\,^{1}/_{3}$, stemming from the assumption that the primary species present at pH 6.0 is $V_{10}O_{28}^{6-}$ (pK_a 6.14). Histidines were assigned a charge of $^{1}/_{2}$. Otherwise, full charges and default parameters within GRASP were used.

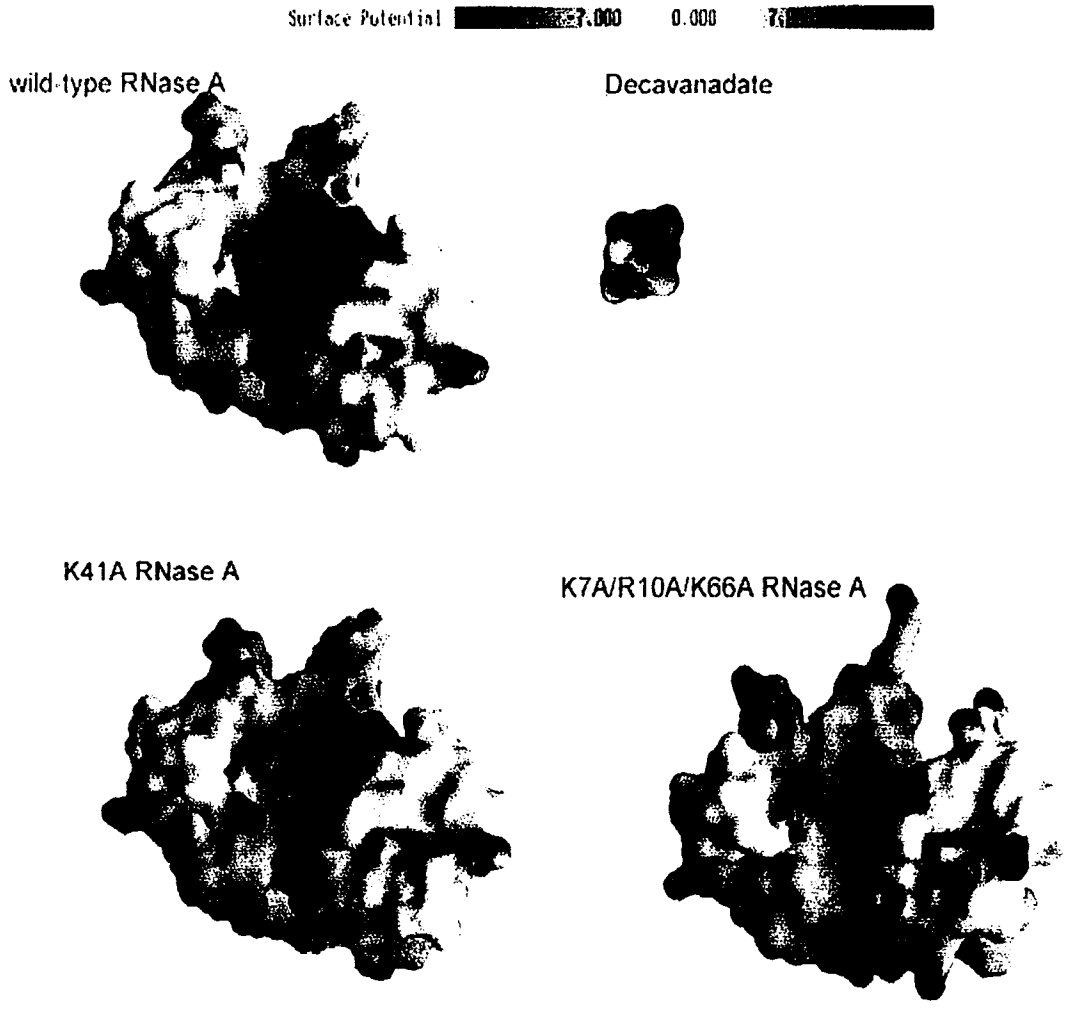
Surface Potential
0.000
wild-type RNase A
Decavanadate
K41A RNase A
K7A/R10A/K66A RNase A

Chapter 5

The Sulfur Shuffle:

Activation and Inactivation of K41C Ribonuclease A

Introduction

The activity levels of enzymes *in vivo* and *in situ* are exquisitely controlled by layers of regulatory mechanisms. Many of these modalities of enzymatic control are lost *in vitro*. Nonetheless, the commercial and technological roles of enzymatic processes *in vitro* are of greater significance than ever before, with applications ranging from food processing (Suckling, 1990) to biotechnology (Eun, 1996). Such uses of enzymes are likely to benefit from added degrees of control.

Controlling enzyme activity *in vitro* is important in molecular biological manipulations in which a ribonuclease, generally ribonuclease A (RNaseA; EC 3.1.27.5), is added in one step, but where residual ribonucleolytic activity is detrimental in later steps. The ribonuclease protection assay (RPA), a method for detecting and quantitating RNA transcripts, is a prime example of this sort of manipulation (Zinn *et al.*, 1983; Ausubel *et al.*, 1994). Available methods of controlling RNase A activity tend to suffer from a lack of specificity, stability, or effectiveness. For example, diethyl pyrocarbonate (DEPC) effectively destroys ribonucleolytic activity but can also alter nucleic acids and any other proteins that are present. Inhibitors such as nucleoside vanadyl complexes and aurintricarboxylic acid are not specific for RNase A, and will inhibit a number of other nucleic-acid binding enzymes, including polymerases. In addition, nucleoside vanadyl complexes are prone to air oxidation. Affinity labels and mechanism-based inactivation reagents have been created. However, the affinity labels bind weakly with dissociation constants greater than 20 mM (Hummel *et al.*, 1987) and the mechanism-based inactivators apparently modify nonessential residues (Stowell *et al.*, 1995), therefore both types of compounds leave uninhibited a significant proportion of the activity.

We have engineered into RNase A a mechanism of *in vitro* control. This method of modulating activity is similar to many natural regulatory mechanisms in that it employs

reversible covalent modification. Specifically, we have replaced a critical lysine residue with a cysteine, and this cysteine residue can be used as a "hook" on which to hang activating or deactivating entities. The K41C RNase A variant can be activated by chemical modification with cysteamine (2-aminoethanethiol), thus replacing the primary amine. Cysteamine can be removed later by gentle treatment with dithiothreitol (DTT) or another reducing agent. An inhibitory ligand at the end of a thiol-reactive linker can be added to achieve more complete inactivation. A few other enzymes have been activated and deactivated by reversible modification of a newly introduced cysteine (Pease *et al.*, 1987; Gloss & Kirsch, 1995), but further inactivation via additional covalent changes to the cysteine is a feature unique to the present work. Similar regimes of transient activation and inactivation may be applicable to other enzymes with critical active-site lysine residues, including other phosphoryl transferases and nucleases.

Materials and Methods

Materials. The oligonucleotide used for site-directed mutagenesis was synthesized bearing a trityl group and was purified using an Oligo Purification Cartridge (OPC) from Applied Biosysytems (Foster City, CA). The *E. coli* strain used for protein production, BL21(DE3), was from Novagen (Madison, WI). Ellman's reagent, dithiothreitol (DTT), HEPES free acid, MES free acid, and cysteamine·HCl were from Sigma Chemical (St. Louis, MO). Poly(cytidylic acid) [poly(C)] was from either Midland Certified Reagents (Austin, TX) or Sigma Chemical. All materials for ribonuclease protection assays were from Ambion (Austin, TX), except for the [α-^{32}P]UTP, which was from DuPont NEN Products (Boston, MA), and electrophoresis and autoradiography materials, which were from Fisher (Chicago, IL) and Eastman Kodak (Rochester, NY). All starting materials for the synthesis of 2,4-dinitrophenyl 3-phosphoryl disulfide were from Aldrich Chemical

(Milwaukee, WI), and the purity of these reagents was assessed by ^{1}H NMR and/or thin layer chromatography (TLC) prior to use.

Spectroscopy and Protein Quantitation. Measurements of ultraviolet (UV) and visible absorption were made with a Cary Model 3 spectrophotometer from Varian (Sugar Land, TX). Protein concentrations were determined based on the wild-type value of $\epsilon^{0.1\%}$ = 0.72 at 277.5 nm (Sela *et al.*, 1957). This relationship was assumed to be valid for all forms of K41C RNase A studied. The veracity of this assumption is supported by the fact that DTT treatment of K41C-NTB RNase A quantified in this manner yields a value of 1.0 ± 0.2 equivalents of NTB, as expected.

K41C-NTB RNase A. Mutation of the cDNA that codes for RNase A was made by the method of Kunkel (Kunkel et al., 1987) using the oligonucleotide AAAGTGGTTAACTGGACAGCATCGATC. Mutant cDNA was expressed in *E. coli* strain BL21(DE3) under the control of the T7 RNA polymerase promoter. The resulting protein was purified as described previously (delCardayre *et al.*, 1995). After purification, the new sulfhydryl at position 41 was protected from inadvertent reaction by treatment with 5,5′-dithio-bis(nitrobenzoic acid), (Ellman's reagent or DTNB). The resulting protein (K41C-NTB RNase A) was separated from any unprotected protein by cation exchange FPLC (MonoS column; Pharmacia, Piscatawy, NJ) using a linear gradient of NaCl (0 – 200 mM) in 50 mM HEPES-NaOH buffer, pH 7.7. The protected protein eluted from the column at ~60 mM NaCl, and the unprotected K41C protein eluted at ~80 mM. The protected protein, as eluted, was stable for several months when stored at 4 °C.

K41C-Cysteamine RNase A. The reaction between K41C-NTB protein and cysteamine was initiated by adding cysteamine•HCl (2 - 10 μL of a 0.010 M solution in 0.10 M Tris-HCl buffer, pH 7.7) to one mL of 50 mM HEPES-NaOH buffer, pH 7.7,

containing K41C-NTB RNase A (0.3 - 0.7 mg/mL). The reaction mixture was incubated at room temperature, and its progress was monitored by following the increase in absorbance of visible light at 412 nm, resulting from the release of the NTB group (ϵ_{412} = 14,500 $M^{-1}cm^{-1}$). Excess cysteamine and released nitrothiobenzoate were removed by subsequent dialysis.

Poly(C) Cleavage Assay. Ribonucleolytic activity was assessed by using poly(C) as a substrate. Prior to assay, poly(C) was precipitated from aqueous ethanol (70% v/v), solubilized in assay buffer, and quantitated for total cytidyl concentration by absorbance at 268 nm [$\epsilon = 6200$ $M^{-1}cm^{-1}$ (Yakovlev *et al.*, 1992)]. Assays of poly(C) cleavage were performed at 25 °C in 0.10 M MES-NaOH buffer, pH 6.0, containing NaCl (0.10 M). Cleavage of poly(C) was monitored by UV absorption at 250 nm using $\Delta\epsilon = 2380$ $M^{-1}cm^{-1}$ (delCardayre & Raines, 1994). Concentrations of poly(C) in assays ranged from 0.02 mM to 1.2 mM, in terms of individual cytidyl units. Initial rates of cleavage were fit to the Michaelis-Menten equation using the program HYPERO (Cleland, 1979).

Deactivation with DTT. Aqueous DTT was added to a solution of K41C-cysteamine (K41C-csa) RNase A in 50 mM HEPES-NaOH, pH 7.7. The protein solution had been dialyzed previously to remove any residual free cysteamine. The reaction was allowed to proceed at room temperature and aliquots were removed periodically to assay for poly(C) cleavage activity.

Ribonuclease Protection Assay. *Probe Creation.* The MAXIscript In Vitro Transcription Kit (Ambion; Austin, TX) was used with the supplied linearized template, which encodes a 250-bp mouse β-actin gene fragment. ^{32}P was incorporated into the transcribed RNA by T7 RNA polymerase, using [α-^{32}P]UTP (800 Ci/mmol) in the transcription reaction, along with the recommended levels of the supplied non-radioactive

NTP's. Transcription was allowed to proceed for 55 min at 37 °C. Template DNA was then digested with DNase I. The resulting RNA fragment was purified by removing small molecules via a Nick column (Pharmacia; Piscatatawy, NJ), and then by acrylamide gel electrophoresis. The RNA that eluted from the excised gel band exhibited 3500 cpm/μL. *Hybridization.* Whole mouse and whole yeast RNA samples (7 and 15 μg, respectively) were co-precipitated with probe RNA (8×10^4 cpm) at –20 °C using 2.5 volumes of EtOH. Resuspension of the resulting pellet in 20 μL of the supplied buffer was followed by heating to 90 °C, slow cooling to 44 °C, maintenance of this temperature overnight, and an additional 30 min incubation at 25 °C immediately prior to the addition of ribonucleases. *Digestion.* After hybridization, unprotected RNA was digested either with the supplied ribonuclease cocktail (0.1 μg RNase A and 2 Ambion units RNase T1 per tube) or with K41C-csa RNase A (15 μg per tube). Digestion took place in 0.20 mL of the supplied digestion buffer over 30 min at room temperature. Digestion was terminated in one of the following ways: addition of the solution supplied by Ambion, addition of DTT to a final concentration of 1 mM, or addition of DTT to 1 mM followed by a single phenol/chloroform extraction. Sample precipitation was either as specified by Ambion at -20 °C or with 2.5 volumes of EtOH at 0 °C. *Autoradiography.* Precipitated samples were resuspended in 95% (v/v) formamide, heated to 90 °C, and loaded in their entirety onto a denaturing (8 M urea) 5% (w/v) acrylamide gel. After running the gel until the bromophenol blue dye was ¾ of the way to the bottom, the gel was transferred to a paper backing, dried, and exposed to x-ray film for 120 h.

Synthesis of 2,4-Dinitrophenyl 3-Phosphopropyl Disulfide.

p-Methoxybenzylmercaptan. *p*-Methoxybenzylmercaptan was prepared from *p*-methoxybenzylchloride and thiourea. A 1:1 ratio of the reactants was refluxed under N_2(g)

in acetonitrile 1 h, and then stirred for an additional 12 h. After 12 h, the reaction mixture was concentrated under reduced pressure to give a white solid. The solid was then dissolved in an aqueous solution of potassium carbonate and sodium bisulfite, and heated to 80 °C, in order to hydrolyze the amidine groups. The product was subsequently acidified, extracted into chloroform, dried over $MgSO_4$, and evaporated to give a slightly yellow oil. ^{1}H NMR ($CDCl_3$, ppm) 7.22-7.25 and 6.86-6.83 (two m, 2H each, -C_6**H**$_4$-), 3.79 (s, 3H, -OC**H**$_3$), 3.70 (d, J = 7.4 Hz, 2H, -C**H**$_2$SH), 1.73 (t, J = 7.4 Hz, 1H, -**SH**).

Propane-3-ol p-Methoxybenzyl Thioether (**3**). Equimolar amounts of *p*-methoxybenzylmercaptan and 3-bromo-1-propanol in acetonitrile were stirred under N_2(g) in the presence of potassium carbonate. The reaction was allowed to proceed, with stirring, overnight at room temperature. Compound **3** was isolated by silica chromatography, with 1:1 ethyl acetate:hexane as the mobile phase, and then evaporated under reduced pressure to give a colorless oil. ^{1}H NMR ($CDCl_3$, ppm) 7.21-7.26 and 6.84-6.87 (two m, 2H each, MeOC$_6$**H**$_4$-), 3.80 (s, 3H, -OC**H**$_3$), 3.71 (t, J = 6.1 Hz, 2H, -C**H**$_2$OH), 3.68 (s, 2H, -C$_6$H$_4$C**H**$_2$S-), 2.53 (t, J = 7.0 Hz, 2H, -SC**H**$_2$CH$_2$-), 1.81 (m, 2H, -CH$_2$C**H**$_2$CH$_2$-), 1.61 (br s, 1H, CH$_2$O**H**).

3-Phosphopropyl p-Methoxybenzyl Thioether (**6**). [Compound **6** was generated by a method analogous to that of Kraszewski & Stawinski, (1980).] Bis-triazole *p*-nitrophenylphosphate (**2**), was generated by the reaction of *p*-nitrophenyl-phosphorodichloridate (**1**) plus triazole and triethylamine (TEA) in tetrahydrofuran, under N_2(g), first at 0 °C and then at room temperature, for a total of 30 min. Compound **3** was then added (500 mg; 2.36 mmol) in a ratio of 3:1 relative to the dichloridate, along with 1.3 equivalents of 1-methylimidazole, relative to **3**. The reaction proceeded, still under N_2(g), for another 30 min. H_2O and TEA were then added to hydrolyze the triazole groups. After 2 h, the reaction mixture was concentrated under reduced pressure to give a yellow solid. The

yellow solid was dissolved in chloroform and washed with aqueous $NaHCO_3$, then concentrated to give a yellow oil. The yellow oil was dissolved in deionized H_2O and purified by two chromatographic steps, ion exchange (Sephadedx SP C-25) and RP-C18 (isocratic; 1:1 MeOH:H_2O mobile phase), to give the phosphodiester **5** in 62% yield from alcohol **3**. MS of **5** (FAB, m/e): 412.1 [calcd. for $C_{17}H_{19}NO_7PS$ 412.06]. Phosphodiester **5** was then hydrolyzed in 1 N NaOH at 90 °C for 16 h, and the resultant phosphomonoester (**6**) was neutralized and purified chromatographically on DEAE sephadex, a strong anion exchange medium. Elution off the DEAE was effected by a linear gradient (0.1 - 1 M) of H_2CO_3•TEA, which was removed as the product was dried under reduced pressure, yielding the sodium salt of **6** in 75% yield from **5**. ^{1}H NMR (D_2O, ppm) 7.06-7.10 and 6.72-6.76 (two m, 2H each, $MeOC_6\mathbf{H}_4$-), 3.73 (quart., J = 6.4 Hz, 2H, -$C\mathbf{H}_2OPO_3^{-2}$), 3.61 (s, 3H, -$OC\mathbf{H}_3$), 3.50 (s, 2H, -$C_6H_4C\mathbf{H}_2S$-), 2.37 (t, J =7.5 Hz, 2H, -$SC\mathbf{H}_2CH_2$-), 1.70 (quint,J = 6.6 Hz, 2H,-$CH_2C\mathbf{H}_2CH_2$-). ^{31}P NMR (D_2O, ppm relative to phosphoric acid) 1.36 (s, decoupled).

Dinitrophenyl 3-phosphopropyl disulfide (**7**). The simultaneous removal of the *p*-methoxybenzyl group from the sulfur and creation of the disulfide was accomplished by the method of (Johnson *et al.*, 1994). Thioether **6** was stirred with an equimolar amount of 2,4-dinitrophenylsulfenyl chloride in acetic acid, at room temperature for 30 min. The reaction mixture was then concentrated by evaporation and dissolved in methanol. The product (**7**) was crystallized with the addition of diethylether, and isolated by filtration to yield disulfide **7** as the free acid in 35% yield from **6**. ^{1}H NMR (CD_3OD,ppm) 9.04 and 8.58-8.62 (s and m, respectively, 1H and 2H, respectively, $(NO_2)_2C_6\mathbf{H}_3$-), 4.06 (quartet, J = 6.2 Hz, 2H, -$CH_2C\mathbf{H}_2OPO_3^{2-}$), 2.96 (t, J =7.2 Hz, 2H, -$SC\mathbf{H}_2CH_2$-), 2.05 (quintet, J =6.5 Hz, 2H, -$CH_2C\mathbf{H}_2CH_2$-). ^{31}P NMR (D_2O, ppm relative to phosphoric acid) 0.8 (s, decoupled).

K41C-MPP RNase A. K41C RNase A was isolated freshly from the K41C-NTB form of the protein by DTT treatment and cation exchange chromatography on a mono S column (FPLC, conditions described above). The protein (6 μM) was then reacted with a 10-fold molar excess of 7 and re-isolated by cation exchange. The addition of the MPP moiety causes the protein to elute off the Mono S column at 45 mM NaCl, rather than at ~80 mM NaCl.

Zymogram Assay. Very small amounts of ribonucleolytic activity can be detected in Laemmli gels impregnated with RNA or with poly(C) (Blank *et al.*, 1982; Raines & Kim, 1993). Here, zymogram assays were performed in an 18% (w/v) acrylamide gel containing poly(C) (0.5 mg/ml). K41C RNase A (0.4 μg) or K41C-MPP RNase A (0.4 μg) were loaded onto the gel in a non-reducing glycerol loading buffer (<20 μL). The gel was run at 50 mV until the sample had entered the resolving gel, and then the voltage was increased to 200 mV. After electrophoresis, the gel was washed for 5 min per wash, twice with 20% (v/v) isopropanol, and twice with 0.050 M Tris-HCl buffer, pH 7.0. The gel was then incubated for 30 min in an additional 35 mL of 0.050 M Tris-HCl buffer. Poly(C) remaining within the gel was stained with 0.2% (w/v) toluidine blue and destained with H_2O. Bands from ribonucleolytic activity where poly(C) is absent show up as clear to light blue against the deep purple background.

Results and Discussion

RNase A has eight cysteine residues in its amino acid sequence, which produce four disulfide bonds in the native protein. Site-directed mutagenesis has introduced a ninth cysteine at several different positions, including residues 1 (B. M. Fisher, personal communication), 19 (M. C. Hebert, personal communication), 41 (Chapter 2), and 88 (P.A.

Leland, personal communication). These protein variants all fold properly to yield proteins with a single free sulfhydryl at the desired position along with the eight native disulfides, and these new cysteine residues are available to react with a variety of sulfhydryl-specific reagents.

Disulfide-exchange is one type of reaction in which the newly introduced cysteine can participate, leaving the protein involved in an intermolecular disulfide bond. Intermolecular disulfide bonding is often remarkably reversible due to facility of thiol-disulfide interchange reactions (Raines, 1997). The modified protein is thus susceptible to reaction with secondary modifying reagents, as well as reduction to the protein bearing a free sulfhydryl. We have exploited this versatility, vis-à-vis position 41, to modulate the ribonucleolytic ability of RNase A. Scheme 5.1 shows the forms of K41C RNase A that have been prepared and studied

We have shown previously that the replacing Lys41 of RNase A with a cysteine residue reduces k_{cat}/K_m by nearly 10^5-fold and k_{cat} by 2×10^4-fold (Chapter 2). We have also shown that the introduction of a cationic proton-bearing amine by way of modification of Cys41 compensates for much of the lost catalytic activity. K41C RNase A is unstable if stored for long periods of time, presumably due to air oxidation, and consequently has been stored only after protection with Ellman's reagent (DTNB). The resultant nitrothiobenzoate-protected protein (K41C-NTB RNase A) contains the first disulfide in which Cys41 will participate. This protein reacts rapidly with cysteamine, releasing one equivalent of nitrothiobenzoate and creating K41C-csa RNase A. This reaction can be monitored by its absorbance at 412 nanometers. The reaction with 25 μM enzyme and a 2.5-fold molar excess of cysteamine was more than half complete after 2 minutes and more than 80% complete after 6 minutes. The value of k_{cat}/K_m for poly(C) cleavage for K41C-csa

RNase A is 1100-fold greater than that of K41C RNase A, while the value of k_{cat} is 130 times that of K41C RNase A (Table 5.1).

The stability of the engineered, intermolecular disulfide bond with cysteamine contrasts sharply with that of the native, intramolecular ones. Approximately 80% of RNase A molecules retain their native disulfide bonds after exposure to 0.10 M DTT for 2 h (1200-fold molar excess)(Li *et al.*, 1995). We have observed that DTT concentrations below 10 mM (700-fold molar excess) for 45 min have little or no effect on intramolecular disulfide bonds of K41C RNase A, as monitored by enzymatic activity. In contrast, the cysteamine disulfide bond can be removed completely with as little as 20 μM DTT (one equivalent) in less than 30 min. At higher levels of DTT, deactivation is even faster (Figure 5.1).

The simple removal of cysteamine from K41C-csa RNase A results in a large reduction in catalytic activity. To assess its practical utility, this deactivation method was tested in a ribonuclease protection assay (RPA). RPA's utilize a labeled piece of anti-sense RNA to probe for an RNA transcript of interest (Figure 5.2). Hybridization is followed by digestion of any unbound RNA, using a ribonuclease that is specific for single-stranded RNA. RNase A is such an enzyme. The labeled probe that has been protected from degradation by the presence of the cognate RNA is then isolated by gel electrophoresis and visualized by autoradiography. If ribonucleolytic activity is not adequately controlled after the digestion step, both prior to and during electrophoresis, the signal resulting from the protected probe will be lost. The standard protocol (Ausubel *et al.*, 1994) removes ribonucleolytic activity with a protease treatment (Proteinase K) followed by a phenol/$CHCl_3$ extraction. A commercially available RPA kit (Ambion, Austin, Texas) uses a method of inactivation that is a "trade secret." In order to test the effectiveness in an RPA of K41C-csa RNase A and subsequent reductive deactivation, whole mouse RNA was assayed with a ^{32}P-labeled RNA probe for actin mRNA (Figure 5.3). The Ambion

inactivation method was compared with DTT deactivation and with DTT deactivation plus phenol/$CHCl_3$ extraction. It is apparent that DTT deactivation is inadequate when used alone and useful only when coupled with phenol/$CHCl_3$ extraction. Even though K41C RNase A has many orders of magnitude less activity than does wild-type or K41C-csa RNase A, it is still too active of a catalyst to be tolerated in the RPA. DTT deactivation followed by phenol/$CHCl_3$ extraction appears to be roughly equivalent to Ambion's proprietary method and is probably also similar in effectiveness to a proteinase K treatment followed by phenol/$CHCl_3$ extraction.

The unique chemistry of the sulfhydryl at position 41 of K41C RNase A can be used as a target for additional modifications leading to more complete inactivation. We chose to do this by synthesizing a modification reagent that creates another disulfide, altering the protein again in a reversible fashion. (Irreversible modifications via alkylation reactions comprise another type of option, not explored here.) We have chosen to investigate the attachment of 3-mercaptopropyl-1-phosphate (MPP) to the sulfur of Cys41. Computer modeling indicated that the propyl linkage would allow the phosphoryl group of MPP to assume a position similar to that of inorganic phosphate or sulfate moieties observed in crystallographic studies. In order to attach MPP, 2,4-dinitrophenyl 3-phosphopropyl disulfide (**7**) was synthesized. Synthesis proceeded in three phases (Scheme 5.2). In the first two phases the MPP moiety was made by modifying 3-bromo-1-propanol, first with an appropriately protected thiol, then with a triazolephosphate. After the triazole groups had been removed, the final phase created the desired disulfide, by using 2,4-dintrophenyl-sulfenylchloride to replace the protecting group on the sulfur of MPP.

Compound **7** reacts readily with Cys41. K41C RNase A was reacted with a 10-fold molar excess of **7**, and the reaction was 90% complete within 25 minutes. K41C-MPP was isolated from any traces of unreacted protein by an additional cation exchange step.

Zymogram analysis of K41C-MPP RNase A indicates that this protein has significantly less ribonucleolytic activity than does K41C RNase A (Figure 5.4).

Spectrophotometric assays of poly(C) cleavage were used in an attempt to quantify the residual catalytic activity and assess kinetic parameters. Changes in absorbance were followed over 5 h. Rates of increase in absorbance were consistently greater than instrumental drift, but instrumental drift severely impacted the reproducibility of the measurements. The measured rates averaged 4(±1)% of the rates expected for the K41C enzyme under identical conditions. However, no steady-state kinetic parameters were determined because of the technical problems associated with the lack of assay sensitivity. If the effect of adding MPP to K41C RNase A is assumed only to be on K_m, the effective molarity of inorganic phosphate can be computed by rearranging the equation describing competitive inhibition. Specifically,

$$v = \frac{k_{cat} \times E \times S}{K_m\left(1 + {}^{[I]}\!/_{K_{ph}}\right)}$$

can be rearranged to give

$$[I] = (k_{cat} \times E \times S \times K_{ph}/(K_m \times v)) - (S \times K_{ph}/K_m) - K_{ph}$$

where K_{ph} is the inhibition constant of phosphate and [I] is the effective molarity of inorganic phosphate at the active site. If the inhibition constant of inorganic phosphate (K_{ph}) is taken to be 4.6 mM (Anderson *et al.*, 1968) and the previously determined K41C RNase A kinetic parameters are used (Chapter 2), the average effective molarity associated with

the measured rates of poly(C) cleavage is 0.3 M. This value can be compared with the actual molarity of the phosphoryl group of MPP, which was equivalent to [E] and ranged from 0.7 to 3.5 μM in these experiments.

Once K41C RNase A has been modified with MPP, the noncovalent interactions with the phosphate group appear to markedly increase the stability of the intermolecular disulfide bond. DTT and β-mercaptoethanol were used over a range of conditions that are benign to the K41C protein in attempts to remove the MPP group. At low and moderate ionic strengths, no increase in activity was observed by zymogram analysis after incubation with up 2 mM DTT for up to 24 h. Even in the presence of 1 M inorganic phosphate and 0.10 mM DTT, no measurable gain in activity was observable. At a very high phosphate concentration (2.5 M) and 2 mM DTT, a gain of activity comparable to 10-30% reversal to K41C was observed over 90 minutes.

Conclusion

The unique reactivity of the sulfhydryl group allows for rapid and specific control of enzymatic activity. The activity of K41C RNase A has been increased 1100-fold by modification with cysteamine, and decreased 25-fold by modification with 3-mercaptopropyl-1-phosphate. The activity can thus be readily modulated over a range spanning a factor of $10^{4.4}$. An analogous control mechanism could concievably be installed into the active site of any enzyme of known three-dimensional structure if an essential amino acid functional group is available for replacement with a cysteine.

Acknowledgement

The chemical synthesis of **7** was designed and implemented by Dr. Steven K. Holmgren with assistance from Ms. Juneko E. Grilley and helpful advice from Dr. Cathy L. Dantzman. These contributions were integral to the success of this work and are deeply appreciated.

Scheme 5.1 Overall scheme of modifications activating and deactivating K41C RNase A.

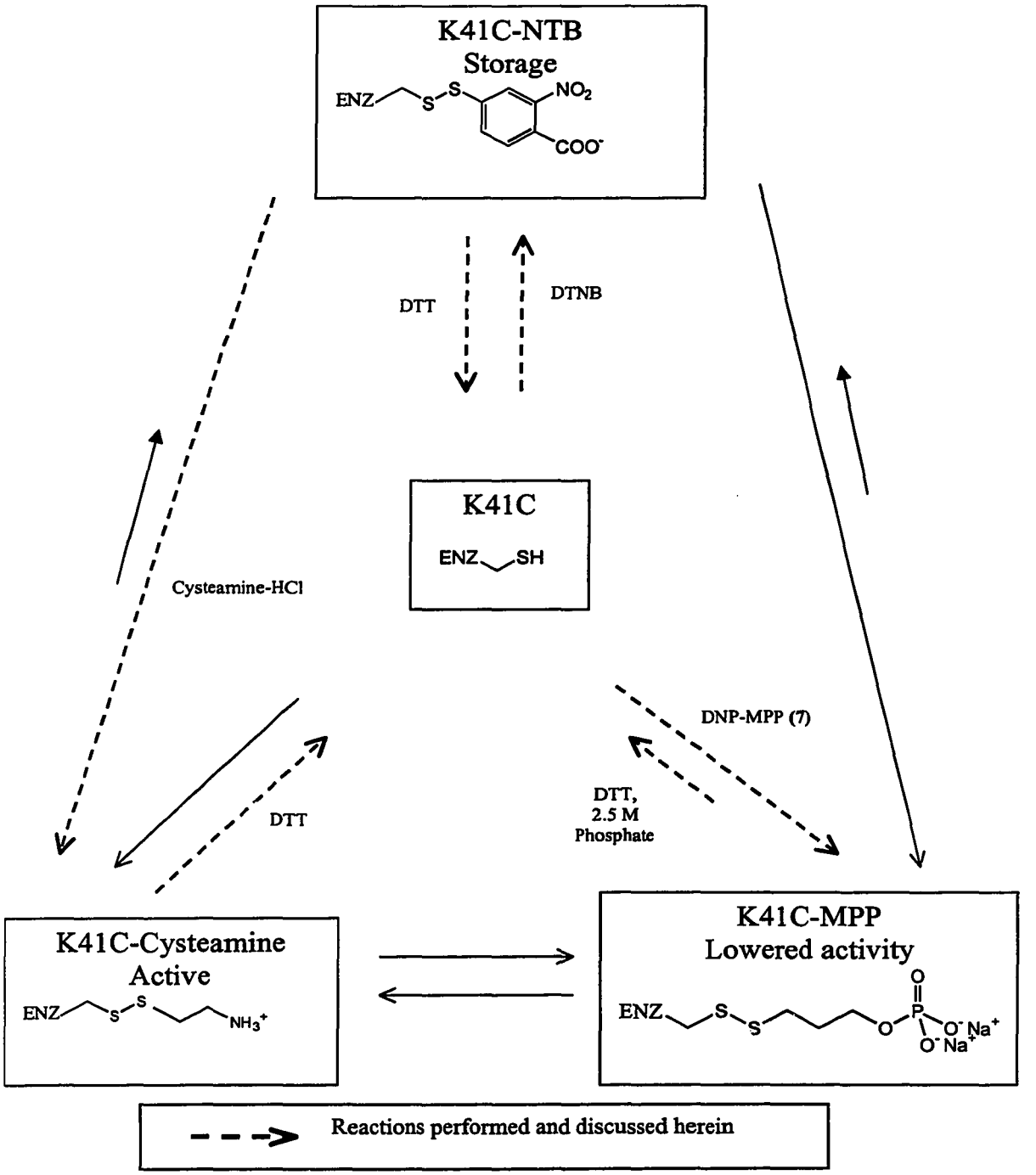

Scheme 5.2 Synthesis of Dinitrophenyl 3-Phosphopropyl Disulfide.

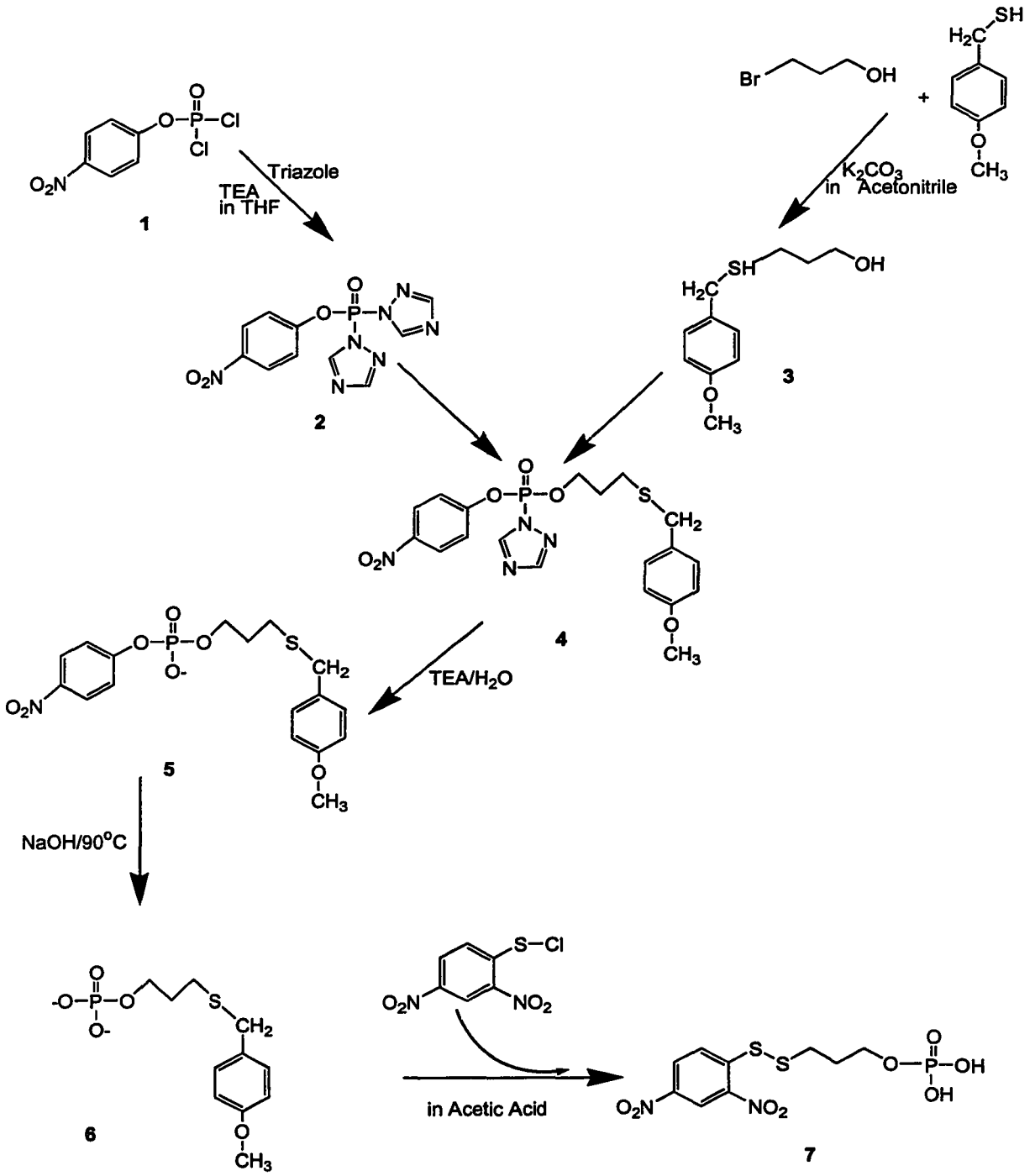

Table 5.1: Steady-State Kinetic Parameters for Catalysis of Poly(C) Cleavage by K41C Ribonuclease A before and after Cysteamine Modification[a].

RNase A	k_{cat} (s^{-1})	K_m (mM)	k_{cat}/K_m ($M^{-1} \times s^{-1}$)	$\Delta\Delta G_{tx}$ (kcal/mol) [c]
wild-type	604 ± 47	0.091 ± 0.022	$(6.5 \pm 1.2) \times 10^6$	0.0
K41C	0.026 ± 0.004	0.36 ± 0.12	$(7.3 \pm 1.5) \times 10$	6.8
K41C-csa	3.6 ± 0.1	0.043 ± 0.009	$(8.5 \pm 1.5) \times 10^4$	2.6

[a] Data were obtained at 25 °C in 0.10 M MES buffer, pH 6.0, containing NaCl (0.10 M).
[c] $\Delta\Delta G_{tx} = RT \ln (k_{cat}/K_m)_{w.t.}/(k_{cat}/K_m)_{variant}$.

Figure 5.1 DTT deactivation of K41C-csa RNase A. Protein was present at 20 μM. Reaction in 50 mM HEPES, pH 7.7, 25 °C. Two levels of DTT were tested: 20 mM (△), and 320 mM (●).

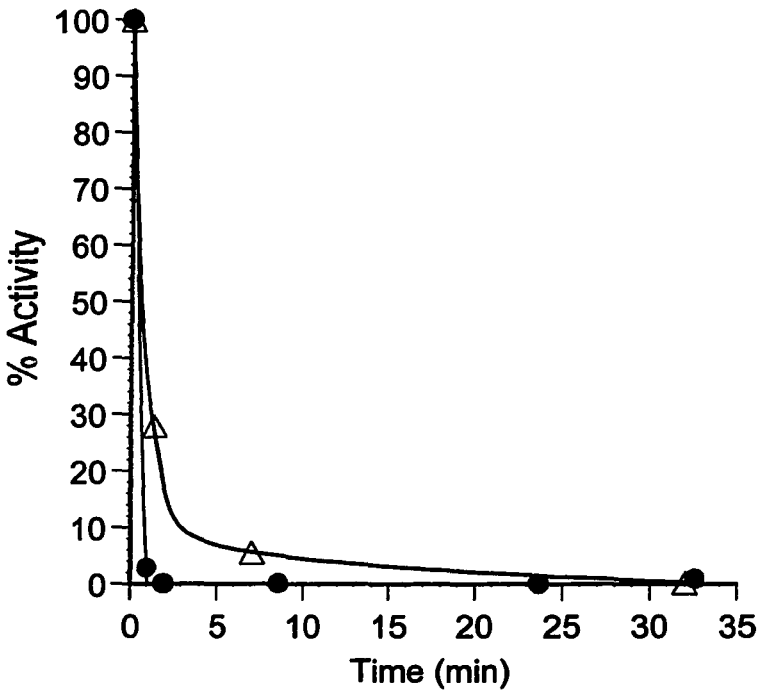
100
90
80
70
60
50
40
30
20
10
0
% Activity
0
5
10
15
20
25
30
35
Time (min)

Figure 5.2 The Ribonuclease Protection Assay (RPA). In an RPA, a labeled probe is hybridized in solution with an RNA sample containing the target RNA. This step is generally performed overnight. After the hybridization step, excess single-stranded (ss) probe molecules are degraded by ribonuclease treatment. Probe molecules hybridized to target molecules are protected from the action of ribonuclease by virtue of being in a double-stranded complex with their cognate target RNA. Protected molecules are then seperated on an acrylamide gel and visualized by autoradiography.*

* Adapted from the Ambion Catalog, Ambion Inc., Austin, Texas

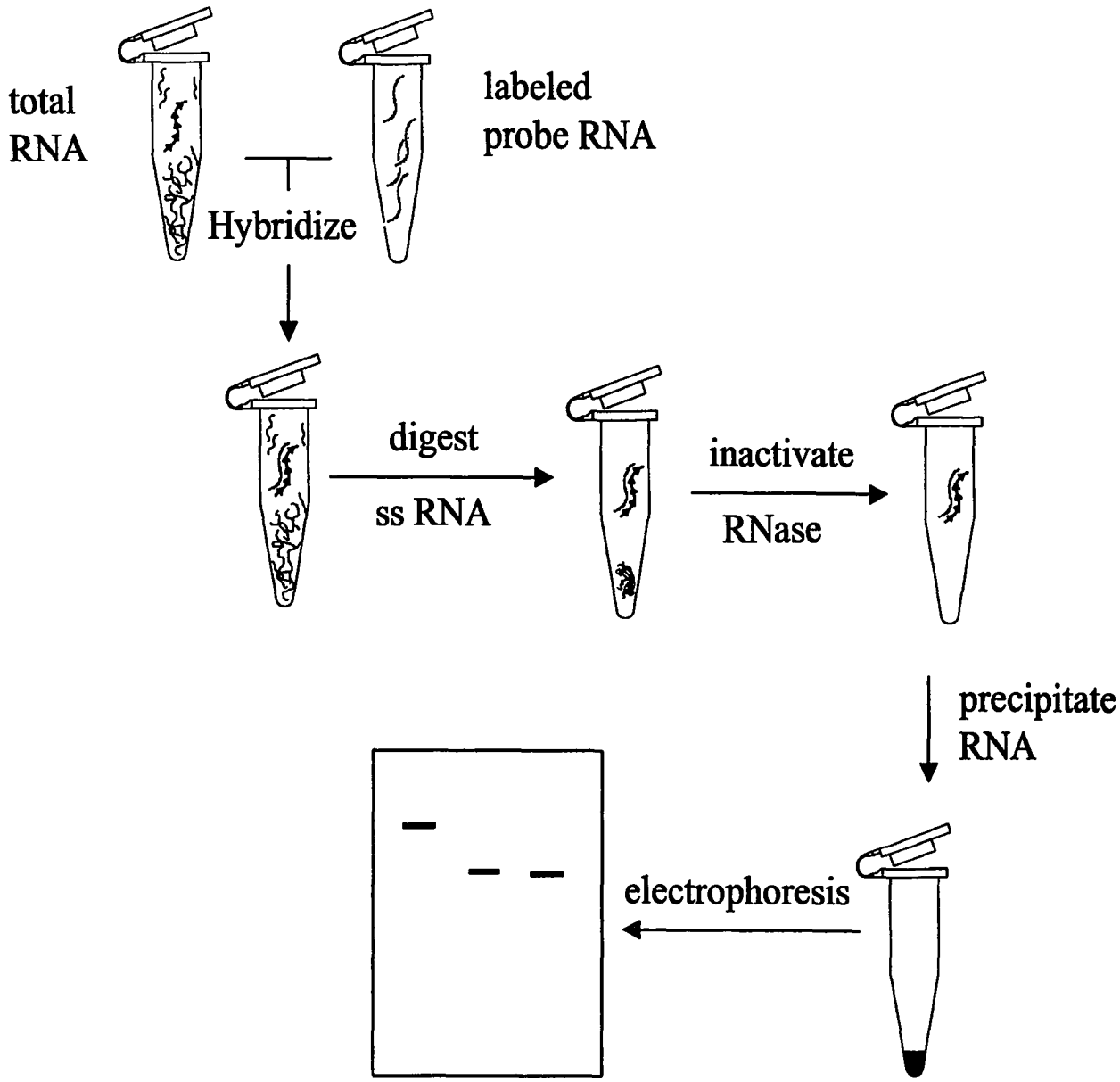
total
RNA
labeled
probe RNA
Hybridize
digest
ss RNA
inactivate
RNase
precipitate
RNA
electrophoresis

Fig 5.3 Autoradiogram probing for the protection of an antisense probe specific for β-actin mRNA. Lanes A, B, and C compare three methods of removing K41C-csa ribonuclease A prior to electrophoresis.

Lane	Probe	Total RNA	Ribonuclease A	Inactivation
A	Mouse β-actin	Mouse	K41C-csa	DTT followed by phenol/$CHCl_3$
B	Mouse β-actin	Mouse	K41C-csa	DTT
C	Mouse β-actin	Mouse	K41C-csa	Dx solution*
D	Mouse β-actin	Mouse	wild-type A plus RNase T1	Dx solution*
E	Mouse β-actin	Yeast	K41C-csa	Dx solution*
F	Mouse β-actin	Yeast	wild-type A plus RNase T1	Dx solution*
G	Mouse β-actin	Yeast	None	Dx solution*

* Dx solution is sold by Ambion, Inc. and is a proprietary formulation for which little information is available

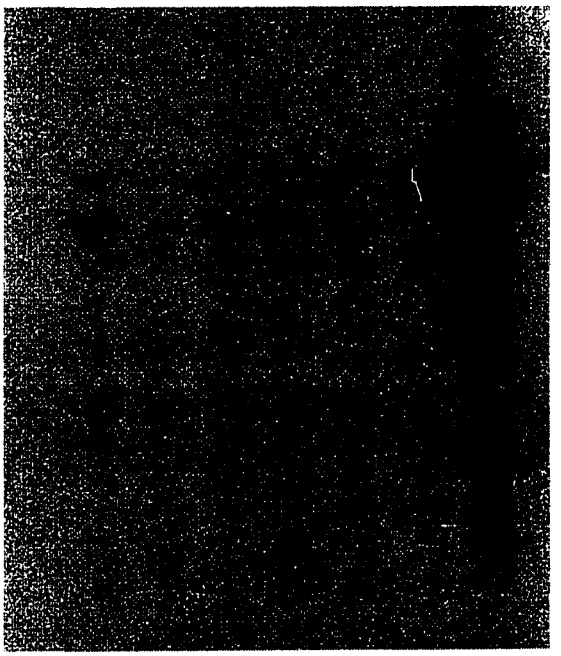

A B C D E F G

Fig 5.4 Zymogram electrophoresis of K41C ribonuclease A and K41C-MPP ribonuclease A. Lane A: 0.4 μg of K41C RNase A. Lane B: 10 μL of Mono S column eluent (negative control). Lane C: empty. Lane D: 0.4 μg of chromatographically purified K41C-MPP RNase A.

A B C D

Bibliography

Alber, T., Gilbert, W., Ponzi, D. & Petsko, G. (1982). The Role of Mobility in Substrate Binding and Catalytic Machinery of Enzymes. In *Mobility and Function in Proteins and Nucleic Acids* (R. Porter, M. D. O'Connor & J. Whelan, Ed.), pp. 4-24, Pitman, London.

Albert, A., Goldacre, R. & Phillips, J. (1948). The Strength of Heterocyclic Bases. *J. Chem. Soc.* **III**, 2240-2249.

Allinger, N. L., Yuh, Y. H. & Lii, J.-H. (1989). Molecular Mechanics. The MM3 Force Field for Hydrocarbons. *J. Am. Chem. Soc.* **111**, 8551-8556.

Anderson, D. G., Hammes, G. C. & Walz, F. G. J. (1968). Binding of Phosphate Ligands to Ribonuclease A. *Biochemistry* **7**, 1637-1645.

Anfinsen, C. B. (1973). Principles that govern the folding of protein chains. *Science* **181**, 223-230.

Angus-Dunne, S. J., Batchelor, R. J., Tracey, A. S. & Einstein, F. W. B. (1995). The Crystal and Solution Structure of the Major Products of the Reaction of Vanadate with Adenosine. *J. Am. Chem Soc.* **117**, 5292-5296.

Anonov, I. V., Gurevich, A. Z., Dudkin, S. M., Karpiesky, M. A. & Sakhorovsky, V. G. (1978). Complexes of Ribonuclease A with 2'-Deoxy-2'Fluororibose Substrate Analogs Studied by Nuclear Magnetic Resonance. *Eur. J. Biochem* **87**, 45-54.

Ausubel, F. M., Brent, R., Kingston, R. E., Moore, D. D., Seidman, J. G., Smith, J. A. & Struhl, K., Eds., *Current Protocols in Molecular Biology Volume 1* , vol. 1 (John Wiley & Sons, Boston, 1994).

Barnard, E. A. (1969). Biological function of pancreatic ribonuclease. *Nature* **221**, 340-344.

Barnard, E. A. & Stein, W. D. (1959). The Histidine Residue in the Active Centre of Ribonuclease, I.A Specific Reaction with Bromoacetic Acid. *J. Mol. Biol.* **1**, 339-358.

Bartlett, P. A. & Marlowe, C. K. (1983). Phosphonamidates as Transition-State Analogue Inhibitors of Thermolysin. *Biochemistry* **22**, 4618-4624.

Baumann, W. K., Bizzozero, S. A. & Dutler, H. (1970). Specificity of alpha-Chymotrypsin. Dipeptide Substrates. *FEBS Lett.* **8**, 257-260.

Beaven, G. H., Holiday, E. R. & Johnson, E. A. (1955). Optical Properties of Nucleic Acids and Their Components. In *The Nucleic Acids* (E. Chargraff, Davidson, J. N., Ed.), pp. 493-553, Academic Press, Inc., New York, NY.

Beintema, J. (1987). Structure, properties and molecular evolution of pancreatic-type ribonucleases. *Life Chem. Rep.* **4**, 333-389.

Berger, S. L. & Birkenmeier, C. S. (1979). Inhibition of Intractable Nucleases with Ribonucleoside-Vanadyl Complexes: Isolation of Messenger Ribonucleic Acid from Resting Lymphocytes. *Biochemistry* **18**, 5143-5149.

Bevington, P. R. (1969). *Data Reduction and Error Analysis for the Physical Sciences*, McGraw-Hill, New York.

Blank, A., Sugiyama, R. H. & Dekker, C. A. (1982). Activity staining of nucleolytic enzymes after SDS-PAGE: use of aqueous isopropanol to remove detergent from gels. *Anal. Biochem.* **120**, 267-275.

Borah, B., Chen, C., Egan, W., Miller, M., Wlodawer, A. & Cohen, J. S. (1985). Nuclear magnetic resonance and neutron diffraction studies of the complex of ribonuclease A with uridine vanadate, a transition-state analogue. *Biochemistry* **24**, 2058-2067.

Bordwell, F. G. (1988). Equilibrium Acidities in Dimethyl Sulfoxide Solution. *Acc. Chem. Res.* **21**, 456-463.

Boyd, D. B., Kustin, K. & Niwa, M. (1985). Do Vanadate Polyanions Inhibit Phosphotransferase Enzymes? *Biochim. Biophys. Acta* **827**, 472-475.

Breslow, R. (1991). How do imidazole groups catalyze the cleavage of RNA in enzyme models and in enzymes? Evidence from "negative catalysis". *Acc. Chem. Res.* **24**, 317-324.

Breslow, R. & Labelle, M. (1986). Sequential General Base-Acid Catalysis in the Hydrolysis of RNA by Imidazole. *J. Am. Chem. Soc.* **108**, 2655-2659.

Brown, D. M. & Todd, A. R. (1955). Evidence on the Nature of Chemical Bonds in Nucleic Acids. In *The Nucleic Acids* (E. Chargraff, Davidson, J. N., Ed.), pp. 3-7, Academic Press, Inc., New York, NY.

Brown, L. R. & Bradbury, J. H. (1976). The Role of Lysine-41 in Ribonuclease A Studied by Proton-Magnetic-Resonance Spectroscopy of Guanidinated Ribonuclease A. *Eur. J. Biochem* **68**, 227-235.

Bruenger, A., Brooks III, C. & Karplus, M. (1985). Active site dynamics of ribonuclease. *Proc. Natl. Acad. Sci. USA* **82**, 8458-8462.

Calnan, B. J., Tidor, B., Biancalana, S., Hudson, D. & Frankel, A. D. (1991). Arginine-Mediated RNA Recognition: The Arginine Fork. *Science* **252**, 1168-1171.

Chargraff, E., Davidson, J. N. (1955). Introduction. In *The Nucleic Acids* (E. Chargraff, Davidson, J. N., Ed.), pp. 3-7, Academic Press, Inc., New York, NY.

Choate, G. & Mansour, T. E. (1979). Studies on Heart Phosphofructokinase, Decavanadate as a Potent Allosteric Inhibitor at Alkaline and Acidic pH. *J. Biol. Chem.* **254**, 11457-11462.

Cleland, W. W. (1979). Statistical analysis of enzyme kinetic data. *Methods Enzymol.* **63**, 103-138.

Cleland, W. W. & Hengge, A. C. (1995). Mechanisms of Phosphoryl and Acyl Transfer. *FASEB J.* **9**, 1585-1594.

Crans, D. C. (1994). Enzyme Interactions with Labile Oxovanadates and Other Polyoxometalates. *Comments Inorg. Chem.* **16**, 35-76.

Crans, D. C. (1995). Interactions of Vanadates with Biogenic Ligands. In *Metal Ions in Biological Systems; Vanadium and Its Role in Life* (H. Sigel & S. A., Ed.), pp. 147-209, Marcel Dekker, Inc., NY.

Crestfield, A. M. & Stein, W. H. (1963). Alkylation and identification of the Histidine residues at the active site of ribonuclease. *J. Biol. Chem.* **238**, 2413.

Dantzman, C. L. & Kiessling, L. L. (1996). Reactivity of a 2'-Thio Nucleotide Analog. *J. Am. Chem. Soc.* **118**, 11715-11719.

Davis, A. M., Hall, A. D. & Williams, A. (1988). Charge Description of Base-Catalyzed Alcoholysis of Aryl Phosphodiesters: A Ribonuclease Model. *J. Am. Chem. Soc.* **110**, 5105-5108.

Deavin, A., Mathias, A. P. & Rabin, B. R. (1966). Mechanism of Action of Pancreatic Ribonuclease. *Biochem. J.* **101**, 14c-16c.

del Rosario, E. J. & Hammes, G. G. (1970). Relaxation Spectra of Ribonuclease. VII. Interaction of Ribonuclease with Uridine 2',3'-Cyclic Phosphate. *J. Am. Chem. Soc.* **92**, 1750.

delCardayre, S. B. & Raines, R. T. (1994). Structural Determinants of Enzymatic Processivity. *Biochemistry* **33**, 6032-6037.

delCardayre, S. B., Ribo, M., Yokel, E. M., Quirk, D. J., Rutter, W. J. & Raines, R. T. (1995). Engineering ribonuclease A: production, purification, and characterization of wild-type enzyme and mutants at Gln 11. *Protein Eng.* **8**, 261-273.

Eckstein, F. (1968). Uridine 2',3' -OO-Cyclophosphorothioate as Substrate for Pancreatic Ribonuclease. *FEBS Lett.* **2**, 85-86.

Eftink, M. R. & Biltonen, R. L. (1983). Energetics of Ribonuclease A Catalysis. 1. pH, Ionic Strength, and Solvent Isotope Dependence of the Hydrolysis of Cytidine Cyclic 2',3'- Phosphate. *Biochemistry* **22**, 5123-5134.

Eftink, M. R. & Biltonen, R. L. (1983). Energetics of Ribonuclease A Catalysis. 2. Nonenzymatic Hydrolysis of Cytidine Cyclic 2',3'-Phosphate. *Biochemistry* **22**, 5134-5140.

Eftink, M. R. & Biltonen, R. L. (1987). Pancreatic ribonuclease A: The most studied endoribonuclease. In *Hydrolytic Enzymes* (A. Neuberger & K. Brocklehurst, Ed.), pp. 333-375, Elsevier, New York.

Eun, H.-M. (1996). *Enzymology Primer for Recombinant DNA Technology*, Academic Press, San Diego.

Fersht, A. (1985). *Enzyme Structure and Mechanism*, Freeman, New York.

Fersht, A. R., Shi, J.-P., Knill-Jones, J., Lowe, D. M., Wilkinson, A. J., Blow, D. M., Brick, P., Arter, P., Waye, M. M. Y. & Winter, G. (1985). Hydrogen bonding and biological specificity analysed by protein engineering. *Nature* **314**, 235-238.

Findlay, D., Herries, D. G., Mathias, A. P., Rabin, B. R. & Ross, C. A. (1961). The Active Site and Mechanism of Action of Bovine Pancreatic Ribonuclease. *Nature* **190**, 781-784.

Findlay, D., Herries, D. G., Mathias, A. P., Rabin, B. R. & Ross, c. a. (1962). The Active Site and Mechanism of action of Bovine Pancreatic Ribonuclease. 7. The Catalytic Mechanism. *Biochem. J.* **85**, 152-153.

Finn, F. M. & Hofmann, K. (1965). Studies of polypeptides. XXXIII. Enzymic Properties of Partially Synthetic Ribonuclease. *J. Am. Chem. Soc.* **87**, 645-647.

Fisher, B. M., Schultz, L. W. & Raines, R. T. (1998). Coloumbic Effects of Remote Subsites On the Active Site of Ribonuclease A. *Biochemistry* **37**, 17386-17401.

Gellman, S. H. (1991). On the Role of Methionine Residues in the Sequence-Independent Recognition of Nonpolar Surfaces. *Biochemistry* **30**, 6633-6636.

Gerlt, J. A. & Gassman, P. G. (1993). Understanding the rates of certain enzyme-catalyzed reactions: proton abstraction from carbon acids, acyl-transfer reactions, and displacement reactions of phosphodiesters. *Biochemistry* **32**, 11943-11952.

Gloss, L. & Kirsch, J. (1995). Examining the Structural and Chemical Flexibility of the Active Site Base, Lys-258, of E coli Aspartate Aminotransferase by Replacement with Unnatural Amino Acids. *Biochemistry* **34**, 1323-12332.

Goddard, J. B. & Gonas, A. M. (1973). Kinetics of the Dissociation of Decavanadate Ion in Basic Solution. *Inorg. Chem.* **12**, 574-579.

Gresser, M. J. & Tracey (1986). Vanadium (V) Oxyanions: Formation of Cyclic Esters with Ethylene Glycol. *J. Am. Chem. Soc.* **108**, 1935.

Gundlach, H. G., Stein, W.H., Moore, S. (1959). The Nature of the Amino Acid Residues Involved in the Inactivation of Ribonuclease by Iodoacetate. *J. Biol. Chem.* **234**, 1754.

Hallick, R. B., Chelm, B. K., Gray, P. W. & Orozco, E. M. J. (1977). The Use of Aurintricarboxylic Acid as an Inhibitor of Nucleases During Nucleic Acid Isolation. *Nucleic Acids Res.* **4**, 3055-3064.

Hanson, J. E., Kaplan, A. P. & Bartlett, P. A. (1989). Phosphonate Inhibitors of Carboxypeptidase A. *Biochemistry* **28**, 6294-6305.

Hine, J. (1975). Structural Effects on Equilibria in Organic Chemistry. In pp. 200, Wiley Interscience, New York.

Hirs, C. H. W., Moore, S., Stein, W.H. (1953). A Chromatographic Investigation of Pancreatic Ribonuclease. *J. Biol. Chem.* **200**, 493-506.

Hirs, C. H. W., Halmann, M. & Kycia, J. H. (1961). The Reactivity of Certain Functional Groups in Ribonuclease A towards Substitution by I-Fluoro-2,4-dinitrobenzene. Inactivation of the Enzyme by Substitution at the Lysine Residue in Position 41. In *Biological Structure and Function. Proceedings of the First*

IUB/IUBS International Symposium (T. W. Goodwin, Lindberg, O., Ed.), pp. 41-57, Academic Press, London.

Hirs, C. H. W., Moore, S. & Stein, W. H. (1960). The Sequence of the Amino Acid Residues in Performic Acid-oxidized Ribonuclease. *J. Biol. Chem.* **235**, 633-647.

Hummel, C. F., Pincus, M. R., Brandt-Rauf, P. W., Frei, G. M. & Carty, R. P. (1987). Reaction of (Bromoacetamido)nucleoside Affinity Labels with Ribonuclease A: Evidence for Steric Control of Reaction Specificity and Alkylation Rate. *Biochemistry* **26**, 135-146.

Jackson, D. Y., Burnier, J., Quan, C., Stanley, M., Tom, J. & Wells, J. A. (1994). A Designed Peptide Ligase for Total Synthesis of Ribonuclease A with Unnatural Catalytic Residues. *Science* **266**, 243-247.

Jencks, W. P. (1966). Current Aspects of Biochemical Energetics. In *Current Aspects of Biochemical Energetics* (N. O. Kaplan & E. P. Kennedy, Ed.), pp. 273-298, Academic, New York.

Jencks, W. P. (1987). Catalysis in Chemistry and Enzymology. In pp. 338, Dover, Mineola, NY.

Jentoft, J. E., Gerken, T. A., Jentoft, N. & Dearborn, D. G. (1981). [^{13}C] Methylated Ribonuclease A; Studies of the Interaction of Lysine 41 with Active Site Ligands. *J. Biol. Chem.* **256**, 231-236.

Johnson, R., Joshi, B. V. & Reese, C. B. (1994). Synthesis of 2' , 3' Dithiouridine. *J. Chem. Soc., Chem. Commun.* , 133-134.

Jones, W. (1920). The Action of Boiled Pancreas Extract on Yeast Nucleic Acid. *Amer. J. Physiol.* **52**, 203-207.

Jubian, V., Dixon, R. P. & Hamilton, A. D. (1992). Molecular recognition and catalysis. Acceleration of phosphodiester cleavage by a simple hydrogen-bonding receptor. *J. Am. Chem. Soc.* **114**, 1120-1121.

Kahne, D. & Still, W. C. (1988). Hydrolysis of a Peptide Bond in Neutral Water. *J. Am. Chem. Soc.* **110**, 7529-7534.

Kartha, G., Bello, J. & Harker, D. (1967). Tertiary Structure of Ribonuclease. *Nature* **213**, 862-865.

Kezdy, F. J. & Bender, M. L. (1962). The Kinetics of the Chymotrypsin-Catalyzed Hydrolysis of p-Nitrophenyl Acetate. *Biochemistry* **1**, 1097-1103.

Knowles, J. R. (1987). Tinkering with Enzymes: What Are We Learning. *Science* **236**, 1252-1258.

Kraszewski, A. & Stawinski, J. (1980). Phosphoryl Tris-Triazole - A New Phosphorylating Reagent. *Tetrahedron Lett.* **21**, 2935-2936.

Krauss, M. & Basch, H. (1992). Is the Vanadate Anion an Analogue of the Transition State of RNase A. *J. Am. Chem. Soc.* **114**, 3630-3634.

Kunitz, M. (1939). Isolation from beef pancreas of a crystalline protein possessing ribonuclease activity. *Science* **90**, 112-113.

Kunkel, T. A., Roberts, J. D. & Zakour, R. A. (1987). Rapid and efficient site-specific mutagenesis without phenotypic selection. *Methods Enzymol.* **154**, 367-382.

Laity, J. H., Shimotakahara, S. & Scheraga, H. A. (1993). Expression of wild-type and mutant bovine pancreatic ribonuclease A in *Escerichia coli*. *Proc. Natl. Acad. Sci. USA* **90**, 615-619.

Leon-Lai, C. H., Gresser, M. J. & Tracey, A. S. (1996). Influence of vanadium (V) complexes on the catalytic activity of ribonuclease A. The role of vanadate complexes as transition state analogues to reactions of phosphate. *Can. J. Chem.* **74**, 38-48.

Li, Y.-J., Rothwarf, D. M. & Scheraga, H. A. (1995). Mechanism of Reductive Protein Unfolding. *Nature Struct. Biol.* **2**, 489-494.

Lide, D. R., ed. (1994). Handbook of Chemistry and Physics. In *Handbook of Chemistry and Physics* (D. R. Lide, Ed.), pp. 9-31, 9-37, CRC Press, Boca Raton, FL, USA.

Lindquist, R. N., Lynn Jr, J. L. & Lienhard, G. E. (1973). Possible transition-state analogs for ribonuclease. The complexes of uridine with oxovanadium(IV) ion and vanadium(V) ion. *J. Am. Chem. Soc.* **95**, 8762-8768.

Lolis, E. & Petsko, G. A. (1990). Transition-State Analogues in Protein Crystallography: Probes of the Structural Source of Enzyme Catalysis. *Annu. Rev. Biochem.* **59**, 597-630.

Manning, J. M. (1993). The Contributions of Stein and Moore to Protein Science. *Protein Science* **2**, 1188-1191.

Markham, R. & Smith, J. D. (1952). The Structure of Ribonucleic Acids. 2. The Smaller Products of Ribonuclease Digestion. *Biochem. J.* **52**, 558-565.

Meot-Ner, M. (1984). The Ionoc Hydrogen Bond and Ion Solvation. 1. NH···O, NH···N, and OH···O Bonds. Correlation with Proton Affinity. Deviation due to Structural Effects. *J. Am. Chem. Soc.* **106**, 1257-1264.

Messmore, J. M., Fuchs, D. N. & Raines, R. T. (1995). Ribonuclease A: Revealing Structure-Function Relationships with Semisynthesis. *J. Am. Chem. Soc.* **117**, 8057-8060.

Miranda, R. R., Expression and site-specific mutagenesis of rat pancreatic ribonuclease, Massachusetts Institute of Technology, Cambridge, MA (1990).

Moore, S. & Stein, W. H. (1973). Chemical structures of pancreatic ribonuclease and deoxyribonuclease. *Science* **180**, 458-464.

Nambiar, K. P., Stackhouse, J., Presnell, S. R. & Benner, S. A. (1987). Expression of bovine pancreatic ribonuclease A in *Escherichia coli. Eur. J. Biochem.* **163**, 67-71.

Neurath, H. (1995). The Golden Years of Protein Science. *Protein Sci.* **4**, 1939-1940.

Nicholls, A. & Honig, B. (1991). A Rapid Finite Algorithm, Utilizing Successive Over-Relaxation to Solve the Poisson-Boltzmann Equation. *J. Comp. Chem* **12**, 435-445.

Parés, X., Nogués, M. V., de Llorens, R. & Cuchillo, C. M. (1991). Structure and function of ribonuclease A binding subsites. *Essays Biochem.* **26**, 89-103.

Pauling, L. (1948). Nature of Forces Between Large Molecules of Biological Interest. *Nature* **161**, 707-709.

Pease, M. D., Serpersu, E. H. & Mildvan, A. S. (1987). Chemical Modification and Spin-Labelling Studies of the Arg 87 to Cys (R87C) Mutant of Staphylococcal Nuclease. *Fed. Proc.* **46**, 1932.

Petterson, L. (1994). Equilibria of Polyoxometalates in Aqueous Solution. In *Polyoxometalates: From Platonic Solids to Anti-Retroviral Activity* (M. T. Pope & M. A., Ed.), pp. 27-40, Kluwer Academic Publishers, Dordrecht, Netherlands.

Petterson, L., Hedman, B., Andersson, I. & Ingri, N. (1983). Multicomponent Polyanions 34. A Potentiometric and 51V NMR Study of Equilibria in the H-HVO4. *Chemica Scripta* **22**, 254-264.

Phillips, M. A., Kaplan, A. P., Rutter, W. J. & Bartlett, P. A. (1992). Transition-Sate Characterization: A New Approach Combining Inhibitor Analogues and Variation in Enzyme Structure. *Biochemistry* **31**, 959-963.

Planas, A. & Kirsch, J. F. (1990). Sequential Protection-Modification Method for Selective Sulfhydryl Group Derivitization in Proteins having More the One Cysteine. *Protein Eng.* **3**, 625-628.

Planas, A. & Kirsch, J. F. (1991). Reengineering the Catalytic Lysine of Aspartate Aminotransferase by Chemical Elaboration of a Genetically Introduced Cysteine. *Biochemistry* **30**, 8268-8276.

Plummer, T. H., Hirs, C. H. W. (1964). On the Structure of Bovine Pancreatic Ribonuclease B. Isolation of a Glycopeptide. *J. Biol. Chem.* **239**, 2530-2538.

Pope, M. T. & Muller, A. (1994). Introduction. In *Polyoxometalates: From Platonic Solids to Anti-retroviral Activity* (M. T. Pope & A. Muller, Ed.), pp. 2-26, Klewer Academic Publishers, Dordrecht, The Netherlands.

Poulson, R. (1977). Isolation, Purification, and Fractionation of RNA. In *The Ribonucleic Acids, second edition* (P. R. Stewart & D. S. Letham, Ed.), pp. 333-337, Springer-Verlag, New York.

Radzicka, A. & Wolfenden, R. (1996). Rates of Uncatalyzed Peptide Bond Hydrolysis in Neutral Solution and the Transition State Affinity of Proteases. *J. Am. Chem. Soc.* **118**, 6105-6109.

Raines, R. T. (1997). Nature's Transitory Covalent Bond. *Nature Struct. Biol.* **4**, 424-427.

Raines, R. T. & Kim, J.-S. (1993). Ribonuclease S-peptide as a Carrier in Fusion Proteins. *Protein Sci.* **2**, 248-356.

Raines, R. T. & Rutter, W. J. (1989). Protein engineering of ribonuclease A. In *Stucture and Chemistry of Ribonucleases, Proceedings of the First International Meeting* (A. G. Pavlovsky & K. Polyakov, Ed.), pp. 95-100, USSR Academy of Sciences, Moscow.

Ray, W. J., Crans, D. C., Zheng, J., Burgner II, J. W., Deng, H. & Mahroof-Tahir, M. (1995). Structure of the Dimeric Ethylene Glycol-Vanadate Complex and Other 1.2-Diol-Vanadate Complexes in Aqueous Solution: Vanadate-Based Transition-State Analog Complexes of Phosphotransferases. *J. Am. Chem. Soc.* **117**, 6015-6026.

Rehder, D. (1995). Inorganic Considerations on the Function of Vanadium in Biological Systems. In *Metal Ions in Biological Systems; Vanadium and Its Role in Life* (H. Sigel & S. A., Ed.), pp. 147-209, Marcel Dekker, Inc., NY.

Richards, F. M. (1992). Linderstrom-Lang and the Carlsberg Laboratory: The view of a post-doctoral fellow in 1954. *Protein Sci.* **1**, 1721-1730.

Richards, F. M. & Vithayathil, P. J. (1959). The preparation of subtilisin-modified ribonuclease and the separation of the peptide and protein components. *J. Biol. Chem.* **234**, 1459-1465.

Richards, F. M. & Wyckoff, H. W. (1971). Bovine pancreatic ribonuclease. In *The Enzymes* (P. D. Boyer, Ed.), pp. 647-806, Academic Press, New York.

Richardson, R. M., Parés, X. & Cuchillo, C. M. (1990). Chemical modification by pyridoxal 5'-phosphate and cyclohexane-1,2-dione indicates that Lys-7 and Arg-10 are involved in the p_2 phosphate-binding subsite of bovine pancreatic ribonuclease A. *Biochem. J.* **267**, 593-599.

Richter, J. & Rehder, D. (1991). Modeling the Transition State of Biological Phosphoester Cleavage: The Complexation of Vanadate (V) by Nucleosides. *Z. Naturforschung* **46b**, 1613-1620.

Roberts, D. V. (1977). *Enzyme Kinetics*, Cambridge University Press, London.

Roberts, G. C. K., Dennis, E. A., Meadows, D. H., Cohen, J. S. & Jardetsky, O. (1969). The Mechanism of Action of Ribonuclease. *Proc. Natl. Acad. Sci. USA* **62**, 1151-1158.

Saenger, W. (1991). Structure and catalytic function of nucleases. *Current Opin. Struct. Biol.* **1**, 130-138.

Schaefer, F. C. & Peters, G. A. (1961). Base-Catalyzed Reaction of Nitriles with Alcohols. A Convenient Route to Imidates and Amidine Salts. *J. Org. Chem.* **26**, 412-418.

Schultz, L. W., Quirk, D. J. & Raines, R. T. (1998). His···Asp Catalytic Dyad of Ribinuclease A: Structure and Function of the Wild-Type, D121N and D121A Enzymes. *Biochemistry* **37**, 8886-8898.

Sela, M. (1962). Inhibition of Ribonuclease by Copolymers of Glutamic Acid and Aromatic Amino acids. *J. Biol. Chem.* **237**, 418-421.

Sela, M., Anfinsen, C. B. & Harrington, W. F. (1957). The correlation of ribonuclease activity with specific aspects of tertiary structure. *Biochim. Biophys. Acta* **26**, 502-512.

Smith, A. A., Carlow, D. C., R., W. & Short, S. A. (1994). Mutations Affecting Transition-State Stabilization by Residues Coordinating Zinc at the Active Site of Cytidine Deaminase. *Biochemistry* **33**, 6468-6474.

Smith, H. B. & Hartman, F. C. (1988). Restoration of Activity to Catalytically Deficient Mutants of Ribulosebisphosphate Carboxylase/Oxygenase by Aminoethylation. *J. Biol. Chem.* **263**, 4921-4925.

Smyth, D. G., Stein, W. H., Moore, S. (1963). The Sequence of Amino Acid Residues in Bovine Pancreatic Ribonuclease: Revisions and Confirmations. *J. Biol. Chem.* **238**, 227-234.

Sowa, G. A., Hengge, A. C. & Cleland, W. W. (1997). ^{18}O Isotope effects Support a Concerted Mechanism for Ribonuclease A. , .

Stankiewicz, P. J., Tracey, A. S. & Crans, D. C. (1995). Inhibition of Phosphate-Metabolizing Enzymes by Oxovanadium (V) Complexes. In *Metal Ions in Biological Systems; Vanadium and Its Role in Life* (H. Sigel & S. A., Ed.), pp. 287-324, Marcel Dekker, Inc., NY.

Stein, W. H. (1964). Structure-activity relationships in ribonuclease. *Fed. Proc.* **23**, 599-608.

Stowell, J. K., Widlanski, T. S., Kutateladze, T. G. & Raines, R. T. (1995). Mechanism Based Inactivation of Ribonuclease A. *J. Org. Chem.* **60**, 6930-6936.

Suckling (1990). *Enzyme Chemistry; Impact and applications*, Chapman and Hall, London.

Tarragona-Fiol, A., Eggelte, H. J., Harbron, S., Sanchez, E., Taylorson, C. J., Ward, J. M. & Rabin, B. R. (1993). Identification by site-directed mutagenesis of amino acids in the B2 subsite of bovine pancreatic ribonuclease A. *Protein Eng.* **6**, 901-906.

Thompson, J. E., Kutateladze, T. G., Schuster, M. C., Venegas, F. D., Messmore, J. M. & Raines, R. T. (1995). Limits to Catalysis by Ribonuclease A. *Bioorg. Chem.* **23**, 471-481.

Thompson, J. E. & Raines, R. T. (1995). Value of General Acid-Base Catalysis to Ribonuclease A. *J. Am. Chem. Soc.* **116**, 5467-5467.

Thompson, J. E., Venegas, F. D. & Raines, R. T. (1994). Energetics of Catalysis by Ribonucleases: Fate of the 2',3'-Cyclic Phosphodiester Intermediate. *Biochemistry* **33**, 7408-7414.

Thompson, R. C. (1973). Use of Peptide Aldehydes to Generate Transition-State Analogs of Elastase. *Biochemistry* **12**, 47-51.

Thorson, J. S., Chapman, E., Murphy, E. C., Schultz, P. G. & Judice, J. K. (1995). Linear Free Energy Analysis of Hydrogen Bonding in Protein. *J. Am. Chem. Soc.* **117**, 1157-1158.

Tlusty, L. L., Abbott, D., Allen, V., Friedhoff, M. J., wirth, K. & Berkness, T., Eds., *Betty Crocker's Cookbook, New and Revised* (Western Publishing Company, Racine, WI, 1986).

Tracey, A. S., Jaswal, J. S., Gresser, M. J. & Rehder, D. (1990). Condensation Reactions of Aqueous Vanadate with Common Nucleosides. *Inorg. Chem.* **29**, 4283-4288.

Tracey, A. S. & Leon-Lai, C.-H. (1991). ^{1}H and ^{51}V Investigations of Complex Formed between Vanadate and Nucleosides. *Inorg. Chem.* **30**, 3200-3204.

Trautwein, K., Holliger, P., Stackhouse, J. & Benner, S. A. (1991). Site-directed mutagenesis of bovine pancreatic ribonuclease: lysine-41 and aspartate-121. *FEBS Lett.* **281**, 275-277.

Ui, N. (1971). Isoelectricpoints and Conformation of Proteins. II. Isoelectric Focusing of alpha-Chymotrypsin and its Inactive Derivative. *Biochim. Biophys. Acta* **229**, 567-581.

Usher, D. A., Erenrich, E. S. & Eckstein, F. (1972). Geometry of the first step in the action of ribonuclease-A. *Proc. Natl. Acad. Sci. USA* **69**, 115-118.

Usher, D. A., Richardson, D. I. & Eckstein, F. (1970). Absolute stereochemistry of the second step of ribonuclease action. *Nature* **228**, 663-665.

Vicentini, A. M., Kieffer, B., Mathies, R., Meycheck, Hemmings, B. A., Stone, S. R. & Hofsteenge, J. (1990). Protein Chemical and Kinetic Characterization of Recombinant Porcine Ribonuclease Inhibitor Expressed in *Saccharomyces cerevisiae*. *Biochemistry* **29**, 8827-8834.

Vithayathil, P. J. & Richards, F. M. (1960). Modification of the Amino Groups of the Peptide Component of Subtilisin-modified Ribonuclease. *J. Biol. Chem.* **235**, 1029-1037.

Weil, L., Siebles, T.S. (1955). Photooxidation of Crystalline Ribonuclease in the Presence of Methylene Blue. *Arch. Biochem. Biophys.* **54**, 368-377.

Westheimer, F. H. (1968). Pseudo-Rotation in the Hydrolysis of Phosphate Esters. *Acc. Chem. Res.* **1**, 70-78.

Wiseman, T., Williston, S., Brandts, J. F. & Lin, L.-N. (1989). Rapid measurement of Bindind Constants and Heat Using a New Titration Calorimeter. *Anal. Biochem.* **179**, 131-137.

Witzel, H. & Barnard, E. A. (1962). Mechanism and Binding Sites in the Ribonuclease Reaction. Kinetic Studies on the Second Step of the Reaction. *Biochem. Biophys. Res. Comm.* **7**, 289-294.

Wladkowski, B. D., Krauss, M. & Stevens, W. J. (1995). Transphosphorylation Catalyzed by Ribonuclease A: Computational Study Using ab Inition Effective Fragment Potentials. *J. Am. Chem. Soc.* **117**, 10537-10545.

Wladkowski, B. D., Svensson, L. A., Sjolin, L., Ladner, J. E. & Gilliland, G. L. (1998). Structure (1.3 Angstrom) and Charge States of a Ribonuclease A-Uridine Complex: Implications for the Phosphate Ester Hydrolysis Mechanism. *J. Am. Chem. Soc.* **120**, 5488-5498.

Wlodawer, A. (1985). Structure of bovine pancreatic ribonuclease by X-ray and neutron diffraction. In *Biological Macromolecules and Assemblies, Vol. II, Nucleic Acids and Interactive Proteins* (F. A. Jurnak & A. McPherson, Ed.), pp. 395-439, Wiley, New York.

Wlodawer, A., Miller, M. & Sjölin, L. (1983). Active site of RNase: neutron diffraction study of a complex with uridine vanadate, a transition-state analog. *Proc. Natl. Acad. Sci. USA* **80**, 3628-3631.

Wolfenden, R. (1969). Transition State Analogues for Enzyme Catalysis. *Nature* **223**, 704-705.

Wolfenden, R. (1976). Transition State Analog Inhibitors and Enzyme Catalysis. *Annu. Rev. Biophys. Bioeng.* **5**, 271-306.

Wyckoff, H. W., Hardman, K. D., Allewell, N. M., Inagami, T., Johnson, L. N. & Richards, F. M. (1967). The structure of ribonuclease-S at 3.5 Å resolution. *J. Biol. Chem.* **242**, 3984-3988.

Yakovlev, G. I., Moiseyev, G. P., Bezborodova, S. I., Both, V. & Sevcik, J. (1992). A Comparative Study on the Catalytic Properies of Guanylyl-specific Ribonucleases. *Eur. J. Biochem.* **204**, 187-190.

Zegers, I., Maes, D., Doa-Thi, M.-H., Poortmans, F., Palmer, R. & Wyns, L. (1994). The Structure of RNase A complexed with 3'-CMP and d(CpA): Active site conformation and conserved water molecules. *Protein Sci.* **3**, 2322-2339.

Zinn, K., DiMaio, D. & Maniatis, T. (1983). Identification of Two Distinct Regulatory Regions Adjacent to the Human β-Interferon Gene. *Cell* **34**, 865-879.